CONTRIBUTED MAP CM-11-A

Arizona Geological Survey
www.azgs.az.gov

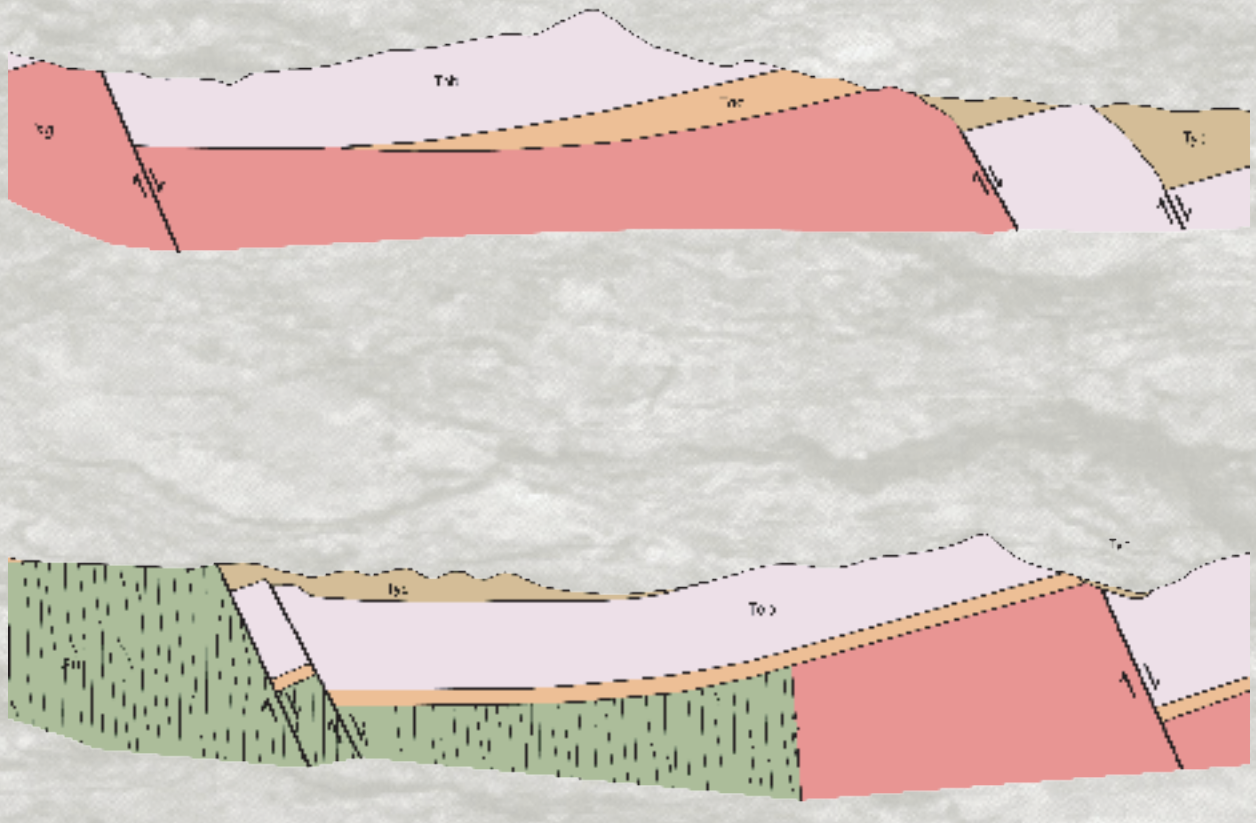

# Tertiary Extension and Fault-Block Rotation in the Transition Zone, Cedar Mountains Area, Arizona

June 2011

Patrick Kennedy Brand and Edmund Stump

ARIZONA GEOLOGICAL SURVEY
Contributed Map CM-11-A, version 1.1

# Arizona Geological Survey Contributed Map Series

The Contributed Map Series provides non-AZGS authors with a forum for publishing documents concerning Arizona geology. While review comments may have been incorporated, this document does not necessarily conform to AZGS technical, editorial, or policy standards.

The Arizona Geological Survey issues no warranty, expressed or implied, regarding the suitability of this product for a particular use. Moreover, the Arizona Geological Survey shall not be liable under any circumstances for any direct, indirect, special, incidental, or consequential damages with respect to claims by users of this product.

The author(s) is solely responsible for the data and ideas expressed herein.

# TERTIARY EXTENSION AND FAULT-BLOCK ROTATION IN THE TRANSITION ZONE, CEDAR MOUNTAINS AREA, ARIZONA

by

Patrick Kennedy Brand and Edmund Stump
Arizona State University

This study was original prepared by Patrick Brand as part of a
thesis presented in partial fulfillment of the requirements for the degree of
Master of Science, with the supervision of Professor Edmund Stump

ARIZONA STATE UNIVERSITY

May 2005

ABSTRACT

New geologic mapping from the Cedar Mountains - Bloody Basin - Cooks Mesa area in the central Arizona Transition Zone presents an enigmatic geologic relationship that has previously gone unstudied. Here, fault blocks of Early Proterozoic basement overlain by Tertiary sedimentary and tuffaceous-lacustrine deposits and capped by a thick accumulation of basalt flows, dated in the project area between 15.1 and 13.5 Ma, are rotated ~20$^{o}$ west to west-southwest along east-dipping normal faults. Half-grabens formed during rotation are filled with a syn- to post-extensional basin-fill conglomerate, and are locally overlain by flat-lying and post-extensional basalts, dated in this study at 6.4 Ma. The extended area is a graben, bounded to the west by the eastern flank of Cooks Mesa, a flat-lying expression of the same general stratigraphy, and to the east by the Mazatzal Mountains. Faults in the project area strike north and northwest and are interpreted to merge with the Cooks Mesa fault, a listric normal fault, at depth. The graben, named in this study the Lower Verde Valley graben, continues southward out of the project area parallel to the Verde River, and northward across the Bloody Basin.

New dates from this research bracket the timing of the extension in the project area between 13.5 Ma and 6.4 Ma. The timing is coeval with the Basin and Range disturbance in Arizona, yet the style of extension in the project area is not consistent with the published understanding of this event. Here, rather than the expected high-angle normal faults and offset without rotation, extension was accommodated by motion along a listric normal fault and rotation of fault blocks. This unusual setting provides a new view into the dynamics of the Basin and Range disturbance in the Arizona Transition Zone.

ACKNOWLEDGMENTS

First and foremost I would like to thank Ed Stump for being such a great advisor. His patience, guidance, and valuable advice played an important role in helping me finish this project. I would also like to thank my supervisory committee members, Steve Reynolds and Ramon Arrowsmith, who were there to help whenever and however needed. Additionally, I want to express my gratitude to Ramon Arrowsmith, Maurits Thayer, Chris Crosby, and most especially, Jessica Block for ArcGIS help and use of the Active Tectonics lab. I appreciate the support of everyone at the Tonto National Forest, especially the people in the Terrestrial Ecosystem Survey, who provided base maps and encouragement. Special thanks go to Melanie Busch, Lucas Delezene, and Shawn Wright, who joined me in the field during this project, for the valuable discussion and company. Finally, I would like to express my gratitude to Sue Selkirk for her patience, Illustrator advice, and merging of digital photos. This work was partially funded through a Graduate and Professional Student Association (GPSA) Research Grant and could not have been completed as thoroughly without it.

TABLE OF CONTENTS


| | Page |
|---|---|
| LIST OF TABLES | viii |
| LIST OF FIGURES | ix |
| LIST OF PLATES | xi |
| INTRODUCTION | 1 |
| Physiographic Provinces | 1 |
| Project Statement | 3 |
| REGIONAL GEOLOGIC FRAMEWORK | 9 |
| Proterozoic | 9 |
| Paleozoic | 11 |
| Mesozoic | 11 |
| Late Mesozoic through Cenozoic | 13 |
| PROJECT AREA GEOLOGIC OVERVIEW | 18 |
| PREVIOUS WORK | 21 |
| MAP UNITS | 24 |
| Early Proterozoic Units | 26 |
| Middle Proterozoic? Units | 35 |
| Tertiary Units | 36 |
| Quaternary and Tertiary Units | 49 |
| Quaternary Units | 50 |
| FAULTS | 51 |
| FIELD RELATIONS | 55 |

Page

GEOCHRONOLOGY ..... 58

INTERPRETATION OF FIELD RELATIONS ..... 64

Older Conglomerate/Basement ..... 64

Chalk Canyon Formation ..... 65

Hickey Formation Basalt…. ..... 67

Younger Conglomerate ..... 68

Younger Basalt ..... 68

TILTING AND EXTENSION ..... 69

Timing……..... 69

Fault Patterns…. ..... 69

Fault Related Folding ..... 74

Lower Verde Valley Graben ..... 77

Amount of Extension ..... 80

REGIONAL SYNTHESIS ..... 82

Verde Valley and Tonto Basin ..... 82

Miocene Extension in the Transition Zone ..... 84

SUMMARY…….. ..... 86

Tertiary Geologic History ..... 86

Conclusions……..... 89

REFERENCES…… ..... 94

APPENDIX Page

A ANALYTICAL TECHNIQUES..... 102

B ANALYTICAL RESULTS ..... 107

## LIST OF TABLES

Table Page

1. $^{40}Ar/^{39}Ar$ analytical results..... 60

LIST OF FIGURES


Figure Page

1. Physiographic provinces of Arizona ..... 2

2. Panoramic photograph of East and West Cedar Mountains area ..... 4

3. Location map of the study area ..... 6

4. Location map for places mentioned in this report ..... 7

5. Map of previous work in the project area ..... 8

6. Mid-Tertiary orogeny tilt-block domains in Arizona ..... 15

7. Map showing the localities where the transition from the mid-Tertiary Orogeny to Basin and Range disturbance can be constrained ..... 17

8. Relationship of project area to the Verde Valley and Tonto Basin ..... 19

9. Generalized stratigraphic column for the project area ..... 25

10. Metarhyolite hand samples from the Rover Peak area ..... 27

11. Slate found to the north of the Rover Peak area ..... 28

12. Field exposures of basement rocks in the Cooks Mesa area ..... 30

13. Hand samples of Cooks Mesa area basement ..... 31

14. Metadiorite from the southwestern corner of the project area ..... 32

15. Hand samples of Verde River Granite from the project area ..... 34

16. Outcrops of the pre-volcanic conglomerate dominated by granite clasts ..... 37

17. Representative hand sample of the basalt of the lower Chalk Canyon Formation ..... 40

18. Field exposure and hand samples of upper Chalk Canyon Formation ..... 41

19. Hand samples of typical Hickey Formation basalts ..... 43

Figure Page

20. Typical field exposure of Hickey Formation basalt with obvious flow banding and fractures showing dip ..... 44

21. Exposures of Hickey Formation basalts across Arizona..... 46

22. Typical field exposures of younger, basalt rich conglomerate ..... 47

23. Typical field relations of Tyc ..... 48

24. Simplified geologic map of the project area ..... 52

25. Geologic map of the Sheep Bridge Area ..... 57

26. Age spectrum and isochron plot for 31304A groundmass concentrate ..... 61

27. Age spectrum and isochron plot for 30704A groundmass concentrate ..... 62

28. Age spectrum and isochron plot for 31404B groundmass concentrate ..... 63

29. Map of Tertiary normal faults in the region..... 75

30. Diagrammatic cross-section depicting the Lower Verde Valley graben ..... 79

31. Diagram summarizing of Tertiary geologic history of the project area..... 90

## LIST OF PLATES

Plate

1. Geologic map of the Cedar Mountains area, Arizona.

2. Cross-sections to accompany the geologic map of the Cedar Mountains area, Arizona.

3. Explanation to accompany the geologic map of the Cedar Mountains area, Arizona.

# INTRODUCTION

## Physiographic Provinces

The present day landscape of Arizona can be subdivided into three major physiographic provinces, known as the Basin and Range, Transition Zone, and the Colorado Plateau (Fig. 1), all of which are the product of a complex late Mesozoic through Cenozoic geologic history.

The Colorado Plateau province includes most of northeastern Arizona, and is characterized by an elevated and generally broad, flat landscape interrupted by volcanic landforms, mesas, and deeply incised canyons. Elevations average between 1500 and 2100 m above sea level (Fig. 1). Geologically, the Colorado Plateau consists of a thick sequence of essentially flat-lying Paleozoic and Mesozoic strata and thin localized deposits of Cenozoic volcanic rocks (Kamilli and Richard, 1998).

The Basin and Range province in southern Arizona is distinguished by narrow, elongate mountain ranges which trend north and northwest and are separated by wide valleys. The rocks composing the mountains are geologically diverse, ranging from Proterozoic to Tertiary in age, while the basins are dominated by Cenozoic sedimentary basin-fill (Kamilli and Richard, 1998). Average basin floor elevations increase eastward across the province, ranging from less than 300 m above sea level in the southwestern part of the state to up to 1500 m above sea level in southeastern Arizona (Fig. 1).

The aptly named Transition Zone province is between the Basin and Range and Colorado Plateau and features characteristics of both. It trends northwest to southeast

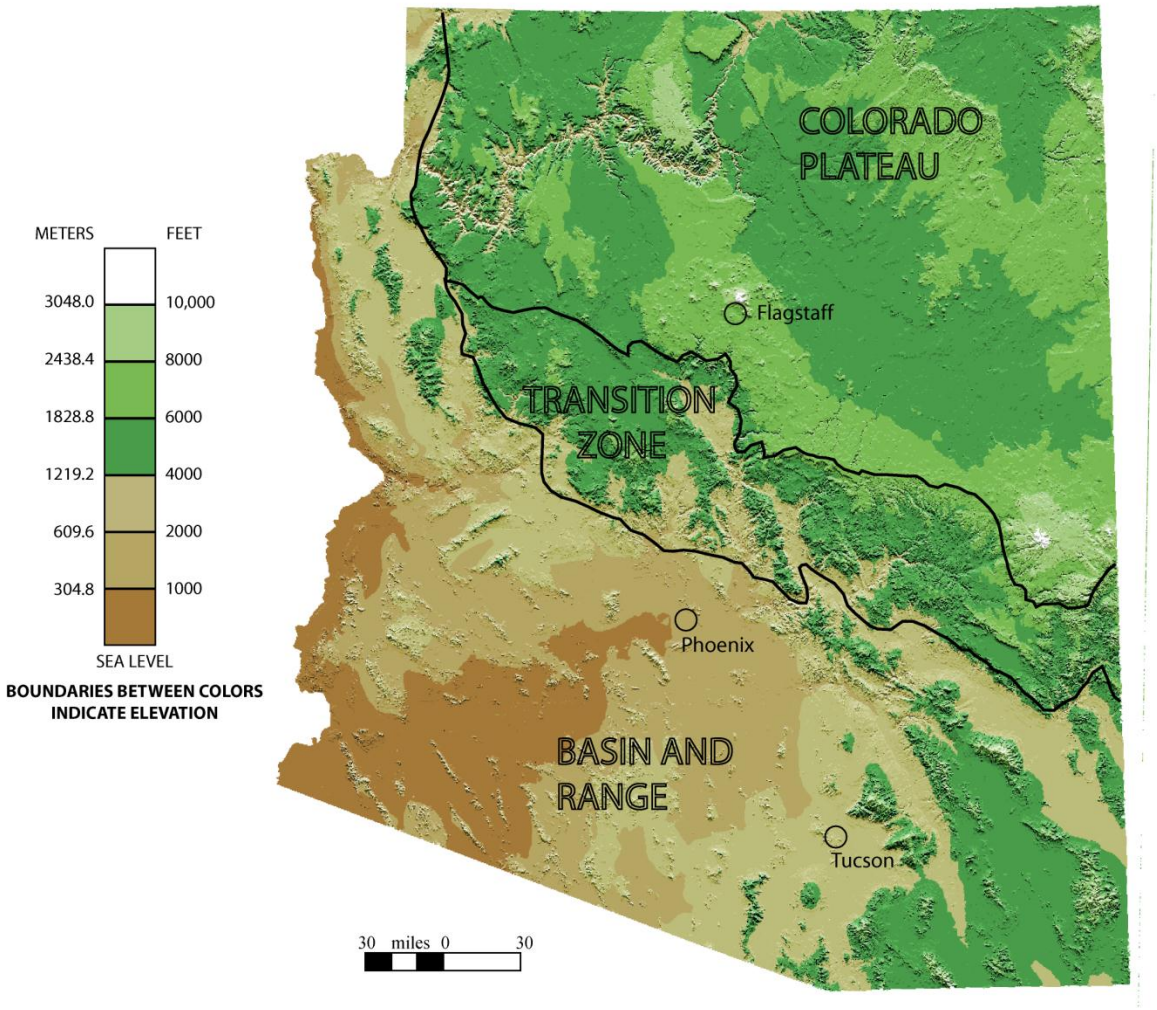


**Figure 1. Physiographic provinces of Arizona. Shaded relief image from United States Geological Survey, Flagstaff, AZ.**

across the state, and is a relatively narrow band, ~100 km wide, of rugged topography, with broad mountain ranges, mesas, and narrow valleys. There are a wide variety of rocks, ranging in age from Proterozoic to Cenozoic (Kamilli and Richard, 1998). Elevations are generally between 900 and 1800 m above sea level (Fig. 1).

**Project Statement**

Large portions of the Transition Zone remain unmapped and unstudied in detail, and therefore we do not have a complete understanding of the tectonic and physiographic development of this area. The East and West Cedar Mountains area is one such locale in the central Transition Zone. Here, one finds an expression of tilted fault-blocks (Fig. 2). Tilted fault-blocks are characteristic of the mid-Tertiary orogeny, the effects of which are confined to the Basin and Range province, and therefore in the Cedar Mountains area are outside the spatial boundaries of this event. Tertiary extension in the Transition Zone is considered to be related to the Basin and Range disturbance. Tilted fault-blocks, however, are not consistent with the general understanding of this latter event in Arizona, which dictates that extension is accommodated by graben subsidence without rotation.

This thesis presents the results of a detailed field investigation of the East and West Cedar Mountains area, which was performed in order to better understand how and when the tilted fault blocks formed, and how this relates to the tectonic and physiographic development of Arizona and the Transition Zone. This study involves new geologic mapping of the entire Rover Peak quadrangle, and adjoining portions of the

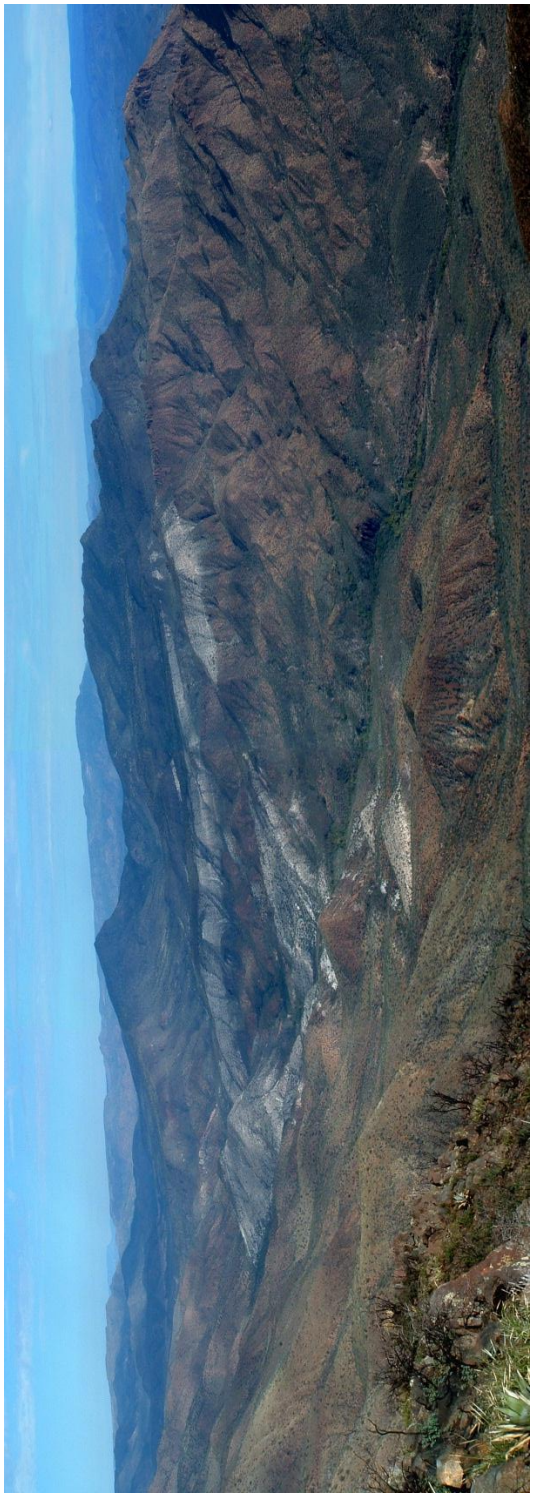

**Figure 2. Panoramic photograph of the East and West Cedar Mountains area, looking north from Humboldt Mountain.**
**Note the tilt-block morphology of East and West Cedar Mountains. Merging of digital photography courtesy of Sue Selkirk.**

Bloody Basin, Cooks Mesa, and Chalk Mountain 7.5' quadrangles (Fig. 3), covering about 75-80 square miles, at the 1:24,000 scale, which was completed over 45 field days between September 2003 and October 2004. Additionally, in combination with the detailed field work, petrographic analysis of selected samples leads to a description of the geology of the area, and construction of cross sections offers a three-dimensional glimpse of the features beneath the surface. Additionally, 3 new $^{40}Ar$-$^{39}Ar$ dates done by Dr. William Macintosh and Lisa Peters at New Mexico Tech help constrain the timing of events in this area by dating of the youngest tilted basalts and oldest non-tilted basalts in the area, important information for truly understanding the evolution of this landscape and geologic history. This project presents conclusions to the objectives set forth above, giving a new view into the tectonic and physiographic development of the Transition Zone and the dynamics of the Basin and Range disturbance.

The East and West Cedar Mountains area lies about 30 miles north of the Phoenix metropolitan area and the city of Cave Creek, Arizona (Fig. 3). The lower Verde River valley marks the eastern edge of the study area, while the western edge is bounded by Cooks Mesa (Fig. 4). The project area extends into the Bloody Basin to the north and ends southward where it ties in with previous geologic mapping efforts (i.e. Gilbert et al., 1998) (Fig. 5). Primary access in the field area is Forest Road 24 and Forest Road 269. Various 4 wheel drive and jeep trails provide additional access throughout the area.

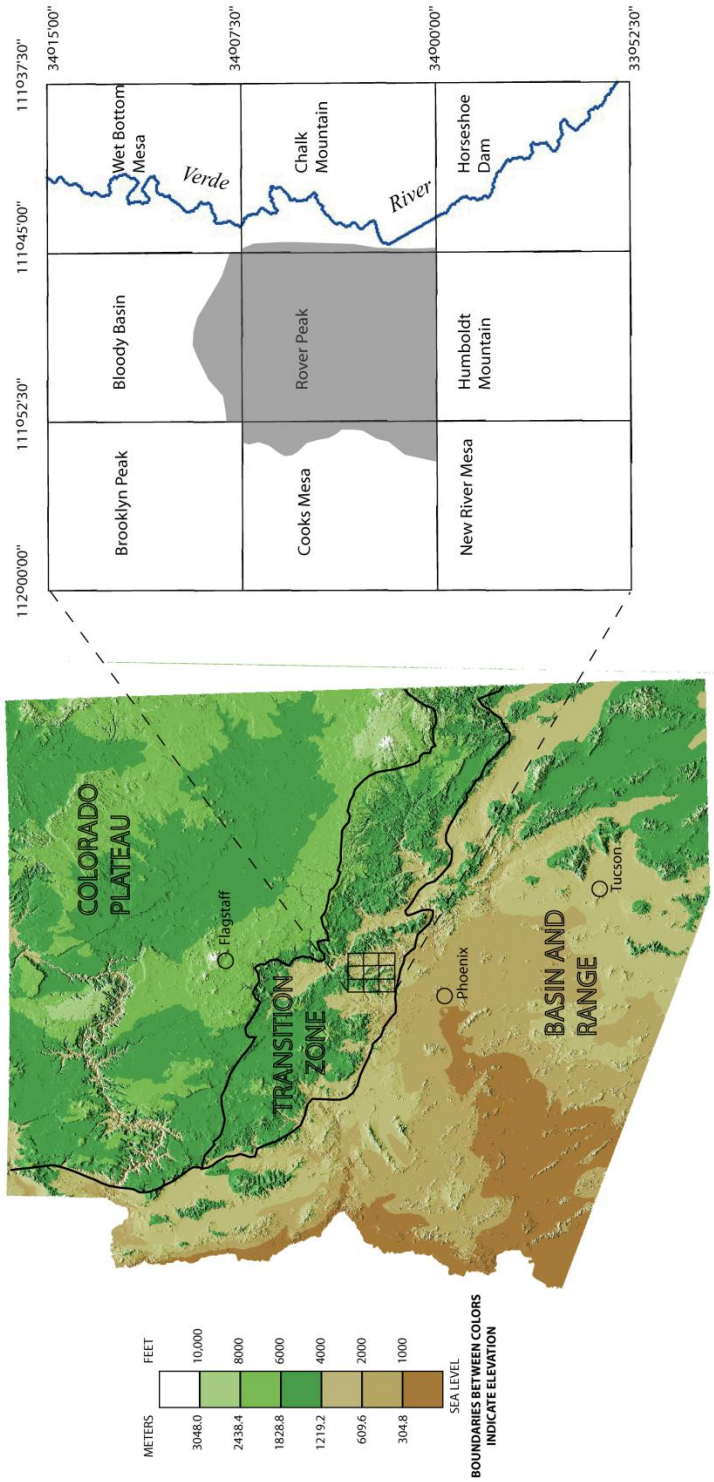


**Figure 3. Location map of the study area. The grid shows USGS 7.5' quadrangles. The shaded portion denotes area of geologic mapping. Shaded relief image from United States Geological Survey, Flagstaff, AZ.**

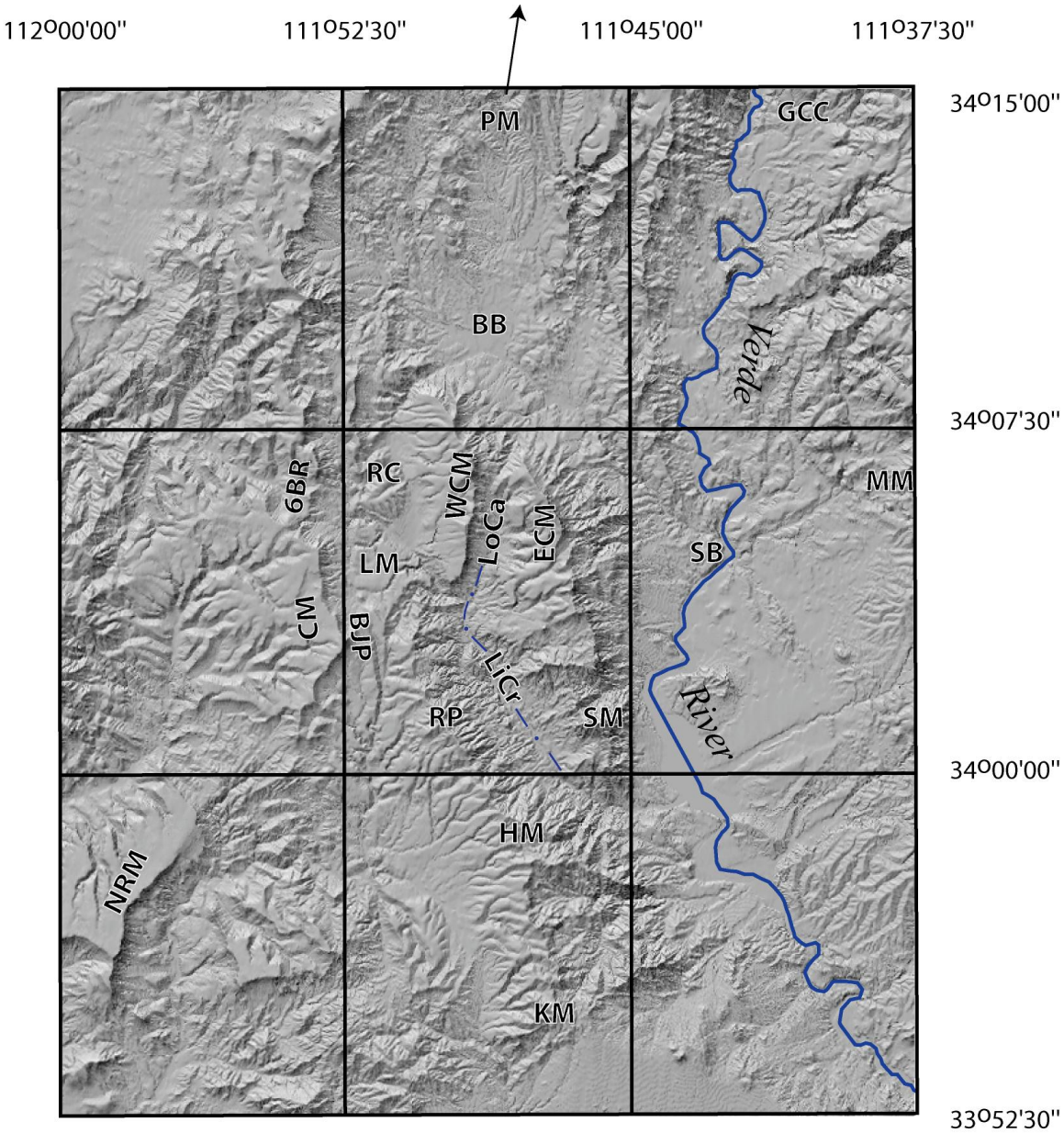


**Figure 4. Location map for places mentioned in this report. WCM=West Cedar Mountain; ECM=East Cedar Mountain; LoCa=Long Canyon; LiCr=Lime Creek; RC=Roundtree Canyon; LM=Lockwood Mesa; RP=Rover Peak; BJP=Blackjack Point; SM=Sunset Mountain; CM=Cooks Mesa; BB=Bloody Basin; 6BR=Six Bar Ridge; NRM=New River Mesa; HM=Humboldt Mountain; KM=Kentuck Mountain; SB=Sheep Bridge; MM=Mazatzal Mountains; PM=Pine Mountain; GCC=Goat Camp Canyon**.

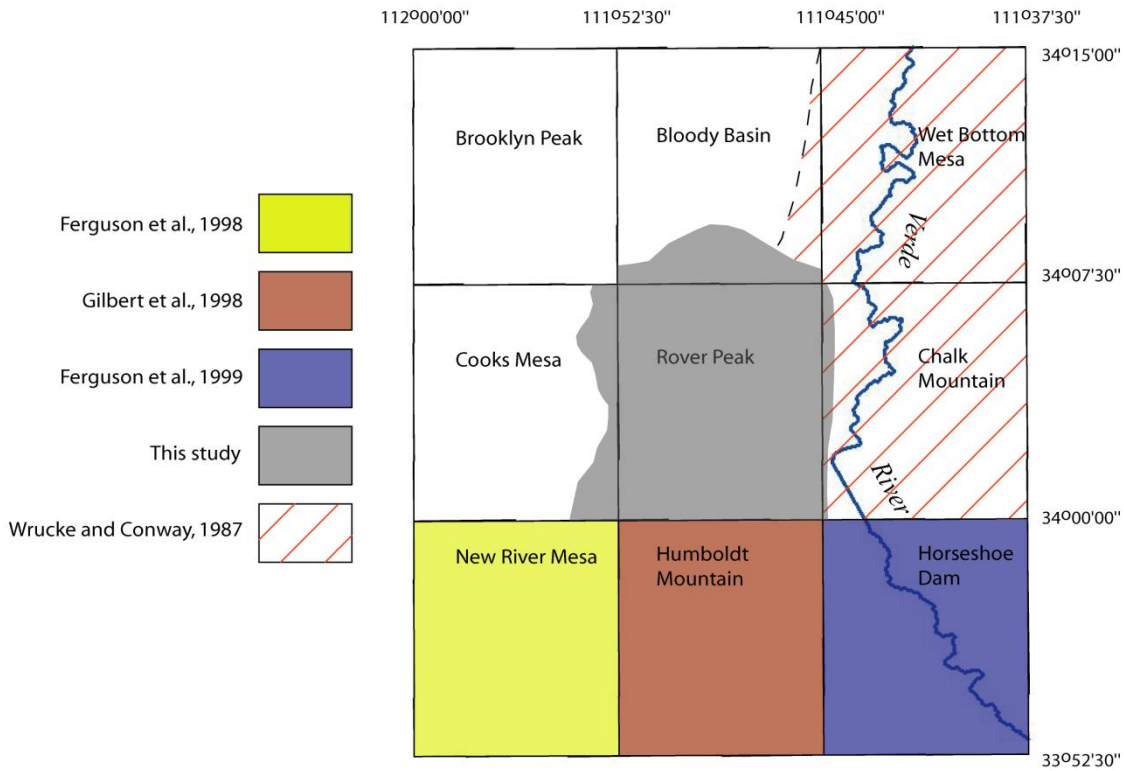


**Figure 5. Map of previous work in the project area. All geologic mapping is at 1:24,000 scale, except Wrucke and Conway (1987), which is at 1:48,000.**

## REGIONAL GEOLOGIC FRAMEWORK

Although this project is a study of Tertiary tectonics and landscape development in the Transition Zone, a complete overview of the geologic history of the region is in order. The Proterozoic through Mesozoic history is an important framework that needs to be reviewed in order for one to understand the subsequent sequence of events. The latest Mesozoic through Cenozoic periods in the Arizona region are, as stated earlier, responsible for the formation of the present landscape of the state. Accordingly, the Proterozoic through Mesozoic will be presented in brief, simplified geological overviews, while the late Mesozoic through Cenozoic will be presented in greater detail. Time boundaries used in this report follow the Geological Society of America 1999 Geological Time Scale.

### Proterozoic

The older Proterozoic geologic history of Arizona is dominated by accretion to the convergent southern margin of the Archean continental core (Dickinson, 1989). The southern margin formed after ca. 2.0 Ga rifting of the Wyoming craton and subsequent formation of oceanic crust in what is now Arizona (Anderson, 1989a). The oldest igneous and metamorphic rocks in Arizona record a period of volcanism, sedimentation, plutonism, and deformation that dates from 1825-1625 Ma (Livingston and Damon, 1968), the details of which are still the subject of debate. It is likely, however, that subduction was involved in their formation, with oceanic crust moving northwest from a

spreading center and formation of northeast-trending volcanic arcs and adjacent sedimentary basins (Anderson, 1980). What is debatable is whether these older Proterozoic rocks were formed in place along the margin of the Archean core, or if they formed and were accreted to the continent after formation in an exotic locale, or perhaps both (Karlstrom et al., 1987). Despite the uncertainty, it is clear that these rocks were accreted to the continental block by the mid-Proterozoic (1600-1500 Ma) (Dickinson, 1989). The older Proterozoic geologic history of Arizona was terminated by the intrusion of transcontinental granitoid batholiths ca. 1450-1400 Ma (Silver et al., 1977).

The younger Proterozoic record begins after an indeterminate period of erosion of the newly consolidated crustal block (Dickinson, 1989), followed by 2.5-4.5 km of sedimentary strata deposited upon the older Proterozoic basement. Sediments are generally coastal plain or epicontinental deposits in the east and more shelf facies to the west, indicating a stable continental shield and platform setting (Elston and McKee, 1982; Shride, 1967; Shafiqullah et al., 1980). Intercalated basalts and diabase sills indicate these units formed at about 1100 Ma (Luchitta and Hendricks, 1983). Little angular discordance exists between the younger Proterozoic rocks and the oldest Paleozoic rocks in Arizona, indicating a long-enduring, stable tectonic setting (Dickinson, 1989).

Today rocks of Proterozoic age are largely exposed throughout the Transition Zone. Scattered outcrops occur in the ranges of the Basin and Range province. On the Colorado Plateau, Proterozoic rocks are only exposed in the bottom of the Grand Canyon (Shafiqullah et al., 1980).

**Paleozoic**

Rifting of the supercontinent Rodinia, assembled during the Proterozoic, began in the latest Precambrian and continued into the earliest Paleozoic. This created smaller continental blocks including North America. As rifting progressed, passive margins developed along the western and southern margins of the North American craton, including most of what is now Arizona (Dickinson, 1989). Seas repeatedly transgressed and regressed, depositing up to several kilometers of carbonate and clastic sediments upon the stable cratonic platform (Shafiqullah et al., 1980). The Paleozoic, in Arizona, was a time of tectonic stability (Coney, 1978a).

Today there are outcrops of the Paleozoic sequence across the entire Colorado Plateau and in scattered outcrops in the southeastern Arizona Basin and Range province (Kamilli and Richard, 1998; Titley, 1984).

**Mesozoic**

By the mid-Mesozoic the tectonic setting of the western margin of the North American block had completely changed from passive to that of active east-directed subduction. Prior to this, throughout the Paleozoic, the entire state of Arizona has a similar geologic history. The Mesozoic, with the inception of a new tectonic regime, marks a point in time when the northeastern and southwestern halves of the state begin completely different geologic histories.

The subduction-related, northwest-trending, magmatic arc ran directly through the southwestern part of the state. Accordingly, the Late Triassic through Late Jurassic are marked in southern Arizona by widespread volcanic activity and emplacement of small granitoid batholiths (Dickinson, 1989; Coney, 1978a). The cessation of magmatism here after the late Jurassic is attributed to a westward shift of the magmatic arc out of the state (Damon et al., 1981). Subsequent backarc extension during the Early Cretaceous caused subsidence and formation of sedimentary basins in southern Arizona, in which over 4 kilometers of muds and clays accumulated in marine and nonmarine environments. This deposition had ceased by the Late Cretaceous (Titley, 1984; Dickinson, 1989).

Northeastern Arizona, however, did not undergo major affects of mid-Mesozoic tectonics or magmatism (Dickinson, 1989). Here, the Mesozoic record is dominated by up to 4 kilometers of clastic sedimentary deposits, specifically continental redbeds, derived from highlands to the south, west, and east (Titley, 1984). It is important to note, however, that there are Cretaceous open-marine shales (Mancos Shale) within the Mesozoic sequence in northeastern Arizona (Nations, 1989).

As is the case with the Paleozoic rocks, one now finds good exposures of these rocks across northeastern part of the Colorado Plateau in Arizona and in scattered exposures in the southeastern Arizona Basin and Range province (Kamilli and Richard, 1998).

**Late Mesozoic through Cenozoic**

The Laramide orogeny began approximately 80 to 75 Ma (Late Cretaceous) as the result of increased convergence rates along the subduction zone (Coney, 1976) that was present along the western margin of North America. It was a period of contractional deformation, thrust faulting, widespread volcanism, and plutonism across Arizona (Coney, 1978a). Maximum convergence rates persisted from 70 to 50 Ma, decreasing the dip of the subducted slab and initiating an eastward sweep of the associated volcanic arc (Coney and Reynolds, 1977, Coney, 1976). By 50 Ma (Early Eocene), the arc had migrated eastward and the Laramide orogeny was terminated in Arizona (Damon et al., 1984).

Crustal thickening and the subduction of progressively warmer, thinner oceanic crust as the East Pacific Rise approached the western margin of North America contributed to widespread epeirogenic uplift of the entire region during and after the Laramide orogeny (Shafiqullah et al., 1980, Damon et al., 1984, Leighty, 1997). This uplift was accompanied by a period of widespread Eocene erosion that removed much of the Laramide volcanic cover, eroding the land surface down over a period of 10 to 30 m.y. (Shafiqullah et al., 1980, Damon et al., 1984). Eocene gravel deposits ("Rim Gravels") on the surface of the modern Colorado Plateau show evidence of transport in a northeasterly direction. These gravels include clasts which originated in southwestern Arizona, indicating that at this time, southwest Arizona was a highland area (Peirce et al., 1979; Potochnik, 1989). After 50 Ma, convergence rates along the western margin of

North America slowed, causing an increase in the dip of the subducting slab which led to the return sweep of the volcanic arc westward, back into central Arizona ~38 Ma. This set the stage for the mid-Tertiary orogeny (Coney and Reynolds, 1977, Damon et al., 1984).

The mid-Tertiary orogeny marks the onset of the separation of the Basin and Range from the Colorado Plateau (Damon et al., 1984). It was characterized by large-magnitude, east-northeast – west-southwest-directed extension along low-angle detachment faults which was responsible for rotation of relatively small, hanging wall, crustal fault blocks. Extreme extension along low-angle detachment faults created and exposed metamorphic core complexes, which formed in footwall rocks at depth along the fault zones (Spencer and Reynolds, 1989, Davis et al., 1980). Magmatism was generally felsic to intermediate in composition and was widespread between 30 and 20 Ma (Damon et al., 1984). It is important to note here that while the affects of the mid-Tertiary orogeny were felt throughout the modern Basin and Range province, they were not felt through the modern Transition Zone or Colorado Plateau (Leighty, 1997; Menges and Pearthree, 1989) (Fig. 6). Extension related to this event had ended by about 17 Ma (Spencer et al., 1995; Shafiqullah et al., 1980).

Between 17 and 15 Ma, magmatism became dominantly basaltic and extension was oriented essentially east-west, had a smaller magnitude, and was characterized by graben subsidence along steep, high-angle normal faults without rotation across the modern Basin and Range province (Shafiqullah et al., 1980, Damon et al., 1984, Leighty, 1997). This event is aptly referred to as the Basin and Range disturbance, and

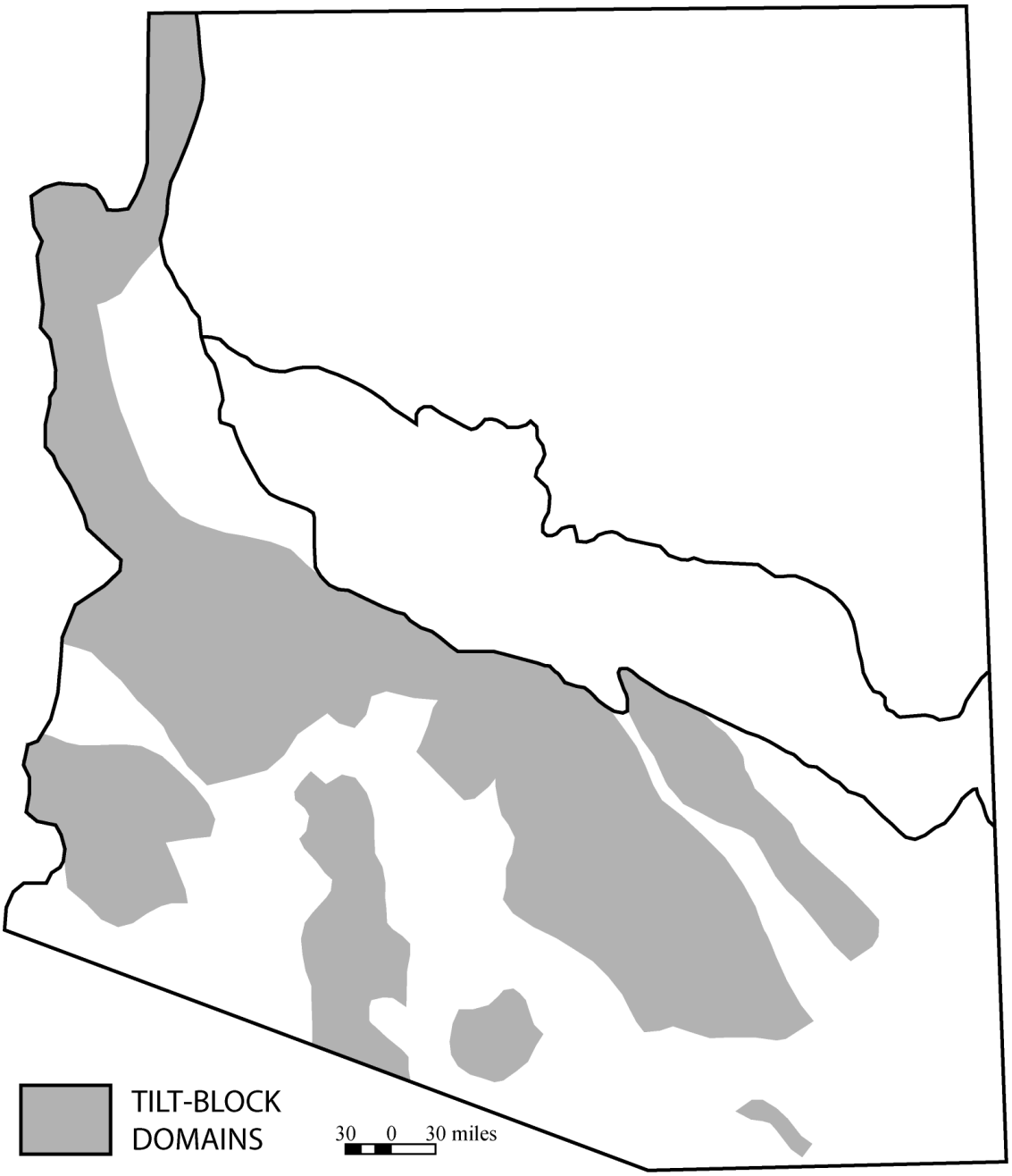


**Figure 6. Mid-Tertiary Orogeny tilt-block domains in Arizona (after Spencer and Reynolds, 1989). Note that none are found in the Transition Zone.**

continues in parts of Arizona through today. Most vertical movement, however, was terminated by 8 - 6 Ma (Shafiqullah et al., 1980; Scarborough and Peirce, 1978).

The change from the mid-Tertiary orogeny to the Basin and Range disturbance was not abrupt, however, as the two events are not separate in time. The period of 24 to 12 Ma is known as the mid-Miocene transition (Shafiqullah et al., 1980) (which should not be confused with the modern transition zone province). Essentially, the transition is a time of overlap between the two tectonic regimes, with processes of the Basin and Range disturbance expanding as those of the mid-Tertiary orogeny faded. The timing of the transition is constrained by dating of the youngest volcanic rock within tilted fault blocks, giving a maximum age for the end of tilting, and the oldest possible, flat-lying, overlying volcanic rock to get a minimum age of the end of tilting. Shafiqullah et al. (1980) document most localities where this is possible (all in the Basin and Range province) (Fig. 7).

As currently understood, these processes have cumulatively acted to separate the modern Basin and Range province from the Colorado Plateau, which has remained relatively undisturbed since the period of Eocene uplift and erosion while the Basin and Range subsided under 2 distinct episodes of extension. The Transition Zone acts as a distributed structural boundary between these two provinces where the differences in extension between the two provinces have been accommodated (Eaton, 1980). It also preserves features which record the transition from the mid-Tertiary orogeny to the Basin and Range disturbance (Leighty, 1997). These characteristics make the Transition Zone an excellent locality for studying the Tertiary tectonic evolution of Arizona.

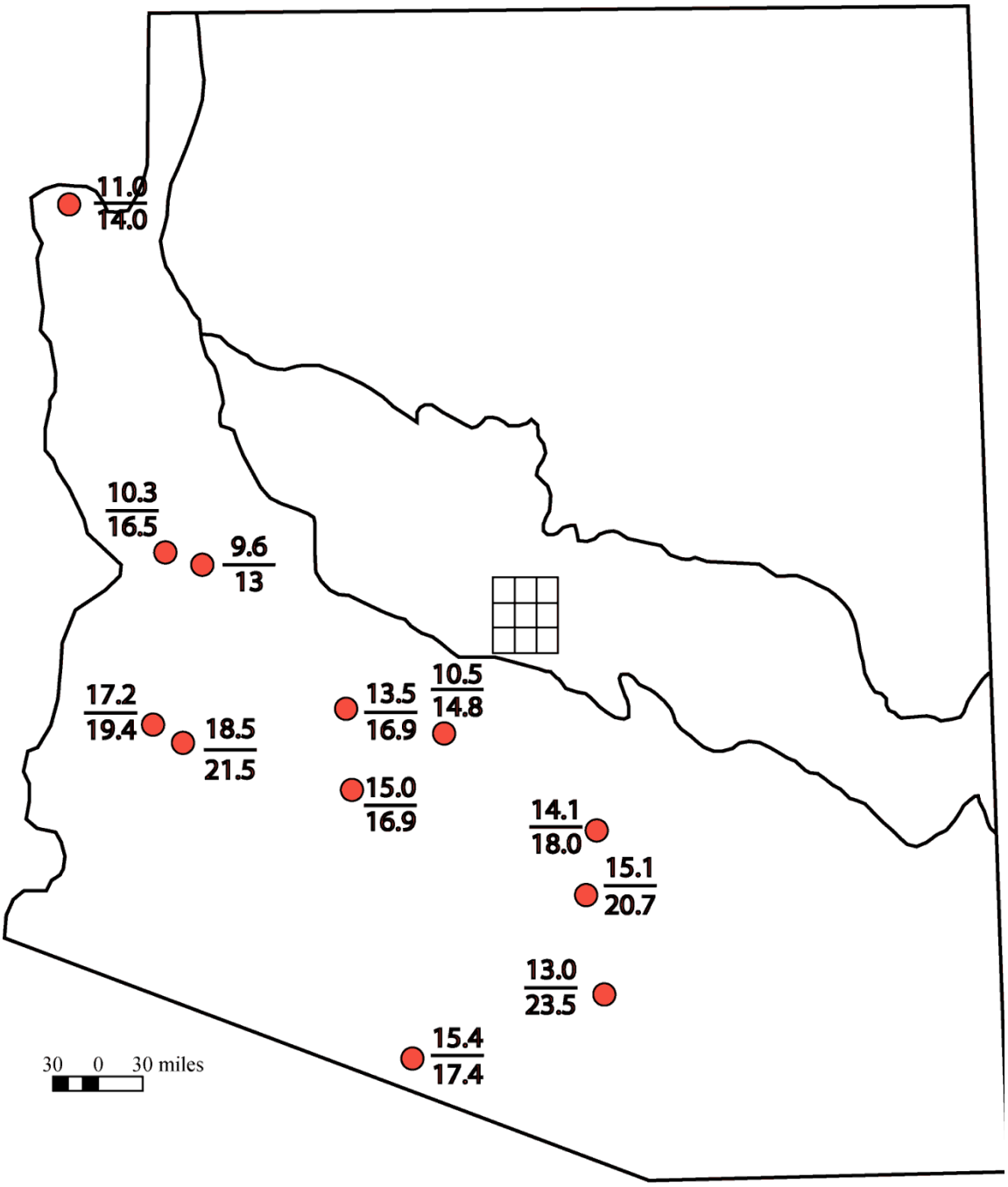


**Figure 7. Map showing the localities where the transition from the mid-Tertiary orogeny to Basin and Range disturbance can be constrained (after Shafiqullah et al., 1980). The number on bottom represents the youngest tilted unit, while the number on top represents the oldest flat-lying unit. The grid shows the project area.**

## PROJECT AREA GEOLOGIC OVERVIEW

The Transition Zone remains unmapped and unstudied in detail across large areas. The Cedar Mountains area is one such place. Here, approximately 30 miles north of Cave Creek, Arizona sit a series of tilted fault blocks dipping ~20$^{o}$ west to west-southwest (Fig. 2). Basalts which cap these tilted fault blocks, collected in reconnaissance fashion by Leighty (1997) have been dated at 14.3 Ma. Therefore, for at least two reasons, this area is recognized as enigmatic. First, tilting of fault blocks, considered to be characteristic of the mid-Tertiary orogeny, has not been observed to affect areas this far north in the modern Transition Zone (Shafiqullah et al., 1980; Leighty, 1997) (Figs. 6, 7). In fact, both to the west and south are flat lying mesas capped by similar aged basalts (New River Mesa, Perry Mesa/Black Mesa) (Gomez, 1979; Leighty, 1997). Secondly, the timing of this event, which must post-date 14.3 Ma, appears to be inconsistent with the generally accepted timing of extension-related tilting in Arizona. The 14.3 Ma age on the tilted basalt implies tilting took place near the end of, or after, the transition period.

Another interesting aspect of this problem can be seen in Figure 8. The area in question aligns almost directly with the junction of the Verde Valley to the northwest and the Tonto Basin to the southeast. These structural basins are both bounded along their southwest edges by escarpments which are controlled by large fault systems with similar behaviors, orientations, and timing of formation. The fault system, however, is more complex at Tonto Basin (Elston, 1984).

The question remains if the proposed field area represents an anomalously located, “last-gasp” of the mid-Tertiary orogeny, or is somehow related to more recent,

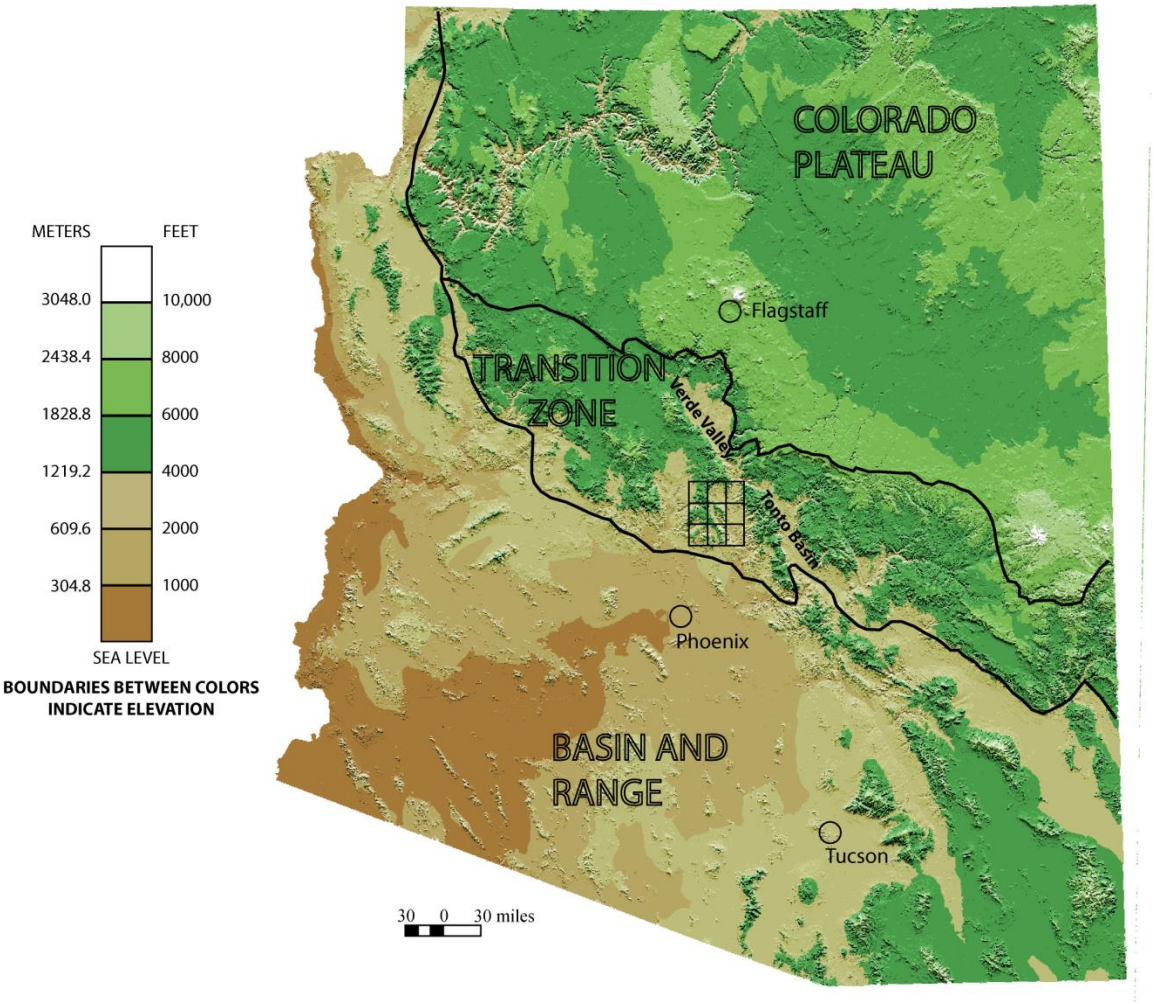


**Figure 8. Relationship of project area (gridded area) to the Verde Valley and Tonto Basin. Shaded relief image from United States Geological Survey, Flagstaff, AZ.**

Basin and Range disturbance fault systems, and possibly those which formed the Verde Valley and Tonto Basin. These questions will be addressed through detailed geologic mapping and dating of appropriate samples of tilted and flat-lying volcanic rocks in order to constrain the timing of this event. It is important to note here that Scarborough and Wilt (1979) have recognized flat-lying volcanic rocks overlying tilted units in the vicinity of this field area, which were determined to be undateable. Also, Wrucke and Conway (1987) produced K-Ar dates on younger basalts in the area of 8.3 ± 2.9 Ma, but the relationship between these younger basalts and the older tilted sequence is unclear. This gives hope that the proper relationships exist in the project area, and therefore, higher precision $^{40}Ar$-$^{39}Ar$ dating can be used to finally constrain the timing of this unique event.

## PREVIOUS WORK

New geologic mapping produced in this project ties in nicely with several maps and studies which have covered adjacent areas to the east and south (Fig. 5). While the project area itself has remained unmapped at a large scale, one study has covered the area in a reconnaissance fashion. The areas immediately to the north and west of the field area remain unmapped and unstudied. This section will briefly discuss what has been learned in the previous studies.

Leighty (1997) studied the project area in reconnaissance fashion, noting that extension in the field area has created west-dipping fault block ranges bounded by major normal faults. The general stratigraphy depicted is an Early Proterozoic basement of dominantly Verde River Granite and metarhyolites of the Red Rock Group in the Lime Creek area. Leighty calls a prevolcanic conglomerate, which overlies basement, the pre-Early Miocene “Bloody Basin fanglomerate”. It is noted that in the East Cedar Mountain block only are the “dominantly Early to Middle Miocene” basalts and tuffaceous limestones of the Chalk Canyon Formation present. The region and tilt-blocks are capped by Middle Miocene Hickey Formation basalts.

Ferguson et al. (1999) have mapped Horseshoe Dam quadrangle, which lies immediately to the southeast of the project area. Here they find Early Proterozoic Verde River/Payson granite overlain directly by Miocene Hickey Formation basalts. Chalk Canyon Formation and older pre-volcanic units are absent. This succession is cut by the major, east side down, Horseshoe Lake fault forming a half-graben with at least 1.5 km offset in the northwestern map area. As the fault continues southward, offset is

accommodated by several east-side down faults which step southeast. Basin-fill units have fanning dips and locally overlap the faults, indicating deposition was syn- to post-extensional.

Gilbert et al. (1998) mapped Humboldt Mountain quadrangle, immediately to the south of the field area. They find that the Proterozoic basement is unconformably overlain by a gently dipping Neogene sedimentary and volcanic complex. The oldest of these units is the pre-volcanic, weakly to non-stratified conglomerate, interpreted only as middle Tertiary in age. This is overlain by the equivalent of the Early to Middle Miocene Chalk Canyon volcanic rocks and capped with basalts correlative with Middle Miocene Hickey Formation. The Horseshoe Lake fault continues through this quadrangle, with at least 2500 ft of offset, and into the project area, as does the Lime Creek fault, another high-angle, east side down normal fault. The overall pattern of Tertiary normal faulting in this region tilts the Miocene strata 5-15$^{o}$ to the west.

The New River Mesa quadrangle to the southwest has been the subject of two studies. Gomez (1979) studied the south-central portion of the quadrangle, and in this project informally named the Chalk Canyon Formation. The region was noted to be the boundary between tilted and dropped blocks to the south and flat-lying mesas to the north. According to Gomez (1979), the stratigraphy was Proterozoic basement overlain by Early to middle Oligocene pre-volcanic “fanglomerate”, overlain by an andesite of probable middle Oligocene age, the middle Oligocene to Middle Miocene Chalk Canyon Formation, and capped by the Middle Miocene Hickey Formation basalts. Ferguson et al. (1998) completed the mapping of this quadrangle, with similar results. The New River

Mesa fault, which strikes north-northeast through the quadrangle, is a high-angle, down to the east fault with up to 300 m of offset. It is also separates gently dipping (5-15$^{o}$) Miocene strata on the east from flat-lying Miocene strata to the west.

The areas to the east of this study have been mapped by Wrucke and Conway (1987), and although at a scale of 1:50,000, it is quite detailed. The focus of the study is on the Proterozoic rocks of the Mazatzal Wilderness, but has excellent Tertiary coverage near the project area nonetheless. The map ties in nicely with the eastern boundary of this project area, along the Verde River. Here, they report, is an extensive exposure of Tertiary rocks. The area is extensively faulted, and here they find mostly Miocene Hickey Formation basalts overlying local deposits of a Miocene or older, “older conglomerate” (all pre-volcanic clasts) and one exposure of Early Proterozoic Payson granite, tilted ~20$^{o}$ to the west. These are buried under deposits of a Miocene conglomerate, rich in volcanic clasts, which are capped with younger, flat-lying basalts of Miocene age. Near the Sheep Bridge area along the Verde River, just to the east of the project area, field mapping was checked in a small, less than 1 square mile area. The field relations described above were proven to be accurate.

## MAP UNITS

Eight bedrock units were mapped in this project, ranging in age from Early Proterozoic to Late Miocene, presented here in order from oldest to youngest. The oldest units are undifferentiated metamorphic rocks and a granite batholith. These are overlain by pre-volcanic sedimentary rocks, followed by the Chalk Canyon Formation (lower volcanic-dominated section and upper limestone and tuffaceous lacustrine deposit). These units are overlain by a thick section of Hickey Formation basalt, which caps the tilted fault blocks and mesas of the area. Filling half-grabens between tilted fault-blocks, and therefore deposited in lower areas, is a sedimentary unit composed dominantly of conglomerates but with some lacustrine deposits and sandstone rock types. The youngest bedrock unit in the study area is younger basalt that overlies the young conglomerates. In the extreme eastern portion of the field area, Tertiary and Quaternary units went undifferentiated. Additionally, two Quaternary units, colluvium and alluvium, were mapped when necessary. Figure 9 presents a generalized stratigraphic column of the bedrock units. The geologic map of the project area is presented on Plate 1.

In addition to field descriptions of these units, 49 samples were collected for more detailed description, and 28 of these were selected for thin section description. The following section will provide a summary description of each unit. The first section of each description will be direct observations, while the second will be interpretive of unit name and age when possible.

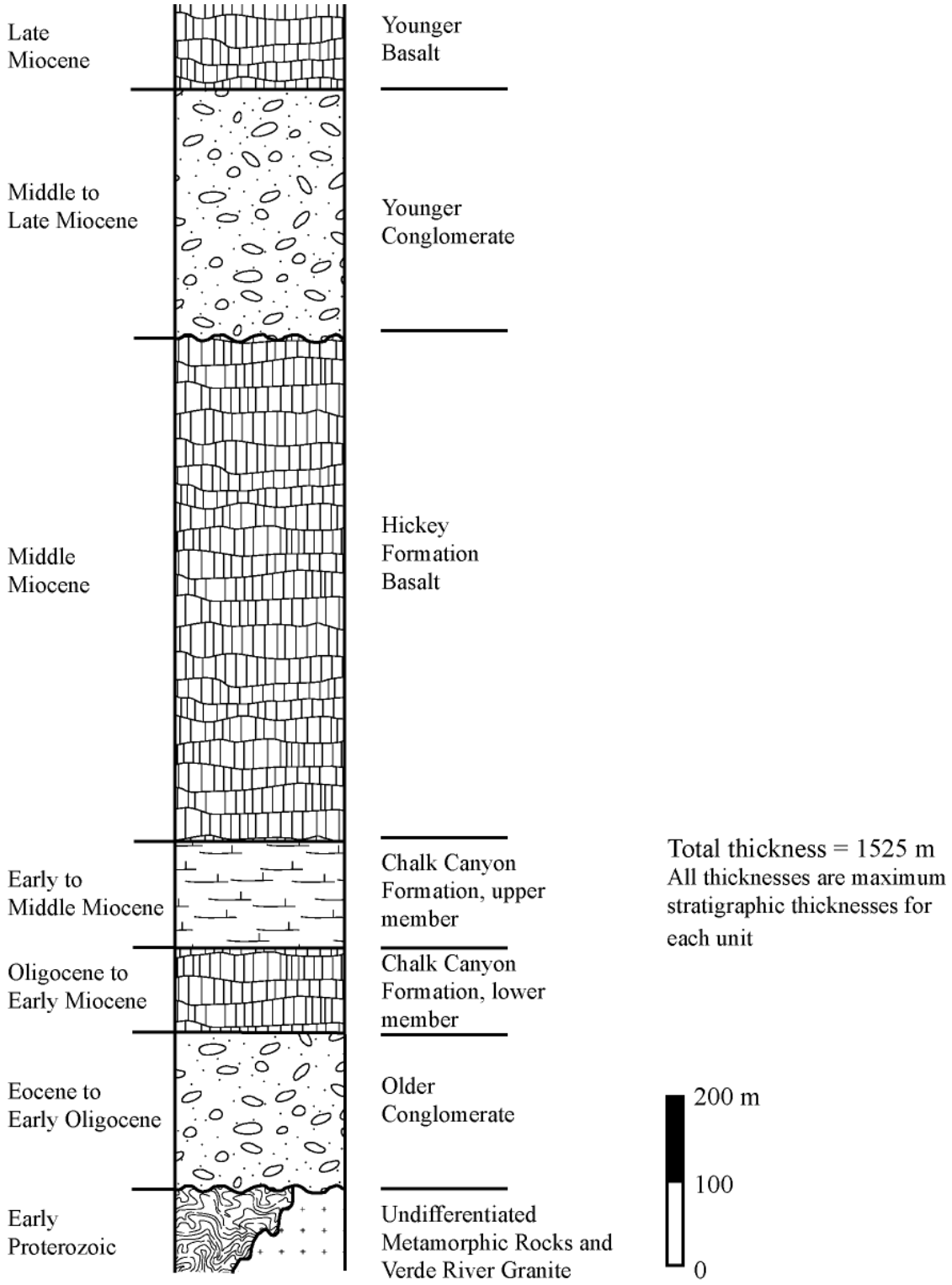


**Figure 9. Generalized stratigraphic column for the project area.**

## Early Proterozoic Units

### *Xm – Metamorphic Rocks Undifferentiated:*

This map unit is simply undifferentiated metamorphic basement. Although not differentiated for mapping purposes, this section will provide an overview of the different rock types present. The Rover Peak area (Fig. 4), in the southern portion of the mapping area (Plate 1), is dominated by a highly altered metarhyolite. This unit is coarsely crystalline, with about 30% altered feldspars (sometimes present as distinct phenocrysts). Quartz and feldspar intergrowths are common in the groundmass, with myrmekitic and granophyric textures common. Muscovite is also present in variable amounts. (Fig. 10)

Moving northward from Rover Peak and into the Cougar Canyon area in the central part of the mapping area (Plate 1), there is a collection of several varieties of slate (Fig. 11). These include several meta-sedimentary and meta-volcanic units, all with slaty cleavage. Examples are a dark, sometimes purplish, finely-laminated rock composed of fine-grained quartz, feldspars, and some muscovite. This is probably a meta-mudstone. Another example is a coarser equivalent of the previous unit. It is brown to grey in color, and appears to have a similar lithology. It is interpreted to be a meta-greywacke. The third unit found in the area is a light grey to light brown, cross-bedded unit. Beds appear to be compositionally banded, as they are alternating light and dark. The texture of the clasts appear to be angular and fragmental, indicating this may have been an explosively derived unit, such as a tuff.

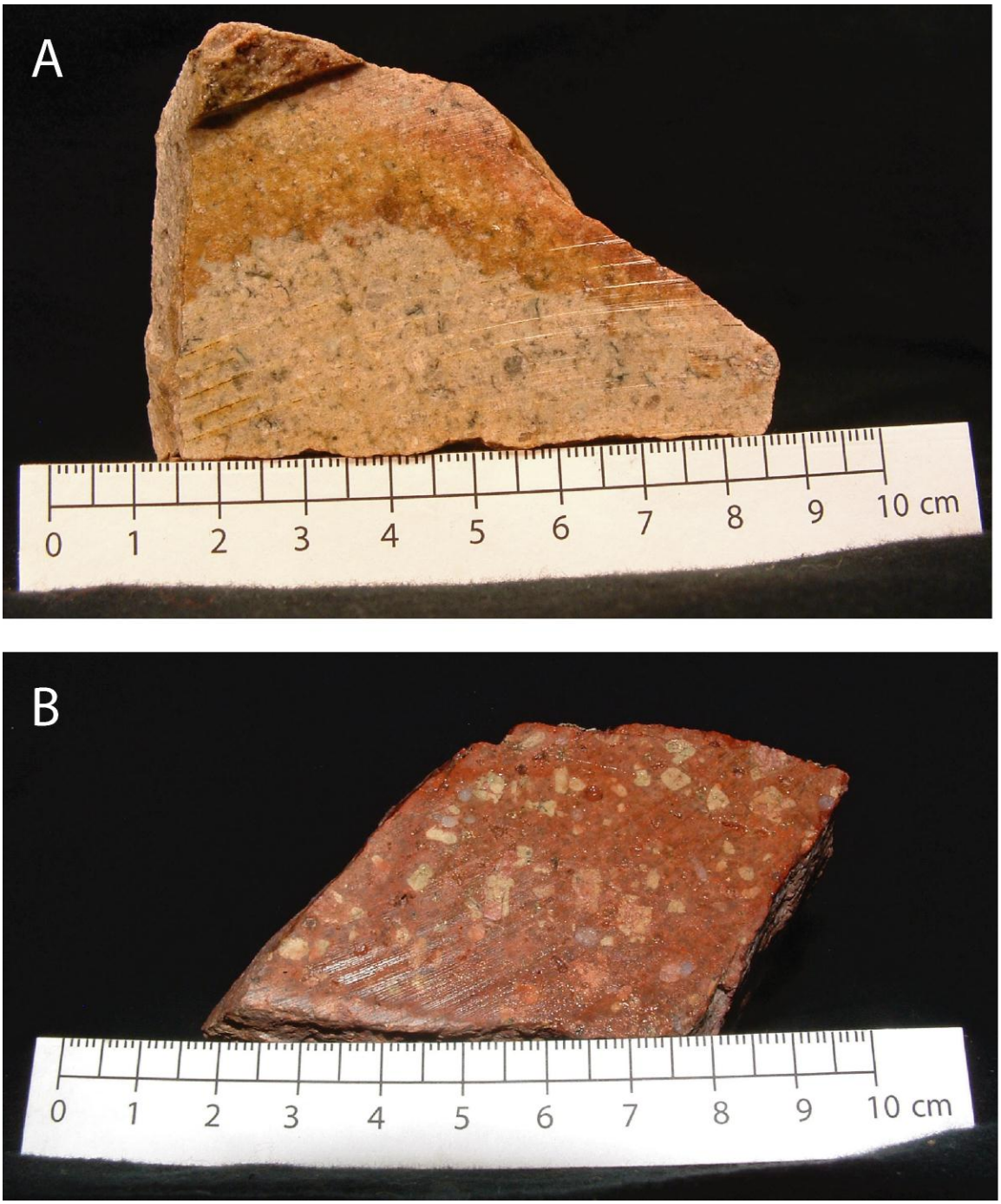


**Figure 10. Metarhyolite hand samples from the Rover Peak area. A) is coarsely crystalline variety, while B) has ~0.5 cm feldspar phenocrysts.**

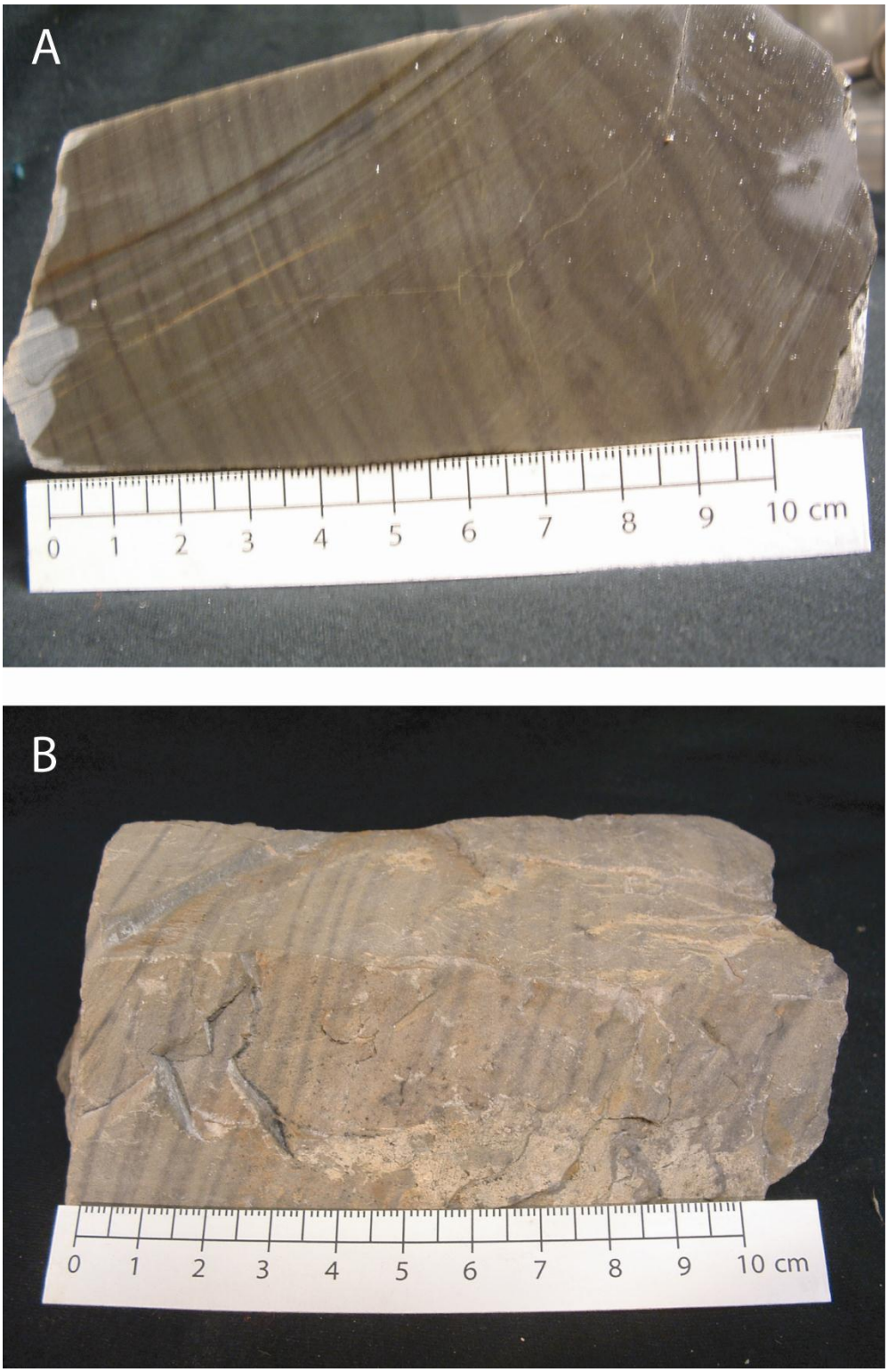


**Figure 11. Slate found to the north of the Rover Peak area. A) shows cross-bedding on a cut surface, while B) shows slaty cleavage on a weathered surface.**

In the Cooks Mesa area (Fig. 4), the basement units include schist, gneiss, and an intimately associated pegmatitic intrusion which remains undifferentiated (Figs. 12, 13). The gneiss is dark in overall color, with small bands of more felsic material, and is coarsely crystalline. The composition is dominated by quartz, muscovite, and chlorite. It is difficult to determine a protolith, but it was probably volcanic or sedimentary in origin. The schist is a highly foliated unit that is coarsely crystalline and grey to green in color. It is compositionally dominated by quartz, muscovite, chlorite, sericite, and oxides. There is also possible crenulation cleavage present. Again, a protolith is difficult to associate, but it is probably volcanic or sedimentary in origin. Finally, intermingled throughout this area there is a very coarse, felsic pegmatite. It is composed of orthoclase, quartz, muscovite, plagioclase, and variable amounts of garnet. A perthitic texture in the orthoclase is common.

The southwestern portion of the mapping area (Plate 1) has very different lithologic character. Here the rocks are dominantly more intermediate to mafic in composition, and have a high percentage of hornblende or actinolite, which could be replacing pyroxene, in addition to plagioclase. There are also smaller amounts of various opaque minerals. It appears that its protolith was most likely a diorite (Fig. 14).

The project area lies in the Proterozoic Central Volcanic Belt of Anderson (1989b). Within this region, it lies between two northeast trending shear zones, the Moores Gulch Shear Zone to the west and the Slate Creek Shear Zone to the east (Anderson, 1989b; Karlstrom et al., 1987; Wessels and Karlstrom, 1991). This relationship places the project area as part of the Tonto Basin Supergroup, which includes

**Figure 12. Typical exposure of basement in the Cooks Mesa area. A) is a field exposure of schist. B) is a close-up of the same exposure.**

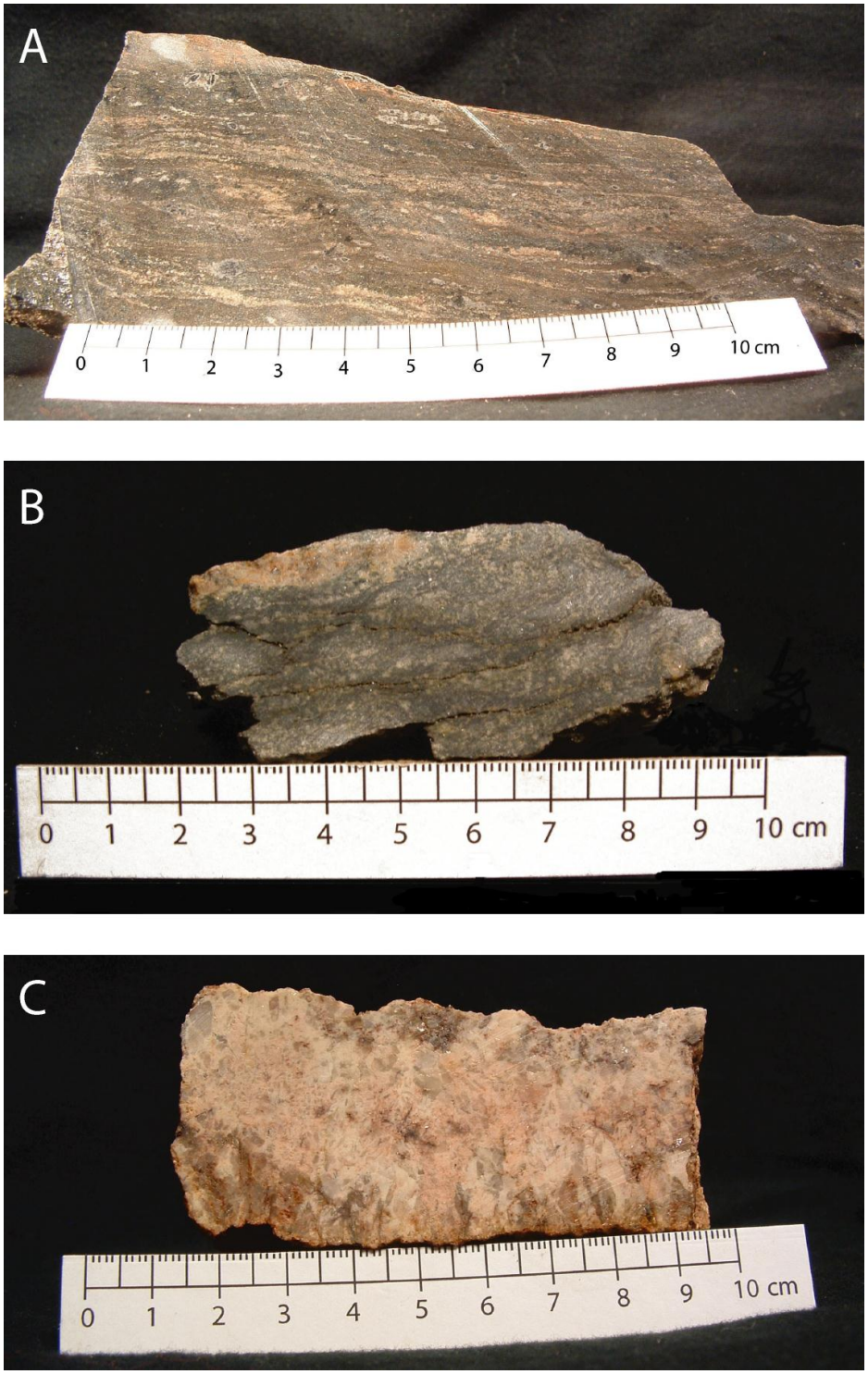


**Figure 13. Hand samples of Cooks Mesa area basement. A) gneiss, which is dark in overall color with small bands of more felsic material. B) highly foliated schist. C) coarse, felsic pegmatite.**

**Figure 14. Metadiorite hand sample from the southwestern corner of the project area.**

the Union Hills Group, Alder Group, Red Rock Group, and Mazatzal Group (Conway and Silver, 1989; Reynolds and DeWitt, 1991). This is in agreement with Leighty (1997), who noted the presence of Red Rock Group in the Rover Peak area. Unfortunately, field relations were not studied in enough detail to definitively state which members of the Tonto Basin Supergroup the metamorphic rocks described above area are correlative with.

***Xg – Granite / Verde River Granite***

This unit is characteristically pink to red color, with a coarsely crystalline texture (all less than 1cm) (Fig. 15). The mineralogy is dominantly orthoclase, quartz, and plagioclase, with variable amounts of biotite (1-10%). In the northernmost portion of East Cedar Mountain block (Plate 1), the granite is tannish brown, coarsely crystalline (0.5 – 1 cm) with slightly porphyritic texture (plagioclase phenocrysts), composed of quartz, orthoclase, plagioclase, and biotite. For mapping purposes, it remains undifferentiated. Unmapped linear bodies of plagioclase porphyry also intrude throughout. Reddish brown in color, with a porhyritic texture, it is composed of ~30 % pink plagioclase phenocrysts (0.5 – 1 cm) in a finely crystalline, brick red groundmass.

Prior to 1989, granites in the region were considered to be Payson Granite, and this nomenclature is followed on mapping near the eastern boundary of the project area by Wrucke and Conway (1987). In 1989, however, Anderson (1989b) redefined all of the granites in the project area as part of the Verde River Granite Batholith, dated at 1709 +/-

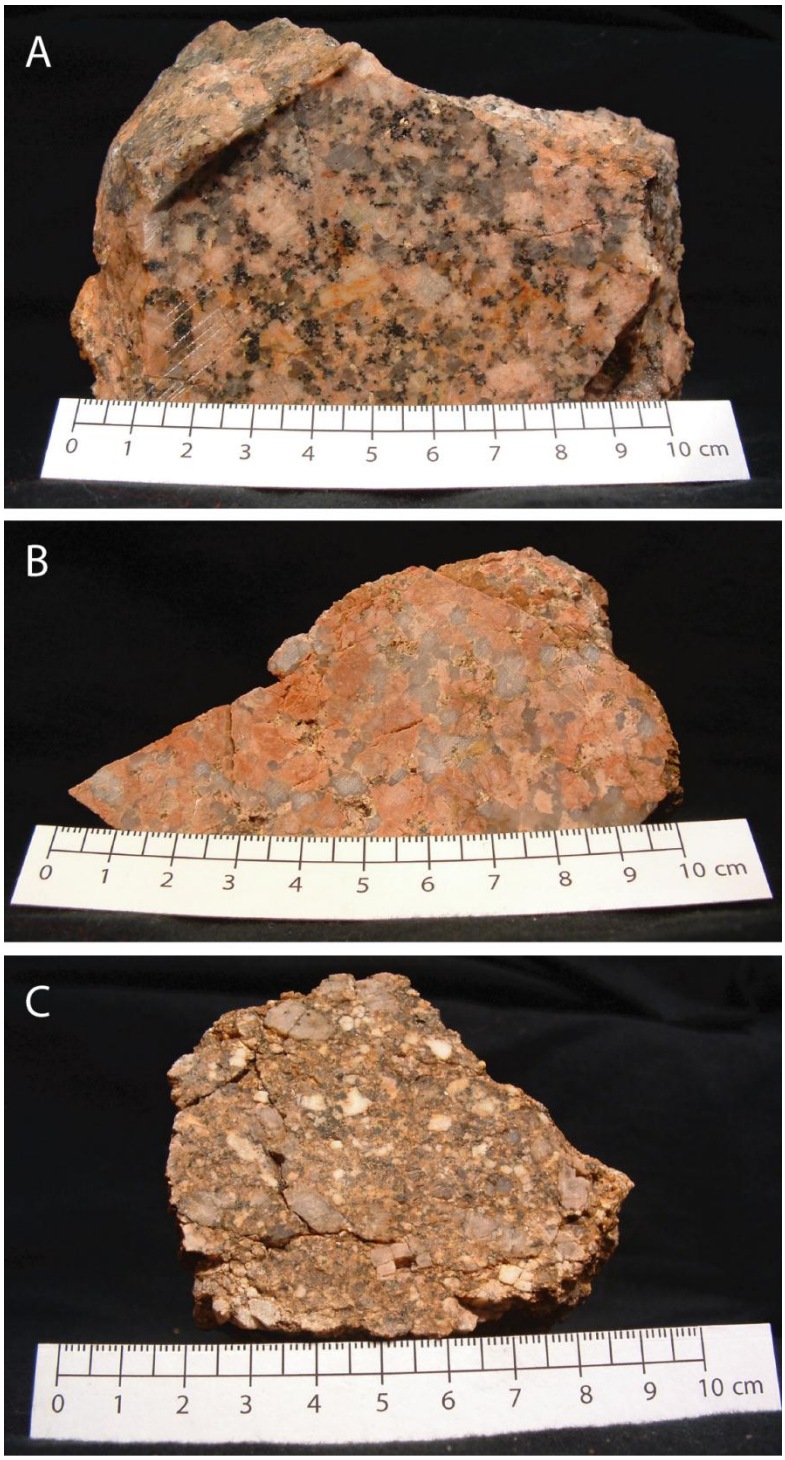


**Figure 15. Hand samples of Verde River Granite from the project area. A) is the biotite rich variety. B) is the biotite poor variety. C) is the brown granite found in the East Cedar Mountain block.**

3 Ma (Silver et al., 1986). The Verde River Granite Batholith is one of the largest plutonic bodies in central Arizona. Ferguson et al. (1999), in mapping the Horseshoe Dam quadrangle, acknowledge the granite in the area has been assigned to the Verde River Granite, but prefer and use the term Payson Granite based upon precedence of the term. Leighty (1997) considers granites in the project area to be part of the Verde River Granite Batholith. This author prefers the interpretations of Anderson and Leighty, and for the purposes of this project the granite will be referred to as the Verde River Granite. The northeast East Cedar Mountain granite may be a different granite body, but alternatively it may be a "feldspar-phenocrystic margin" of the Verde River Granite, as described by Anderson (1989b).

## Middle Proterozoic? Units

### *Yq – Quartz Dike*

This unit occurs throughout the Early Proterozoic units, and are milky white, coarsely crystalline quartz veins. The unit is only mapped in one locality where it is substantially large.

There are no real constraints on the age of this unit in the project area. One can only say the quartz dikes are younger than the Early Proterozoic they cut through, and are older than the Tertiary units which unconformably overlie it. Gilbert et al. (1998),

working in the Humboldt Mountain quadrangle to the south, have assigned quartz dikes which cut through Middle Proterozoic intrusives a Middle Proterozoic age.

## Tertiary Units

### *Toc – Older Conglomerate*

This is a reddish to orangish sedimentary unit with variable rock types. Its characteristic feature is that it is always composed entirely of detritus of basement units (Fig. 16). The most common rock types include 1) bedded granitic conglomerates: poorly sorted, clast supported, 100% granite and plagioclase porphyry clasts, rounded to subrounded, ranging from 5 – 25 cm, in a matrix of fine granitic grus (i.e. East and West Cedar Mountains area exposures); 2) non-bedded granitic conglomerates and breccias: poorly sorted, 100% granitic and plagioclase porphyry clasts, 5 cm – 50 cm clasts, angular to rounded in a coarse granitic grus (i.e. Blackjack Point area exposures); and 3) bedded granitic and metamorphic conglomerates: subangular to rounded clasts, equal mix of metamorphic rocks (slates, phyllites), granite and plagioclase porphyry clasts, 5 cm – 15 cm, sandy matrix of chiefly granitic debris (i.e. The Island area exposures). Additionally, along Cooks Mesa from just south of The Island to the southeastern corner of the map area, the unit grades upwards into a white, apparently lacustrine and tuffaceous influenced deposit at the top of the section. It is not uncommon, however, for

**Figure 16. Outcrops of the pre-volcanic conglomerate dominated by granitic clasts. This is an exposure of the non-bedded breccia variety found near Blackjack Point.**

variations of and between these end member rock types. Thicknesses of the unit can be more than 200 m, but average about 75 m in the project area (Fig. 9).

As outlined above, this unit fits the description for a unit reported by numerous workers across Arizona, throughout the Transition Zone, and perhaps even on the Colorado Plateau. In all cases, it is generally regarded as one of the oldest Tertiary units found in Arizona. In the Transition Zone, and in the general vicinity of the project area, these include the fanglomerates and conglomerates as discussed by Gomez (1979), Elston (1984), Jagiello (1987), and Leighty (1997). Elsewhere in the Basin and Range, this unit matches the description of the lower member of Unit I, as described by Eberly and Stanley (1978), which is constrained to have formed between 53 and 28-26 Ma. Wilt and Scarborough (1981) describe similar units as part of their “pre-ignimbrite” unit, and estimate the age to be 40-25 Ma. Elston and Young (1991), on the other hand, consider this unit to be correlative with the Rim Gravels of the Colorado Plateau. They constrain the age as Late Paleocene to Eocene.

In the project area, this unit can only be constrained to be younger than the post-Laramide erosion period and older than the Early Oligocene lower Chalk Canyon Formation. Based upon the lack of age constraints from the project area and the uncertainties in age described above, one can only say with confidence that the unit is of Paleogene age. For this project, the unit will be referred to as the Older Conglomerate.

***Tccl – Olivine Basalt/ Lower Chalk Canyon Formation***

An olivine basalt, it is dark gray with ~15% olivine phenocrysts completely altered to rust colored iddingsite (Fig. 17). Phenocrysts are up to 3 – 4 mm. The matrix is plagioclase, clinopyroxene, and interstitial olivine. It may have a vesicular texture (with calcitic amygdules) or have platy fractures parallel to flow. At least two flows appear to be present in the area, each overlain by < 1m of basaltic conglomerate with reworked tuffaceous beds. The total thickness of this unit averages about 100 m (Fig. 9).

This unit generally correlates with the lower Chalk Canyon Formation informally described by Gomez (1979) in the New River Mesa area to the southwest, who described the lower Chalk Canyon Formation as basalt flows separated by thin conglomerates and tuffaceous intervals, closely matching the description above. An oreodont fossil found in a lithic tuff near the base of the Chalk Canyon Formation has been determined to be of middle Early Oligocene age (~29-32 Ma) (Gomez, 1979). Additional K-Ar whole rock analysis on a basalt overlying the tuff determined an age of 22.4 +/- 2.6 Ma, or Early Miocene (Lindsay and Lundin, 1972).

***Tccu –Tuffaceous Lacustrine Limestone/ Upper Chalk Canyon Formation***

This is a bedded tuffaceous lacustrine limestone, white in color, with distinct bedding on an outcrop scale from 5-20 cm (Fig. 18). Finer laminations are found on fresh surfaces on a 0.5 cm scale. Rock types vary from low density, reworked, sand-sized

**Figure 17. Representative hand sample of the lower Chalk Canyon Formation basalt.**

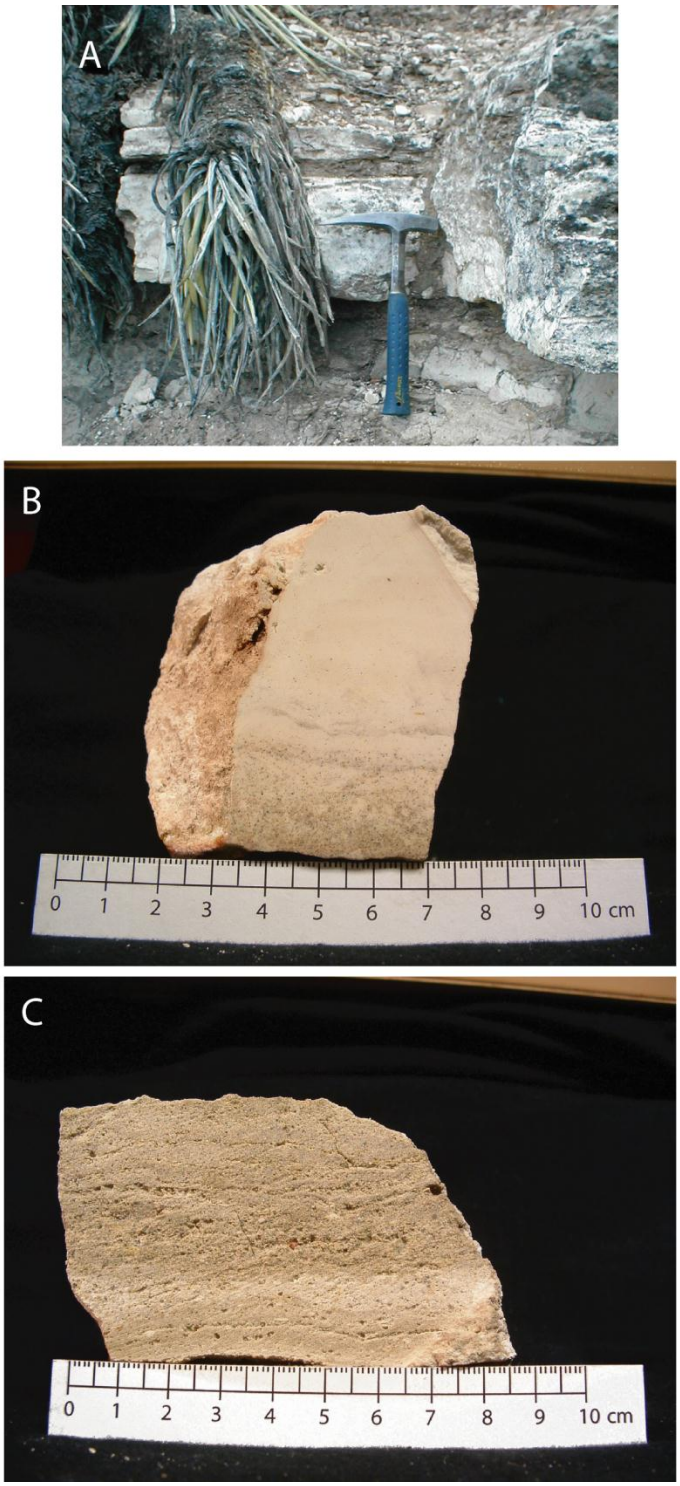


**Figure 18. The upper Chalk Canyon Formation. A) is a typical field exposure. B) is a nice fining upward sequence. C) is a tuffaceous influenced unit.**

tuffaceous material with little limestone to very fine-grained limestones containing coarse gypsum crystals. The unit fines upward from the tuffaceous layers into limestone layers. Locally present are thin basalt flows. Total thickness of the upper Chalk Canyon Formation averages about 125 m (Fig. 9).

In association with the underlying lower member, this unit clearly correlates with the upper Chalk Canyon Formation. Gomez (1979) first described the unit in the New River Mesa area to the southwest as dominated by marl, dolomite, and tuffs, with interbedded basalt flows.

***Tob – Tertiary Older Basalt/ Hickey Formation Basalt***

This unit is a thick accumulation of basalt flows (Figs. 19, 20). It is generally dark gray to black in color, but commonly weathers to brown. Phenocryst assemblage is variable, including olivine; clinopyroxene; clinopyroxene + olivine; and plagioclase + clinopyroxene. Olivine phenocrysts are commonly partially to completely altered to rust colored iddingsite. The groundmass is plagioclase with variable amounts of clinopyroxene and/or olivine. Vesicular textures are common (with calcitic amygdules), and are sometimes stretched and aligned parallel to flow. Flow banding and fractures parallel to flow are also not uncommon (this shows especially well on weathered surfaces). Ophitic and trachytic textures are also present in some flows. Hickey Formation basalts appear to have a maximum thickness of ~600 m in the area (Fig. 9).

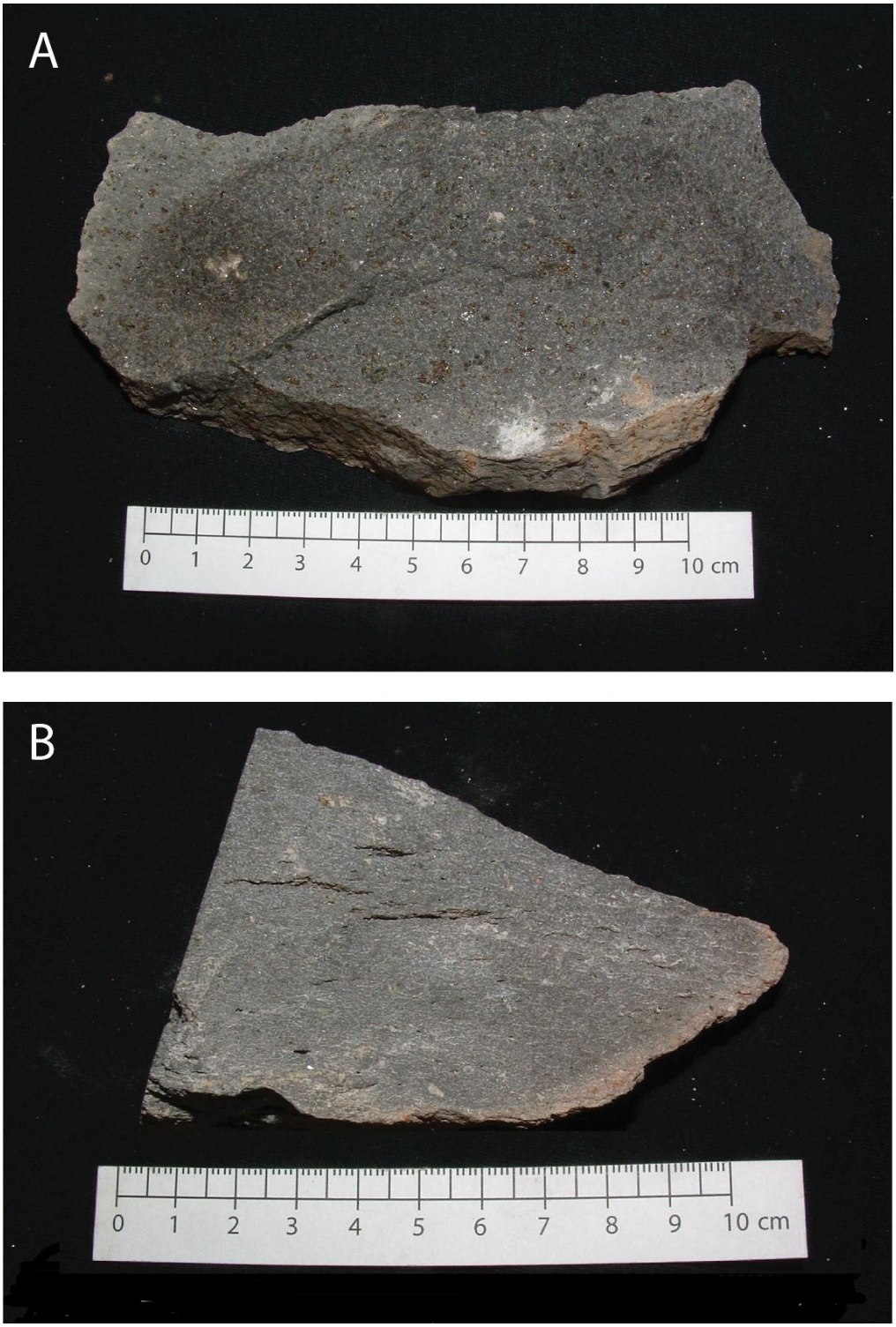


**Figure 19. Hand samples of typical Hickey Formation basalt. A) has olivine crystals completely altered to iddingsite. B) features prominent flow banding.**

**Figure 20. Typical exposure of Hickey Formation basalt in the project area. Note obvious flow banding and fractures**
**that show dip. Photograph taken looking south along the front of East Cedar Mountain.**

Basalt flows capping mesas throughout the Transition Zone are now considered to be correlative with the Hickey Formation basalts. Found throughout the Transition Zone, these rocks are the result of extensive Middle Miocene basaltic volcanism (Fig. 21). (Elston, 1984; Leighty, 1997). Elston (1984) gives an age range of 15 – 11.25 Ma, while Leighty (1997) broadens the range to 16.2 – 9.2 Ma. Maximum thicknesses for Hickey Formation basalts or correlative units have been observed to be >450 m (Leighty, 1997) to >700 m (Wrucke and Conway, 1987).

***Tyc – Younger Conglomerate***

Brown to tan in color, and poorly sorted, this unit consists almost entirely of basalt detritus, with in places up to ~5% granitic clasts (Fig. 22). Clasts vary from subangular to subrounded. Along margins of the unit clasts are generally 0.5 – 1.5 m, locally up to 3 m. Moving away from the margins, there is a fining inward progression where clasts become smaller, averaging 0.5 – 10 cm. Fanning dips within the unit are very slight, such as the incised section in Roundtree Canyon where only approximately $5^{o}$ of angular discordance occurs between beds. In other localities, flat-lying beds unconformably overlie tilted Hickey Formation basalt without any indication of fanning dips (Fig. 23). Thicknesses of the unit are highly variable, but in the Roundtree Canyon area are approximately 200 m, while in the Bloody Basin area they are estimated to be greater than 300 m (Fig. 9).

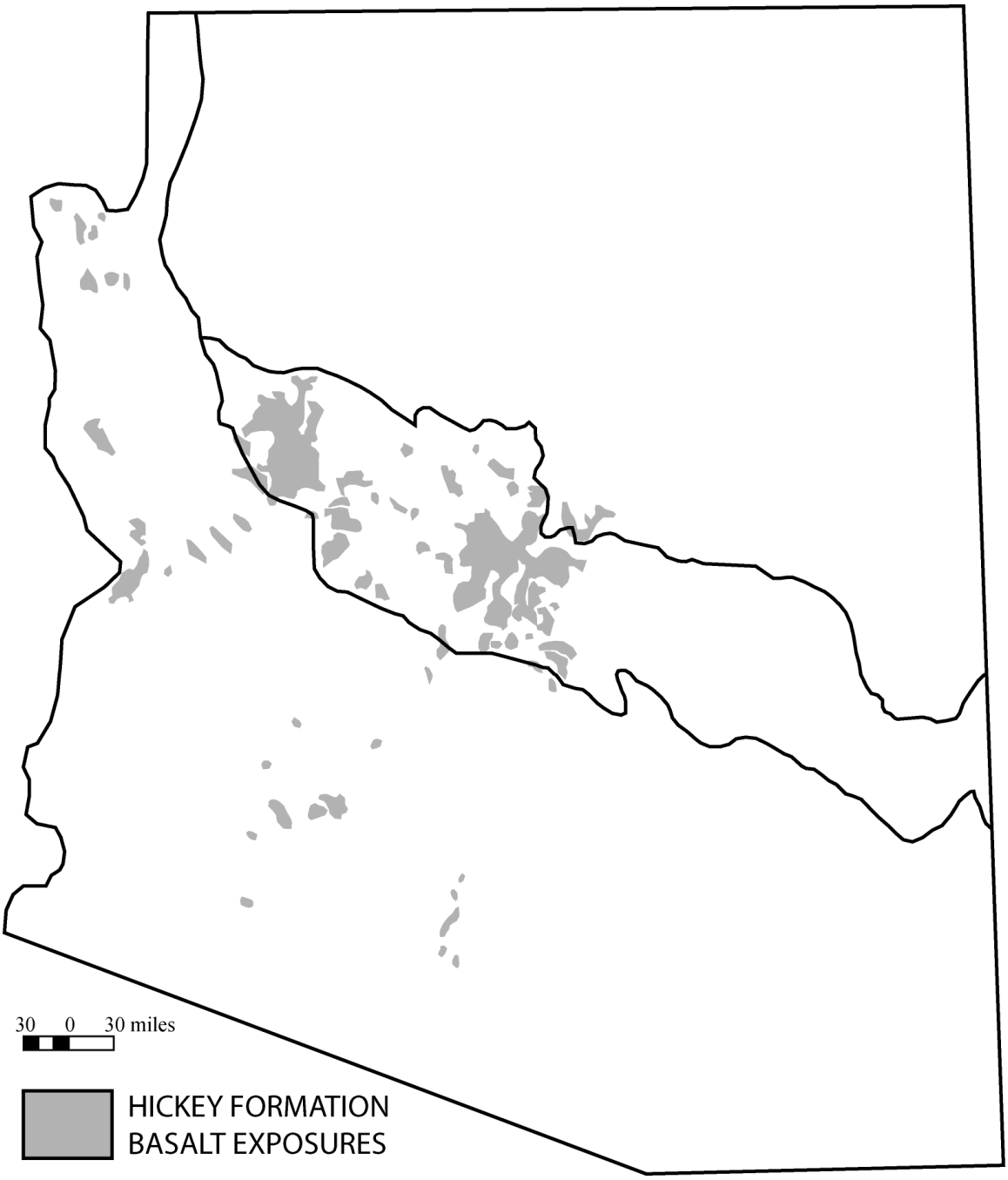


**Figure 21. Exposures of Hickey Formation basalts across Arizona (after Leighty, 1997).**

**Figure 22. Typical field exposure of younger conglomerate. Note all clasts are basalt. A) is an exposure on Lockwood Mesa. B) is an exposure in Roundtree Canyon.**

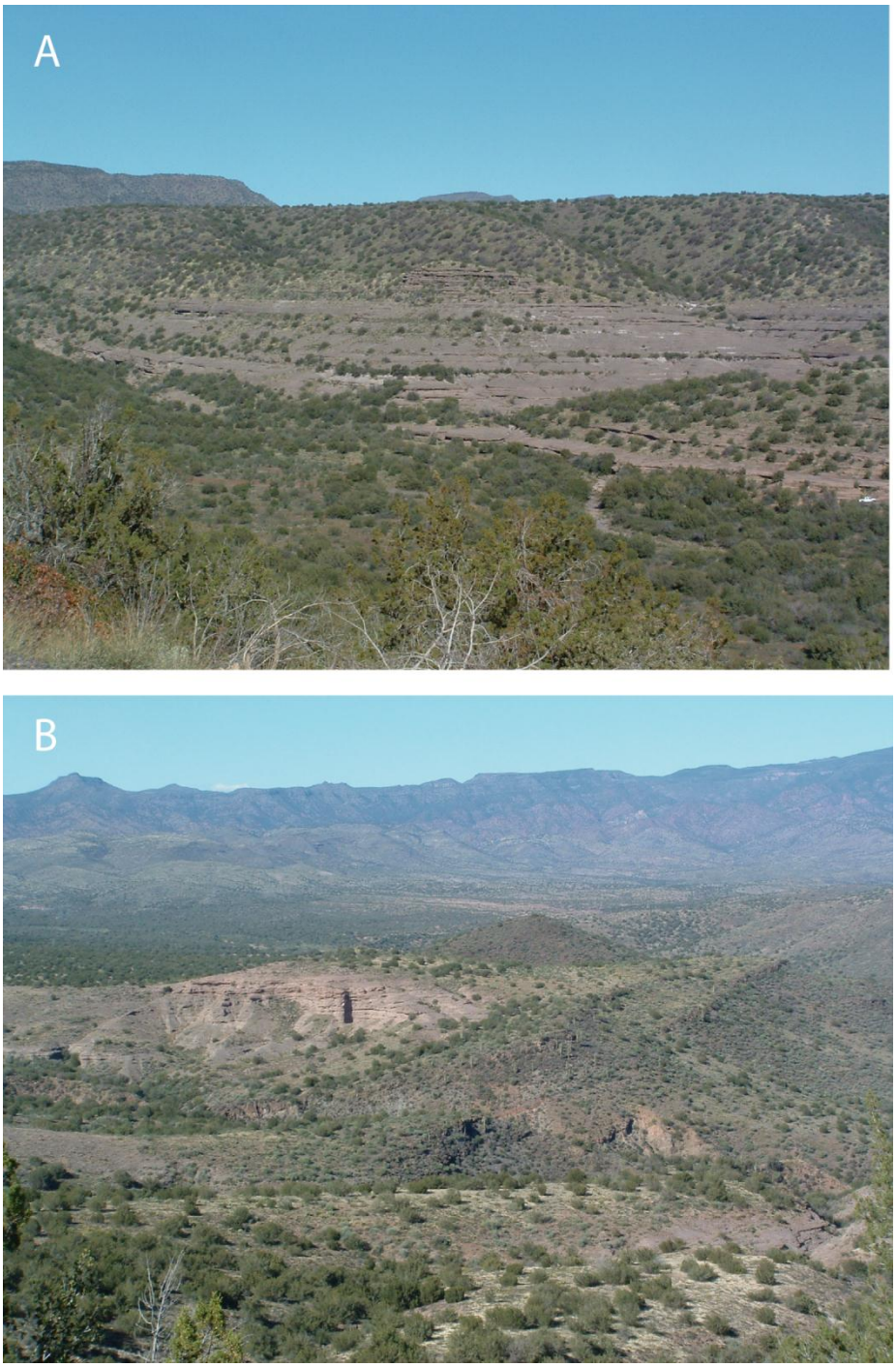


**Figure 23. Field relations of Tyc. A) shows the slightly fanning dips found in Tyc (photo is looking north from Lockwood Mesa across the Roundtree Canyon area). B) shows flat-lying Tyc overlying west-dipping basalts (photo looking north across the Bloody Basin from East Cedar Mountain).**

### *Tyb – Younger Basalt*

A black, mafic, and finely crystalline basalt. It is composed of 5-7% unaltered olivine phenocrysts (1 - 2 mm) in a plagioclase and olivine groundmass. Although any overlying units were not mapped, the unit is at least 100 m thick in the Sheep Bridge area (Fig. 9).

## Quaternary and Tertiary Units

### *QTu – Quaternary and Tertiary Units, Undivided*

QTu is undivided Quaternary and Tertiary map units along eastern border of mapping area, where the work ties into that of Wrucke and Conway (1987). These units include, but are not limited to, Hickey Formation basalts, Younger Conglomerate, Quaternary gravels, and Quaternary colluvium.

## Quaternary Units

### *Qc – Colluvium, undivided*

This unit was mapped only where completely covering bedrock relationships. It consists of poorly sorted, unconsolidated to moderately consolidated deposits found locally on hill slopes.

### *Qal – Alluvium, undivided*

Qal is poorly sorted, unconsolidated deposits of modern stream channels. It was mapped only where sufficiently large.

## FAULTS

The project area appears to be an extended corridor bounded to the west by the eastern flank of Cooks Mesa and to the east by the Mazatzal Mountains. It is dominated by north- and northwest-striking, east-dipping normal faults that form “tilt blocks” that are rotated about 15-20$^{o}$ to the west. These faults cut through all map units older than the younger conglomerates. The faults include some previously recognized in other projects, such as the Horseshoe Dam fault (Ferguson et al., 1999) and the Lime Creek fault (Gilbert et al., 1998).

The Cooks Mesa fault is the master fault in the project area (Plate 1, Fig. 24), and separates the west-dipping tilt-block domain to the east from the relatively undisturbed, flat-lying terrain to the west. The separation of rotated fault blocks to the east from unextended terrain to the west implies that the Cooks Mesa fault is a master fault that is listric at depth.

Moving southward from the northwestern edge of the map area (Plate 1) to Blackjack Point, the Cooks Mesa fault juxtaposes Early Proterozoic metamorphic rocks and Paleogene older conglomerate on the west against Hickey Formation basalt and southward, Younger Conglomerate, to the east. The transition from Hickey Formation basalt to Younger Conglomerate on the east side of the Cooks Mesa fault occurs where a fault immediately to the east of this area splays off of the Cooks Mesa fault to the north. This fault, if fault trace trends are considered, probably merges with the Cooks Mesa fault somewhere in section 29, and continues out of the project area to the north. This fault has offset in the range of 150 – 700 m, with offset increasing northward from the point of the

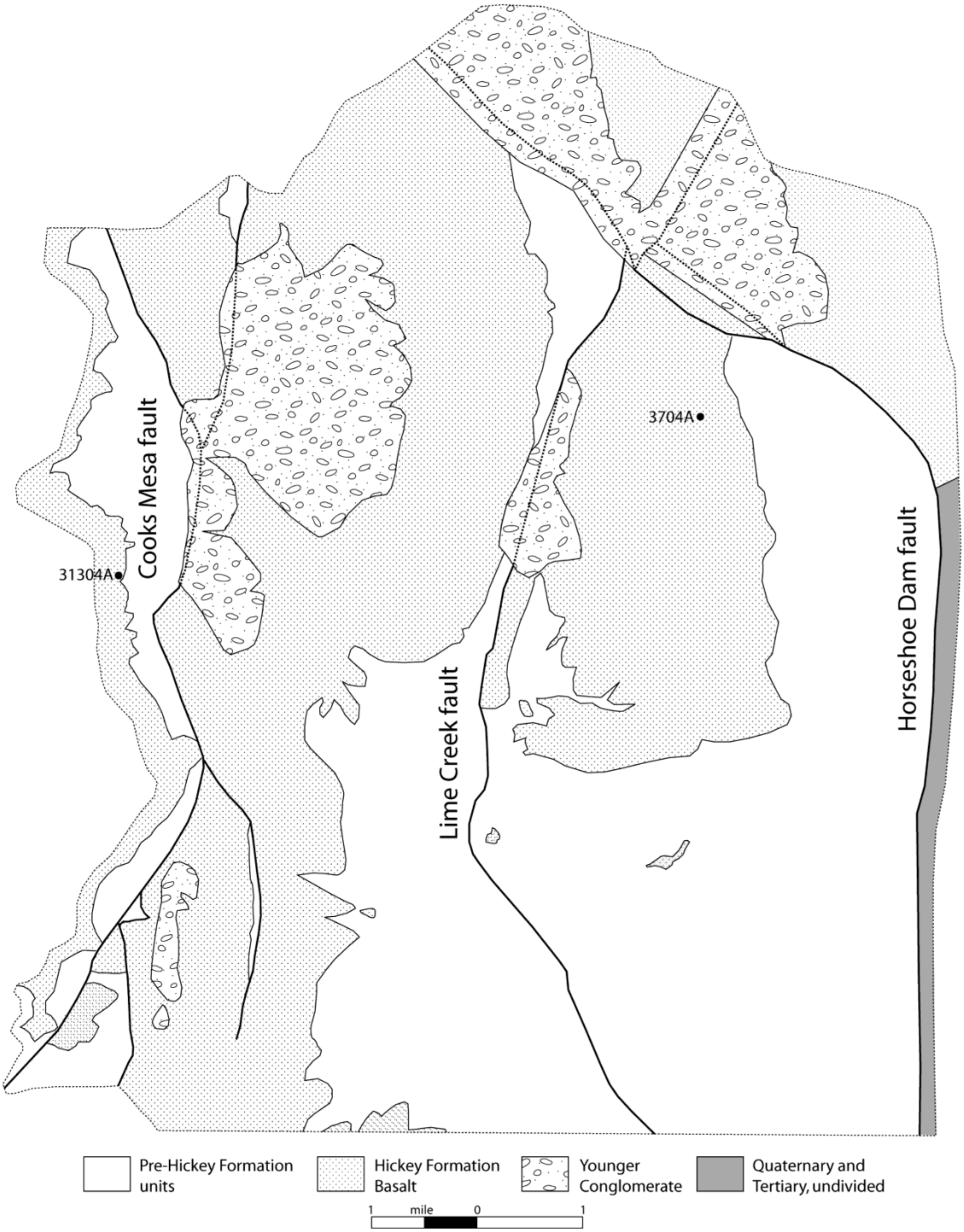


**Figure 24. Simplified geologic map of the project area showing locations of major faults and samples used for geochronology.**

splay. Where exposed, the Cooks Mesa fault is commonly expressed as a zone of basaltic breccia in a calcitic matrix that appears to be dipping ~65$^{o}$ to the east. Also, basement near the fault is commonly brecciated. Offset along the Cooks Mesa fault is variable due to accommodation of total offset along fault splays. In areas without splays, fault offset appears to be ~1500 m.

To the south of Blackjack Point, there are two southward splays from the Cooks Mesa fault (Plate 1, Fig. 24). The first is exposed as a north-striking fault in Cave Creek, which is lost in Hickey Formation basalt on Hickey Formation basalt contacts in both directions. It is probable that this fault would merge with the Cooks Mesa fault near its bend in front of Blackjack Point. The southern extent of the fault is unclear. The fault in Cave Creek appears to offset units by 250 m. The second fault splay occurs further south near The Rincon. This fault appears to continue southward out of the project area. To the west of this fault, the Cooks Mesa fault drops a small fault block without rotation. This fault splay, then, is separating the untilted domain to the west from west-dipping tilt-blocks to the east. Displacement along this fault is ~250 m.

The Horseshoe Dam fault is the easternmost fault in the area (Fig. 24, Plate 1). Along the eastern portion of the mapping area it drops undivided Quaternary and Tertiary units (QTu) to the east and places them against the Early Proterozoic Verde River Granite. Northward along the fault, it makes a northwestern bend, placing west-dipping Hickey Formation basalt against the Verde River Granite. In the northwest bend, the fault breaks into several splays which display a “stepping-down” character to the northeast. This relationship is lost where the Horseshoe Dam fault appears to cut an extension of the

Lime Creek fault (yet to be discussed). Beyond this, the Horseshoe Dam fault continues northwest, with down to the northeast movement placing Hickey Formation basalt of West Cedar Mountain against the Younger Conglomerate of the Bloody Basin, out of the mapping area, where it may merge with the fault that splays off of the Cooks Mesa fault in the northwestern part of the field area. Good exposures of this fault can be observed along Forest Road 269, where it is dipping steeply to the east. Offset along the Horseshoe Dam fault appears to be ~2000 m in the north-striking segment. Offset is ~500 to 1000 m along the northwestern striking segment.

The Lime Creek fault is the third major structure in the project area (Plate 1, Fig. 24). In the south-central portion of the mapping area the Lime Creek fault has a northwest strike. Here down to the east motion juxtaposes Chalk Canyon Formation against Early Proterozoic metamorphic rocks and the Verde River Granite to the west. There is a small paleotopographic high along this section of the fault, resulting in metamorphic on metamorphic fault contact. Moving northward, the Lime Creek fault continues into Long Canyon between East and West Cedar Mountains, and takes on a more north-south strike. Here the fault places west-dipping Hickey Formation basalts to the east against Verde River Granite and Older Conglomerate to the west. The fault is cut by the northwestern extension of the Horseshoe Dam fault, but the continuation of the Long Canyon fault projects out of the study area to the north-northeast. The Lime Creek fault has between 1000 to 1500 m of offset.

## FIELD RELATIONS

The Paleogene Older Conglomerate (Toc) lies unconformably on an exhumed Early Proterozoic bedrock surface. This is best exemplified by the angular unconformities where steeply dipping metamorphic foliation is overlain by flat or gently tilted Toc (Plate 2). Additionally, unit Toc is composed of materials derived from the underlying bedrock, indicating erosion of bedrock units before deposition of Toc. Unit Toc has variable thicknesses (Plate 2), such as in the West Cedar Mountain block, where it pinches out from a thickness of ~ 200 m as one moves southward. These types of relationships are found throughout the field area and indicate that these units were deposited in an environment with a fair amount of relief prior to deposition, locally demonstrated to be as much as 200 m as described above. This indicates that local bedrock highs were the source areas, shedding sediments into local basins.

Significant paleotopography is expressed in relationships between basement and Chalk Canyon Formation and Hickey Formation basalts as well. Bedrock highs are encountered protruding through the Chalk Canyon Formation in the southern portion of the mapping area, causing it to pinch out against the undifferentiated metamorphic rocks (Plate 2; E-E'). This indicates >300 m of relief. There is also evidence of steep paleotopography between the basement and Hickey Formation basalts in the form of a ~50 m escarpment (Plate 2; D-D'), which is covered by Hickey Formation basalts, to the south of Cougar Canyon and east of Blackjack Point near the high point at 4821 ft (Plate 1). Throughout the project area, however, the paleotopography on the surface, which Hickey Formation basalts flowed across, is generally not as steep. For example, gentler

slopes are present along the front of East Cedar Mountain, where ~75 m of this relief occurs.

The lower Chalk Canyon Formation overlies Toc in Lime Creek near the southern portion of the map area (Plate 1). This is a conformable contact, and there are even thin interbeds of granitic clast-rich Toc interbedded with the lower Chalk Canyon Formation basalts.

Hickey Formation basalt directly overlies Toc or Chalk Canyon Formation, and where neither is present, sits directly on Early Proterozoic basement (Plate 2). Despite the evidence for Hickey Formation basalt encountering paleotopography, as discussed above, it appears that the basalt completely flooded the entire region, covering all bedrock highs in the project area.

Tertiary Younger Conglomerate (Tyc) unconformably overlies Hickey Formation basalts, and where immediately adjacent to faults onlaps onto various older units (Plate 2). The unit displays only slightly fanning dips. This is best exemplified in the incised Tyc outcrops in Roundtree Canyon, where only ~5$^{o}$ of angular discordance is exposed within the Younger Conglomerate. Unit Tyc is found in topographically low areas between tilted fault blocks, and where present obscures true fault exposures.

Younger Basalts overlie Tyc in the Sheep Bridge area along the Verde River, just to the east of the project area. Field relations, as mapped by Wrucke and Conway (1987) (Fig. 25), were checked in the field and proven to be correct. A lower basalt (Hickey Formation), tilted ~15$^{o}$ to the west-southwest, is unconformably overlain by a deposit of the Tyc, which is flat-lying, which is capped by a younger, flat-lying basalt.

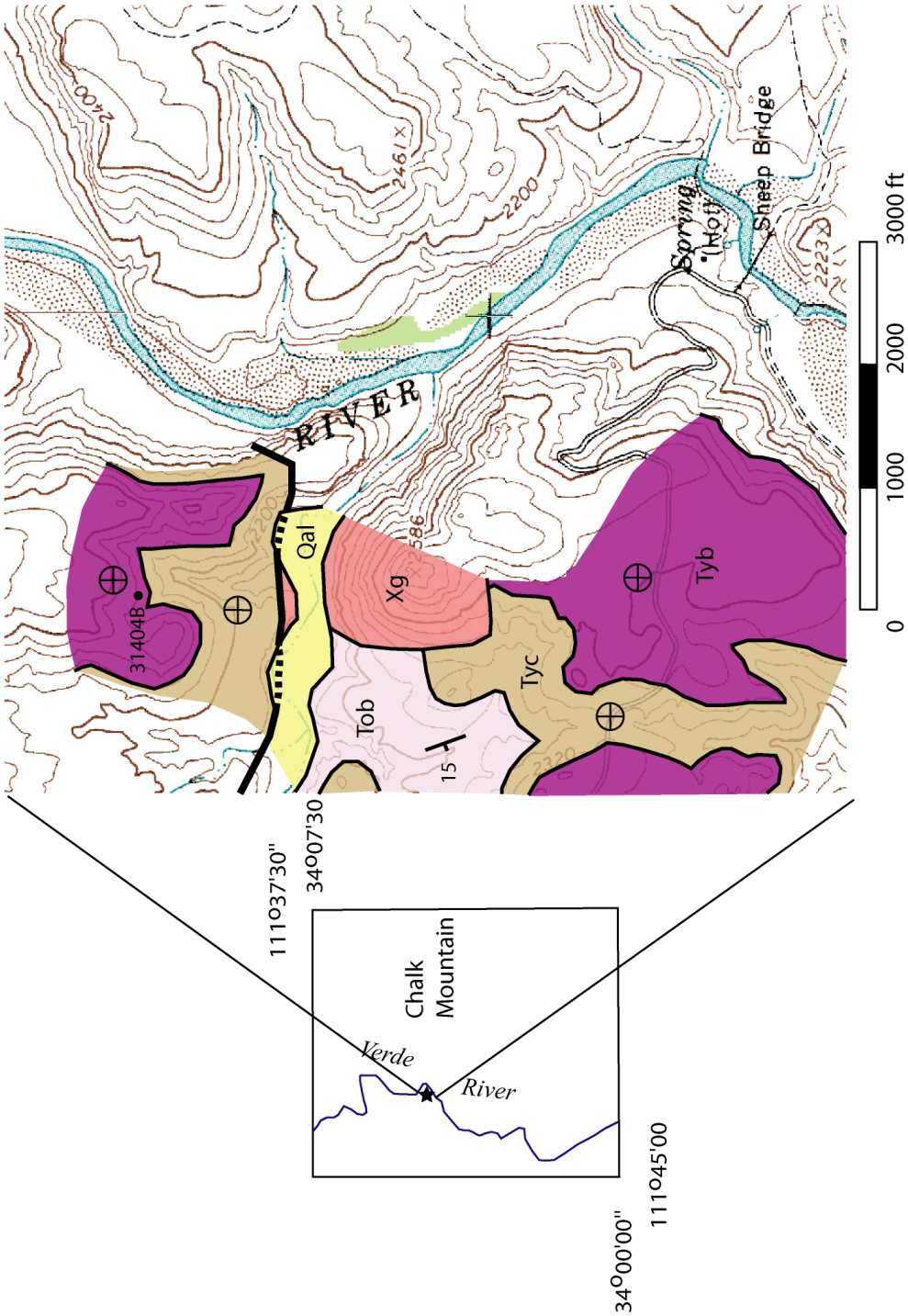


**Figure 25. Geologic map of the Sheep Bridge area (after Wrucke and Conway, 1987). Here, tilted Hickey Formation basalt (Tob)is unconformably overlain by flat-lying younger conglomerate (Tyc), which is capped by younger basalt (Tyb). See Plate 3 for complete explanation and text for unit descriptions. Star on Chalk Mountain 7.5' quadrangle depicts location of the map.**

## GEOCHRONOLOGY

Three basalt samples were selected for dating in order to constrain the timing of tilting and extension in the project area. This work was performed by Lisa Peters at the New Mexico Geochronology Research Laboratory (NMGRL). $^{40}Ar/^{39}Ar$ analyses were performed on groundmass concentrates of each sample. Sample 31304A was collected at the base of the Hickey Formation basalt on Cooks Mesa (Plate 1; Fig. 24). Sample 3704A was collected at the top of East Cedar Mountain and represents some of the stratigraphically highest Hickey Formation basalt in the project area (Plate 1; Fig. 24). Sample 31404B was collected at the base of the Younger Basalt found in the Sheep Bridge area (Fig. 25).

The results of the analysis are presented in Table 1. Hickey Formation basalt sample 31304A had a slightly disturbed spectrum which yielded a weighted mean age of 15.14 ± 0.13 Ma (Fig. 26). The upper Hickey Formation basalt sample, 30704A, had a well behaved spectrum that yielded a weighted mean age of 13.53 ± 0.14 Ma (Fig. 27). The younger basalt sample 31404B had a very disturbed spectrum which yielded a weighted mean age of 6.4 ± 1.3 Ma (Fig. 28). Additional information on analytical procedure and data can be found in Appendices A and B

The weighted mean ages assigned to 3704A groundmass concentrate (13.53±0.14 Ma) and 31304A groundmass concentrate (15.14±0.13 Ma) provide precise, reliable eruption ages for the basalts. Although its petrographic analysis showed no evidence of alteration, the low radiogenic yields and disturbed age spectrum for 31304B groundmass concentrate are strongly suggestive of alteration and perhaps recoil of $^{39}Ar$ (loss of $^{39}Ar$

from the higher K phases to the lower K phases during irradiation). The weighted mean age calculated for steps B-I (6.4±1.3 Ma) is the best estimate of the eruption age of 31304B, but confidence in this date is not high.

TABLE 1. $^{40}Ar$-$^{39}Ar$ ANALYTICAL RESULTS

| Sample | Unit | Location | Phase | Age (Ma)±2σ | Comments |
|---|---|---|---|---|---|
| 3704A | Hickey Formation Basalt, base of Cooks Mesa | lat: 34°6.03' long: 111°47.22' | Groundmass Concentrate | 13.53±0.14 | Well-behaved spectrum |
| 31304A | Hickey Formation Basalt, top of East Cedar Mountain | lat: 34°4.59' long: 111°52.96' | Groundmass Concentrate | 15.14±0.13 | Slightly disturbed spectrum |
| 31404B | Younger Basalt, base near Sheep Bridge | lat: 34°5.47' long: 111°42.99' | Groundmass Concentrate | 6.4±1.3 | Integrated age, disturbed spectrum |

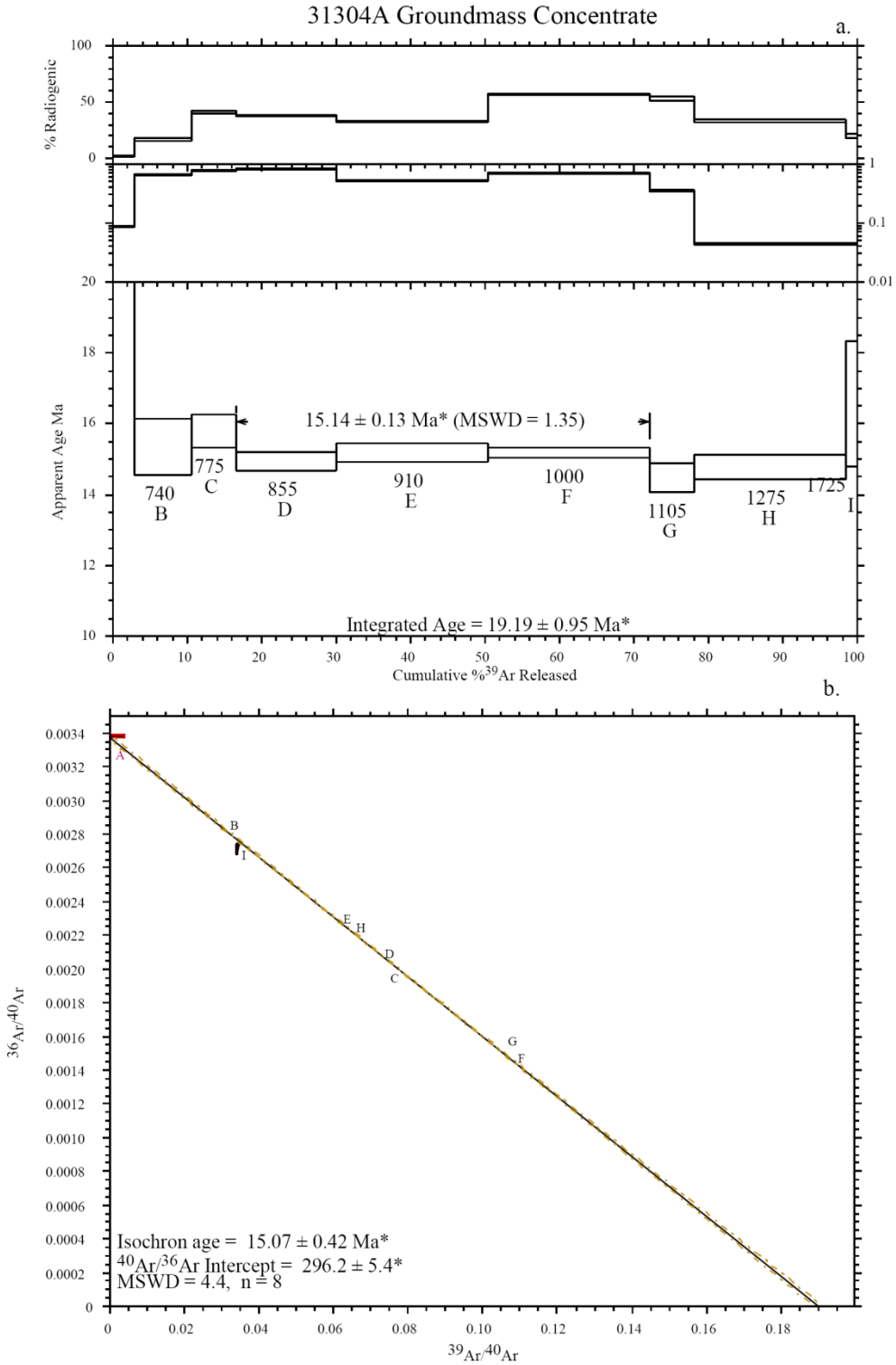


**Figure 27. Age spectrum (a) and isochron plot (b) for 31304A groundmass concentrate.**

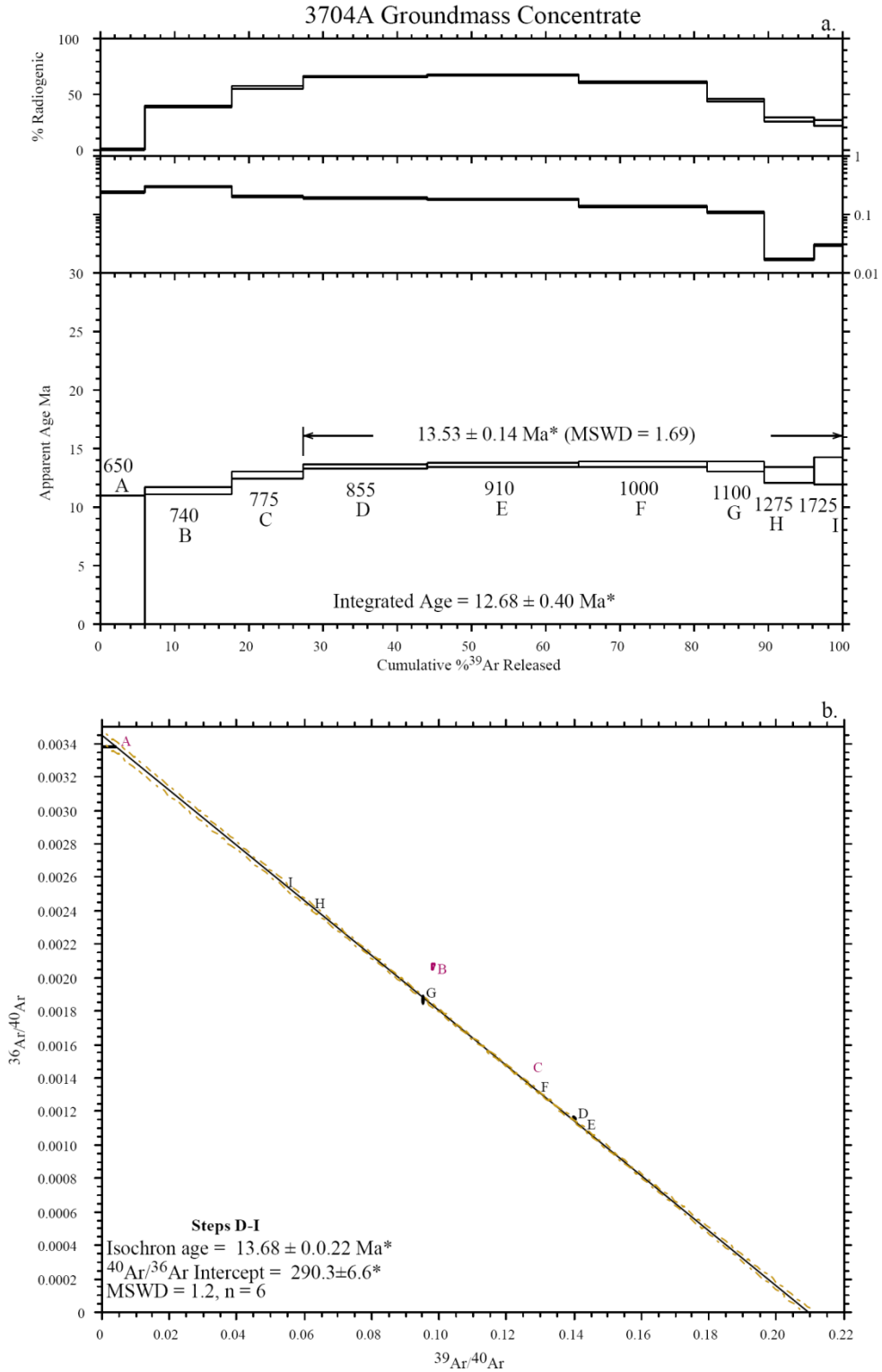


**Figure 28. Age spectrum (a) and isochron plot (b) for 3704A groundmass concentrate.**

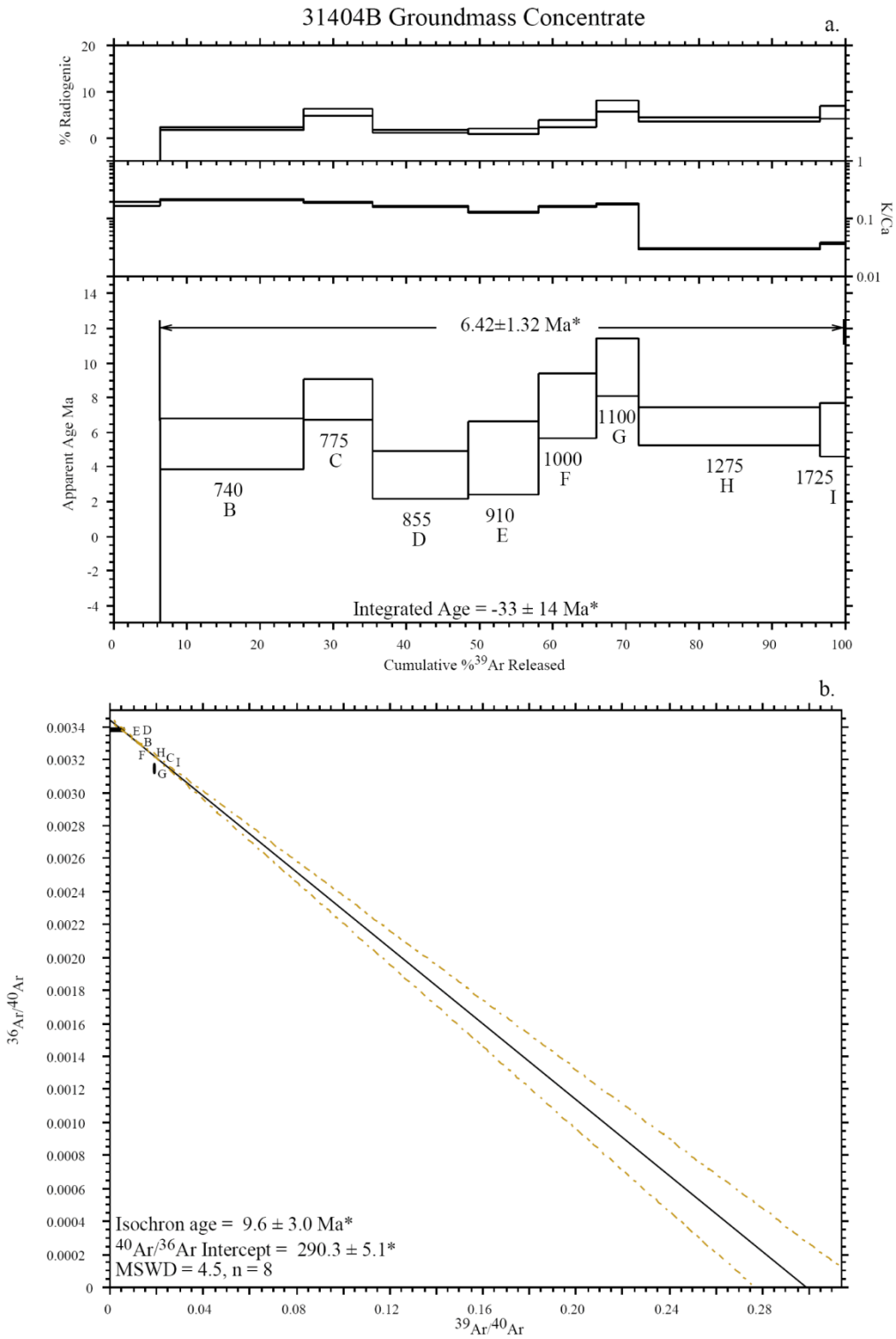


**Figure 26. Age spectrum (a) and isochron plot (b) for 31404B groundmass concentrate.**

## INTERPRETATIONS OF FIELD RELATIONS

### Older Conglomerate/Basement

The depositional environment of the Tertiary Older Conglomerate (Toc) appears to be small, localized basins deriving sediment from nearby sources. The unit is derived from mostly Verde River Granite and greater or lesser amounts of Early Proterozoic metamorphic rocks exposed in the area. The sedimentary characteristics of this unit and lithologic variability within the unit indicate that the basins were small and localized, with little transport. Given the amount of paleotopography throughout the project area, this is not surprising.

The question remains as to the nature of these basins. Were these merely erosionally created topographical basins, or were these created by something else, such as an episode of faulting? Nowhere in the field area do relations show definitive evidence for fault-created basins. The nature of the unit in the project area is to pinch out along moderate to gentle slopes. High-angle terminations of the unit, indicative of fault bounded basins, are absent. Eberly and Stanley (1978) suggest their correlative Unit I was deposited in interiorly drained basins, without any suggestion of tectonism. Elston and Young (1991) also suggest that these units were deposited on an eroded, regional bedrock surface with considerable paleotopography. Working closer to the project area, Gomez (1979) and Elston (1984) suggest that deposition of this unit occurred in topographic lows after an episode of regional uplift. On the other hand, Leighty (1997) suggests a fault-related origin based upon large clast size and local provenance. One

certainly cannot rule out an older period of extension, but field relations in the project area do not exhibit strong evidence for this.

**Chalk Canyon Formation**

The small areal extent of the Chalk Canyon Formation in the project area indicates that is must have been deposited in a small localized basin. It seems probable that this was a fault-created basin, not merely topographic, as the placement of the unit does not match those of the redbed basins. In fact, Chalk Canyon Formation is even placed directly on areas that appear to have been source areas for redbeds, or what were previously highlands. It seems more likely that the fault was probably an older expression of the Lime Creek fault, as the unit is thickest where directly adjacent to the modern Lime Creek fault, and pinches out to the east. Additionally, the unit does not exist to the west of the modern Lime Creek fault. The unit does not appear to have fanning dips, however, so fault motion must have completely pre-dated deposition of the Chalk Canyon Formation in a stable environment.

Timing of faulting may have began as early as the time of deposition of the basal tuff found in the New River Mesa area to the southwest (32-29 Ma) (Gomez, 1979), but must have predated the deposition of the ~22 Ma basalts (Lindsay and Lundin, 1972) and the tuffaceous lacustrine beds. The Chalk Canyon Formation does not display fanning dips, indicating their deposition must completely post-date faulting. These relationships

can bracket faulting between 32 to 22 Ma. This timing is contemporaneous with extension during the mid-Tertiary orogeny in Arizona, and faulting here may be related.

The basalt which dominates the lower member may be related to this extensional setting, while interbedded tuffs may be associated with explosive, silicic volcanic centers found throughout Arizona at this time (i.e. Chiricahuas, Superstitions) (Damon et al., 1984). The tuffaceous/lacustrine upper member represents a more stable environment that followed where the fault-bounded basin would have produced ponded conditions.

One interesting aspect when considering the Chalk Canyon Formation is the apparent absence of underlying Older Conglomerate (Toc) to the east of the Lime Creek fault, while it is present on the west side (Plate 2; C-C'). This is an unexpected situation if one considers that after motion along the paleo-Lime Creek fault the upthrown western-side should have been subject to erosion of Toc while on the down-dropped eastern side Toc would have been buried and preserved, exactly the reverse of what is observed. There are several possible explanations for this, including 1) the paleo-Lime Creek fault is a reactivated Laramide reverse fault, with uplift of the eastern side and removal of Toc during continued Toc deposition to the west, prior to normal motion along the paleo-Lime Creek fault, or 2) the coincidence of the eastward pinch-out of Toc due to paleotopography with the paleo-Lime Creek fault.

**Hickey Formation Basalt**

Field evidence indicates that Hickey Formation basalts flowed over a surface of at least some relief, as there are islands of Early Proterozoic basement sticking out above Toc and Chalk Canyon Formation, and there are relations of basalts encountering paleohills and cliffs. It does seem, however, that most of the paleotopography in the area had been eliminated by the time of Hickey Basalt volcanism, either through erosion, infilling of local basins with either Older Conglomerate or Chalk Canyon Formation, or a combination of both. There is no evidence that Hickey Formation basalts encountered any topographic barriers as they crossed the current location of the Lime Creek fault, indicating that Chalk Canyon Formation had probably filled all the accommodation space created in the small basin created by earlier movement along a "paleo Lime Creek fault". This suggests ~225 m of relief along this paleo-fault (as determined by the thickness of the Chalk Canyon Formation).

It is clear from relations in the field area that Miocene extension and tilting post-date Hickey Formation basalts, and that prior to extension the Hickey Formation basalts must have covered the entire project area. If one considers the adjacent mapping (discussed in the Previous Work section), and considers that the type locality of Hickey Formation is in the Black Hills area to the north (Anderson and Creasy, 1958), it is evident that the Hickey Formation basalts and equivalents must have covered a large portion of the central Arizona Transition Zone during the Middle Miocene. In the project

area, dating indicates that the Hickey Formation basalts accumulated between 15.1 and 13.5 Ma.

**Younger Conglomerate**

This unit unconformably overlies the Hickey Formation basalts and is deposited in half-grabens between tilt-blocks. It displays only slightly fanning dips (Fig. 23), and appears to be in primary sedimentary, rather than faulted, contact with the footwall blocks. It therefore must be a late syn- to post-extensional phase unit. Timing of this unit can be constrained to be between 13.5 and 6.4 Ma.

**Younger Basalt**

Just outside the field area, this unit overlies the late syn- to post- extensional Younger Conglomerate. The unit is not tilted and must post-date the period of fault block rotation. Dating of this sample can therefore provide an upper constraint on the timing of the tilting. In the project area, $^{40}Ar$-$^{39}Ar$ dating indicates the unit is ~6.4 Ma. The age of the younger basalt indicates that its eruption is synchronous with that of the 'Ramp basalts' (8.1 to 6.0 Ma) exposed along I-17. The Ramp basalts were erupted on the Colorado Plateau, and then flowed over the Mogollon escarpment and into the Verde Valley (Leighty, 1998; Peirce and Nations, 1986).

## TILTING AND EXTENSION

### Timing

$^{40}Ar$-$^{39}Ar$ dating from this project brackets the tilting to have occurred between 13.5 and 5-8 Ma, as there is low confidence in the younger age of 6.4 Ma. The period of extension and rotation of fault blocks in the project area is thus synchronous with timing of the Basin and Range disturbance in Arizona. Northwest-striking faults in the northwestern portion of the project area and in adjacent mapping immediately to the east appear to have undergone motion which offsets younger basalts, indicating faulting occurred after 5-8 Ma. This relationship will be discussed in greater detail in a subsequent section.

### Fault Patterns

North and northwest fault strikes form rhomb-shaped fault blocks throughout the project area (Plate 1). Field relations suggest that the fault systems developed contemporaneously during extension, rather than as two separate generations of faulting, and this is in agreement with Leighty (1997), who noted that the evolution of the north and northwest striking faults in the project area is linked in an extensional continuum, rather than as the result of separate events. This relationship is best exemplified where faults bend from one orientation to another, such as the Lime Creek fault and Horseshoe Dam fault (Plate 1). This relationship is in contrast to the idealized continental rift setting,

where one would expect to find parallel normal faults striking perpendicular to the extension direction. This section will address this issue.

Investigation of the literature reveals that these gridded, intersecting fault patterns, which create rhomb shaped fault blocks, have been noted throughout the Basin and Range province (Thompson and Burke, 1974; Scarborough and Peirce, 1978; Menges and Pearthree, 1989). Additionally, they have been found to be a feature of many other continental rift areas including the late Cenozoic Rio Grande Rift and the Paleozoic Oslo graben in Norway (Ramberg and Smithson, 1975; Thompson and Burke, 1974). Several hypotheses have been put forth to explain this feature. Keith and Wilt (1985) suggest that Basin and Range province rhomb-shaped basins opened as strike-slip – associated pull-apart structures. Significant strike-slip motion along basin boundaries, parallel to the extension direction, is invoked as the cause. The main competing theory is simply that extensional faulting patterns are controlled by reactivation of older structures or other pre-existing lineaments in the basement (Ramberg et al., 1978; Scarborough and Peirce, 1978).

Field investigation of the project area found no evidence for any strike-slip motion along faults, and it seems highly unlikely that the theory of Keith and Wilt (1985) is responsible for the rhomb-shaped fault patterns in the area. Additionally, as described in the regional geologic framework, the generally accepted model of Basin and Range disturbance extension does not call for any significant strike-slip motion as a cause.

It is possible that the rhomb-shaped pattern of faulting in the area is directly controlled by older structures, but there is a lack of direct evidence for this in the project

area. In this case, one could consider that the north-south striking faults must represent primary fracture in response to east-west directed extension, while the northwest-striking faults probably would be controlled by reactivation of pre-existing structures. Elston and Young (1991) report that many faults in Arizona have experienced several episodes of reactivation, although they fail to mention specific localities or evidence. They state that these structures have their origin in Precambrian tectonic episodes, then have been subjected to two or more Laramide compressional episodes, and finally were reactivated during Neogene extensional faulting. Structural trends in Proterozoic rocks, however, tend to be north to northeast (Karlstrom et al., 1987) rather than northwest. McKee and Anderson (1971) state, without putting forth evidence, that the northwest striking Verde fault underwent over 300 m of motion during the Proterozoic. In this area, though, penetrative F1 folds trend north-northwest, potentially providing the structural grain for the Verde fault (Lindberg, 1989). Overall, concrete evidence for northwest-trending structures of Proterozoic age is vague, and one cannot say with any certainty that northwest-striking faults in the project area have any Proterozoic origins. Laramide contraction, on the other hand, has been documented to have resulted in a dominant northwest-trending structural grain across Arizona (Coney, 1976). Additionally, Laramide reverse faults have been reported at several localities to have been reactivated in the Tertiary as extensional normal faults. These are the north-striking Canyon Creek and Cherry Creek fault zones and the northwest-striking Verde Fault in central Arizona (Potochnik, 2001; Lindberg, 1989; Faulds, 1988; Young et al., 1987). In the project area, however, there are no Laramide structures reported, nor is evidence found for any. Unless

there are undetected, northwest-trending Laramide structures within the project area, it seems unlikely that reactivation of northwest-trending Laramide structures in the project area, in concert with north-south striking faults related to east-west extension, is the cause of the rhomb-shaped fault blocks.

In this particular case, it seems the most probable explanation for the north and northwest strikes of faults in the project area is the interaction of stress fields in the Transition Zone. This can be seen if one considers measurements of both the modern- and paleo-stress fields in the Basin and Range province and along the margin of the Colorado Plateau in Arizona. Modern stress fields can be considered because their orientations are essentially the same as those which acted to form the modern physiography of Arizona.

In the Basin and Range province, the orientation of the extension direction varies according to author, but generally is considered to have been directed east-west. Thompson and Burke (1974) report that crustal extension was oriented roughly west-northwest to east-southeast. Thompson and Zoback (1979) state the least principal stresses in the Basin and Range to vary between east to west and northwest to southeast. Zoback et al. (1981) define a clockwise change in the orientation of the stress field ~10 Ma. From 20-10 Ma, the least horizontal principal stresses were west-southwest to east-northeast, while after 10 Ma they rotated to west-northwest to east-southeast. In Arizona, this clockwise rotation has been constrained between 14 and 7 Ma. Aldrich and Laughlin (1984) say the Basin and Range is characterized by extension directed between east to west and west-northwest to east-southeast, although the same authors (1986) suggest that

least principal horizontal stress in the western part of the Basin and Range in Arizona is northeast, while in the eastern part of the state it is between northwest to southeast and west-northwest to east-southeast. Zoback and Zoback (1989) also report that the least principal horizontal stresses in the Basin and Range are oriented approximately east-west (between west-northwest and east-northeast). Finally, Leighty (1997) determined that extension in the Basin and Range province was directed east-west. Overall, despite the inconsistencies, one can generalize the extension to have been oriented approximately east to west.

The state of stress along the southwestern margin of the Colorado Plateau is not as extensively studied, but is very well defined. Most authors agree that the modern least principal horizontal stresses in Arizona are north-northeast to northeast (Zoback and Zoback, 1989; Aldrich and Laughlin, 1984; Thompson and Zoback, 1979; Zoback et al., 1981). Basically, the least principal horizontal stresses around the margins of the Colorado Plateau are perpendicular to its margin. This change in the state of stress is suggested to be related to the pronounced lateral variations in the thickness of the lithosphere beneath the Basin and Range and Colorado Plateau (Zoback and Zoback, 1989)

In the Arizona Transition Zone, Aldrich and Laughlin (1986) and Menges and Pearthree (1989) state that the least principal horizontal stresses are mainly perpendicular to the Plateau boundary, which would result in northwest-striking faults. Aldrich and Laughlin (1984), however, report that in the zone between the Colorado Plateau and the Basin and Range the stress state is transitional between those of each respective province.

Hendricks and Plescia (1991) describe the stress field in the central Arizona Transition Zone as complicated, probably a reflection of this transition between the two stress states.

This transitional stress state is the most likely explanation for the simultaneously active north and northwest faults found in the project area. Interaction of the east-west directed extension of the Basin and Range province to the south, resulting in north-south striking-faults, and the northeast directed extension along the southwestern Colorado Plateau margin, resulting in northwest striking faults, must occur in the project area. In the project area, the westward dip of the fault blocks appears to indicate that the extension in the project area was mostly controlled by the east-west directed extension of the Basin and Range province. As one moves to the north of the project area, and closer to the Colorado Plateau margin, major Tertiary faults become almost exclusively northwest-striking (Fig. 29). It is this author's contention that the project area marks the location where these two oblique stress fields interact.

**Fault-Related Folding**

It appears that rock units within the tilted fault block immediately to the east of the Cooks Mesa fault have been subject to fault drag folding in the project area. The effect of this is to drag and fold the units on the downthrown side of the fault so their dip becomes nearly horizontal and then eastward immediately adjacent to the fault (Plate 2). There are several lines of evidence for this relationship. First, the fault block between the Cave Creek fault and the Cooks Mesa fault in the southwest corner of the mapping area

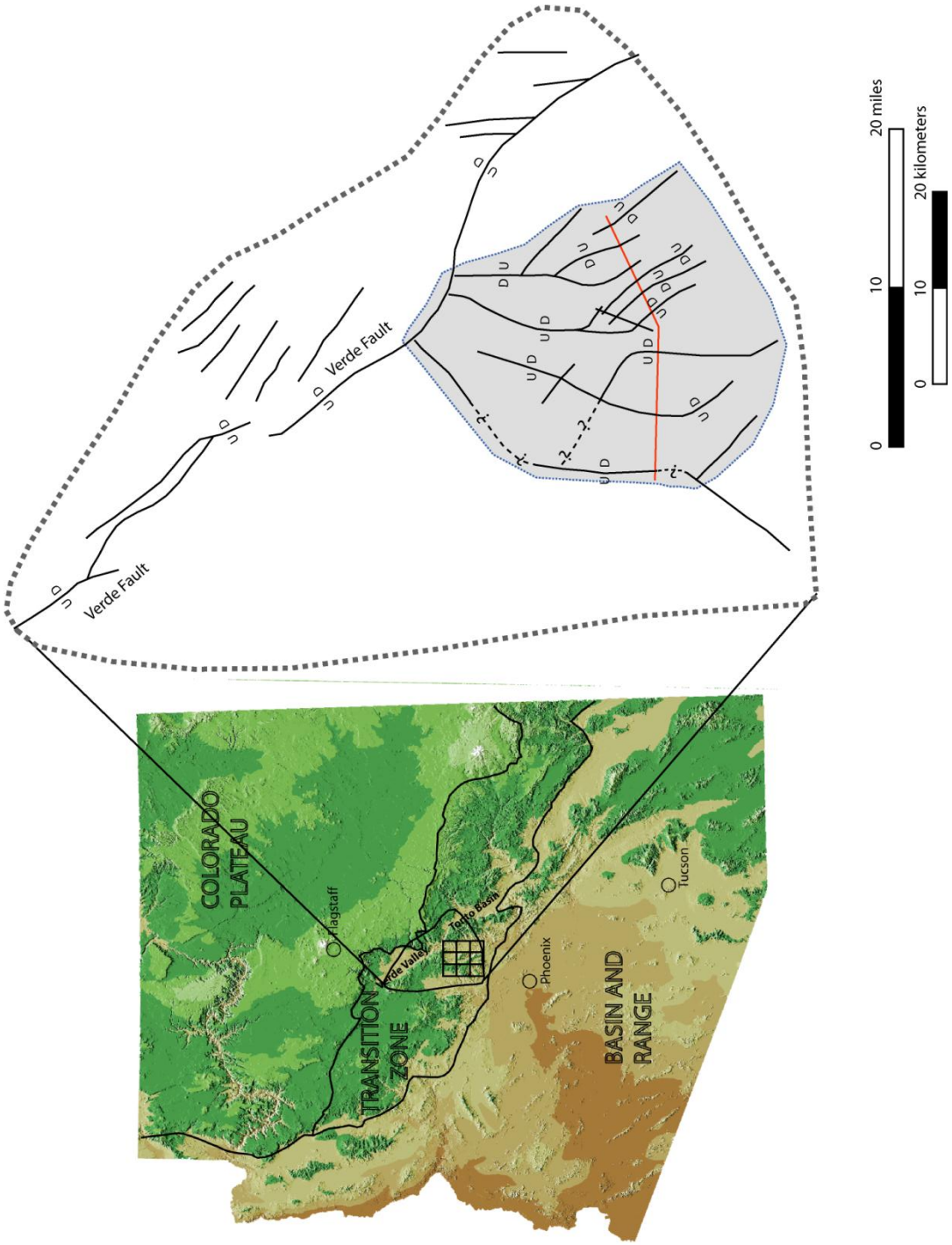


**Figure 29. Map of Tertiary normal faults in the region, and an outline of the approximate area of the Lower Verde Valley graben. Red line indicates approximate line of section used in Figure 28. Modified from Kamilli and Richard (1998) and Wrucke and Conway (1987). Shaded relief image from United States Geological Survey, Flagstaff, AZ.**

and seen in cross section E – E' (Plate 2) has good exposure of a fault drag fold. Immediately to the east of the Cooks Mesa fault in The Rincon area the units dip ~20$^{o}$ east, and as one moves westward they change to a ~15$^{o}$ westward dip. The core of the fold was actually then the locus of a small amount of Younger Conglomerate deposition. Additionally, poorly exposed Hickey Formation basalts immediately to the east of the Cooks Mesa fault in the Lockwood Mesa and Blackjack Point areas appear to be less tilted than the Hickey Formation basalts to the east, but are within the same fault block. Although the strike and dip could not be confidently measured in the flat-lying areas, the landscape implies this relationship as the surfaces along the backside of the fault block become nearly flat as one moves towards the west. The final piece of evidence for this is that without fault drag folding, Hickey Formation basalts appear to be unreasonably thick in the Roundtree Canyon area. Field relations cannot constrain the true thickness at depth of the Hickey Formation basalts, but do indicate the top of the Hickey Formation basalts at depth is much shallower than expected if one merely projects the 15-20$^{o}$ dip under the surface. This relationship is best seen near the line of section C – C' (Plate 2), where adjacent basalt exposures within the same tilt block indicate basalts are as high as ~3750 ft, but through simple tilt projections on a cross-section would appear to be no higher than 1500 ft. This projection, without fault drag folding, would make the Hickey Formation basalts over 2000 ft thicker, more than doubling the maximum thickness of Hickey Formation basalts elsewhere in the project area. Fault drag folding can explain all of the relationships described above.

**Lower Verde Valley Graben**

The Cooks Mesa fault is the master fault in the project area. It separates an area of extension and tilting to the east from an untilted, unextended sequence to the west, indicating that it is listric at depth. The faults to the east are probably planar normal faults which merge with the Cooks Mesa listric fault at depth.

The Cooks Mesa fault continues out of the project area to the north, and based upon topographic relations and strike, it appears that it extends northward until it merges with, or becomes, the northeast striking Pine Mountain fault, originally described by Canney et al. (1967) and Elston (1984). The Pine Mountain fault eventually intersects the Verde fault (Leighty, 1997).

If one considers the mapping of Wrucke and Conway (1987) to the east, it becomes clear that the project area, and the north – south trending portion of the lower Verde River valley to the east, is part of a graben system. To the east of East Cedar Mountain and the Horseshoe Dam fault, Wrucke and Conway (1987) map another east-dipping, high-angle normal fault with down to the east motion and Hickey basalts tilted ~20$^{o}$ to the west. As one moves eastward, and upward in elevation into the Mazatzal Mountains, the faults become west-dipping, high-angle normal faults that cut Hickey Formation basalts, but apparently with little offset. These fault blocks are relatively small, and appear to be falling into the open space created by extension with little to no rotation. The easternmost, west-dipping faults on the eastern margin of this graben

continue northward until they tie into the Verde fault to the north of Goat Camp Canyon and west of the Limestone Hills along the Verde River (Wrucke and Conway, 1987).

It seems, then, that the area bounded by Cooks Mesa on the west and the Mazatzal Mountains on the east is a graben system dominated by a series of west-tilted fault blocks between the major bounding faults. Figure 30 offers a diagrammatical cross section of this feature, herein named the Lower Verde Valley graben. This cross section is based upon the model of a listric normal fault bounding a family of planar normal faults from Wernicke and Burchfiel (1982). The shape of the Cooks Mesa listric fault was determined to a depth of ~6.6km using the method of Gibbs (1983). This is a graphical method that uses roll-over geometry of the tilted-block to construct the change of curvature of a listric fault. Finally, the negative listric fault (concave downward) to the east of the Horseshoe Dam fault resolves spatial problems created at depth when the terrain transfers from tilted to the west to relatively untilted to the east. This type of fault has been observed in the field as well as produced experimentally (Laubach et al., 1992; McClay and Ellis, 1987). Figure 29, a map of major Tertiary faults in the region, also depicts the approximate aerial extent of the Lower Verde Valley graben and shows the line of section used to create Figure 30.

One issue to be considered is that the west-dipping faults to the east of the project area are mapped as cutting younger basalts. These faults are all northwest-striking structures, similar to the northwest-striking segment of the Horseshoe Dam fault. It is the interpretation of the author that this motion represents slight reactivation of the northwest-striking faults in the area after the main pulse of extension and tilting was over.

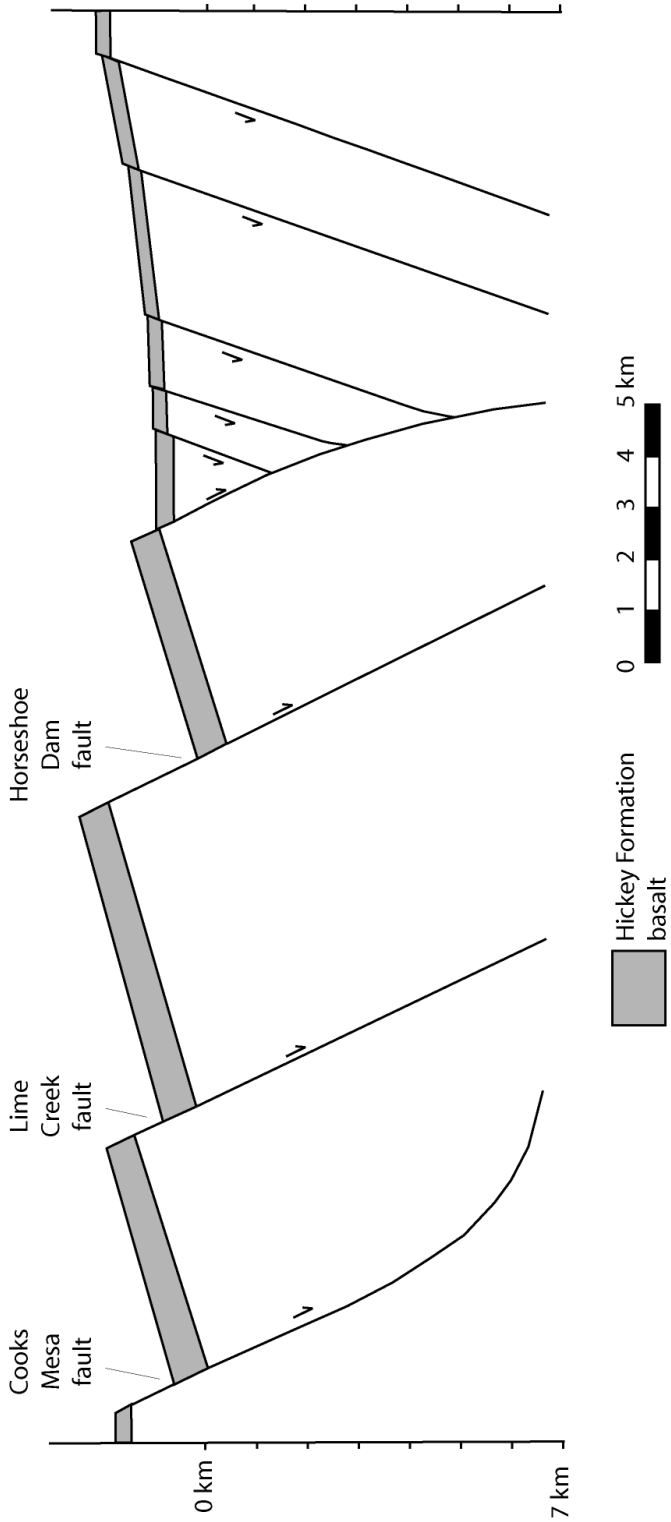


**Figure 30. Diagrammatic cross-section depicting the Lower Verde Valley graben to a depth of ~6.6 km. Model makes some assumptions about mapping to the east of the field area. Model follows Wernicke and Burchfiel (1982), and curvature of listric fault is constructed after Gibbs (1983).**

This motion along northwest-striking faults can be attributed to the continuation of northeast-directed extensional stress along the margin of the Colorado Plateau through the present, while extension related to the Basin and Range (east-west) mostly ended 8-6 Ma (Shafiqullah et al., 1980; Scarborough and Peirce, 1978). The orientation of these faults with respect to this stress state could explain preferential motion along the northwest-striking faults after 8-5 Ma.

Reactivation of northwest-striking faults after the main pulse of extension and rotation in the area explains several observations. First, it may explain why the northwest-striking segment of the Horseshoe Dam fault appears to cut the north-striking Lime Creek fault, although they are part of apparently contemporaneous structures. Additionally, the faulting appears to offset units without rotation, indicating that this episode was separate from the earlier period of extension and rotation. Map relations in this area are not definitive, however, and data is sparse. Further study of these relationships in the field is needed to definitively answer these questions.

**Amount of Extension**

Miocene extension across the project area is calculated to be between 8.5 – 10%, after the methodology of Twiss and Moores (1992, p. 93-94). The timing, as discussed above, is coeval with timing of the Basin and Range disturbance. Estimates for the amount of Basin and Range disturbance extension have been made by several authors. Spencer and Reynolds (1989) suggest 5-15% extension, while Coney (1978b) estimates

15-20%. Menges and Pearthree (1989) suggest horizontal extension between 5-20%. Stewart (1980) proposes 20-30% extension. Zoback et al. (1981) estimate 17-23% extension. Thompson and Burke (1974) estimate 10% extension. All of these estimates consider only extension within the Basin and Range physiographic province.

The estimate of 8.5-10% extension certainly falls within these parameters as defined above. Even if one takes only the higher end of the spectrum when considering Basin and Range disturbance extension, these numbers are still acceptable. Menges and Pearthree (1989) note that total extension related to the Basin and Range disturbance in the Transition Zone may be much less than that within the Basin and Range province.

## REGIONAL SYNTHESIS

### Verde Valley and Tonto Basin

It is difficult to attempt to reconcile extension in the project area with that which formed the Verde Valley and Tonto Basin based upon timing alone. Numerous authors have studied both localities, yet there seems to be little agreement on the timing at either locality.

The Verde Valley is bounded on the southwest by a single, major normal fault, the Verde fault, which splays into several high-angle faults at the southern end of the Verde Valley (Wolfe, 1981). The valley has been described variously as a graben (Young et al., 1987), “trap-door” graben (Elston and Young, 1991), and a half-graben (Leighty, 1997). The timing of late Tertiary movement along the fault is not completely agreed upon. Leighty (1997) proposes formation between 10-6 Ma, apparently based upon cross-cutting relationships with the Hickey Formation basalts (16.2-9.2 Ma) and Perkinsville Formation lavas (6.3-4.6 Ma). Elston and Young (1991) propose formation between 11-8 Ma. Their upper bound is based upon the cutting of the Hickey Formation basalts by the Verde fault, while the lower bound is apparently based upon the onset of sediment accumulation. Several authors provide upper bounds only. Peirce (1984) proposes formation occurred after 10 Ma based upon the Verde Fault cutting Upper Miocene volcanic rocks. Lindberg (1989) suggests only that major motion occurred after Hickey Formation basalts because they are completely offset by the Verde Fault. In view of these results, the timing cannot be constrained more tightly than during the Late Miocene.

Sedimentation in the Verde Valley, however, continued through the Pliocene (Nations et al., 1985).

The Tonto Basin has been described as having similar timing of formation as the Verde Valley (Elston, 1984), however, its formation time has an even broader range of estimates. Nations (1988, 1990) suggests the basin formed through extensional faulting which can only be constrained as occurring between 19 Ma and 5 Ma. The upper bound is constrained through offset of a 19 Ma dacite, while the lower bound is based upon unfaulted basin-fill with Late Miocene to Early Pliocene fossils. Finally, Young (1987) and Faulds (1988) suggest that Oligocene tectonism may have initiated the development of the basin, but that its primary development came in Middle Miocene time. Several lines of evidence for this are given: 1) the scarcity of Oligocene and Early Miocene fanglomerates and Apache Leap Tuff in the Tonto Basin; 2) the thick accumulation of Late Tertiary basin-fill; and 3) interruption of the Oligocene through Middle Miocene episode of internal drainage in the Salt River paleocanyon immediately to east of the Tonto Basin. The Payson Basin, considered to be a northwestern extension of the Tonto Basin (Peirce, 1984), probably began to form sometime after 23 Ma as indicated through relationships with basalts (Muehlberger and Brumbaugh, 1986). Overall, it seems that the main development of the Tonto and Payson Basins can only be constrained between middle Early Miocene (~20 Ma) through the Late Miocene/Early Pliocene (~5 Ma).

**Miocene Extension in the Transition Zone**

The project area encompasses part of a larger structural feature, the Lower Verde Valley graben. The formation of this feature is constrained to have occurred mostly between 13.5 and 6.4 Ma. This timing is contemporaneous with that of the Verde Valley and Tonto Basin formation. This timing is also contemporaneous with the Basin and Range disturbance in Arizona.

The major faults that bound the Lower Verde Valley graben continue northwards out of the field area and eventually tie into the Verde fault, the major fault bounding the Verde Valley. This relationship warrants further study, as it is important to study the interaction of these intersecting fault systems. Additionally, further mapping is needed to the north of the project area to ascertain whether the Cooks Mesa fault does indeed become the Pine Mountain fault and merge with the Verde fault.

The results of this project suggest that the tilting in the Cedar Mountains area is related to the formation of the Lower Verde Valley graben during the Basin and Range disturbance, as opposed to a “last-gasp” of the mid-Tertiary orogeny. Tilting of fault blocks in the project area is explained by extension along the Cooks Mesa fault, a listric normal fault. While unexpected with respect to our general understanding of the dynamics of the Basin and Range disturbance in Arizona, this type of extension is not completely unrecognized across the Basin and Range province. Faulds et al. (1997) have recognized a large, listric normal fault associated with the Basin and Range disturbance in the Hualapai basin of Arizona, while Effimoff and Pinezich (1986) have also

recognized several Basin and Range basins in Nevada that are bounded by major listric normal faults. Finally, it seems probable that extension in the project area is related to the same episode of extension responsible for the formation of the Tonto Basin and Verde Valley, but further work is needed to determine this relationship.

## SUMMARY

### Tertiary Geologic History

The oldest Tertiary unit in the project area is the Paleogene Older Conglomerate. This unit was deposited in small, localized basins on an exhumed basement surface of moderate relief. The relief on this surface is locally up to 200 m, and relief seems to be erosionally formed rather than fault created. Although this unit cannot be directly dated, timing can be constrained in the project area. Deposition probably began during the post-Laramide period of uplift and erosion that beveled the basement surface. Conformably overlying the older conglomerates is the Chalk Canyon Formation. Just to the south of the project area the Chalk Canyon Formation has been constrained to be as old as the Early Oligocene (~29-32 Ma) by an oreodont fossil found in the basal tuff (Gomez, 1979). In the project area, the oldest unit present is the basal basalts of the lower Chalk Canyon Formation, dated at 22 Ma (Lindsay and Lundin, 1972). These factors constrain deposition of the Older Conglomerate to have occurred from Eocene through the end of the Early Oligocene, or between ~55 and ~30 Ma. These age estimates coincide with estimates of correlative units in southern Arizona (Eberly and Stanley, 1978; Wilt and Scarborough, 1981). Elston and Young (1991) correlate these same units with the Rim Gravels of the Colorado Plateau, however, and consider the Rim Gravels to be Late Paleocene to Eocene.

Deposition of the Chalk Canyon Formation in the region must have began ~29-32 Ma through deposition of reworked tuffs (Gomez, 1979). This unit is not recognized in

the project area. The overlying basalts of the lower member, however, have been dated at ~22 Ma (Lindsay and Lundin, 1972), indicating a hiatus 7 to 10 Ma within the lower member. Hickey Formation basalts, which in the area are as old as 15.1 Ma, overlie the upper Chalk Canyon Formation, indicating that Chalk Canyon Formation deposition was complete by this time. The above constraints suggest deposition of the Chalk Canyon Formation may have began as early as 32 Ma, but that the bulk accumulated between 22 and 16 Ma.

There is substantial evidence that the Chalk Canyon Formation was deposited in a fault-bounded basin. The lack of fanning dips in the project area indicates that most of the Chalk Canyon Formation was deposited in a stable environment between 22 and 15 Ma. This suggests the episode of faulting that created the basin must have predated 22 Ma. Faulting may have began by 32 Ma, as indicated by deposition of reworked tuffs in the region, and must have been completed by 22 Ma at the onset of basaltic volcanism of the lower member. Faulting appears to have occurred on a “paleo-Lime Creek fault” with up to 225 m of offset. The 32 to 22 Ma timing bracket suggests this episode of faulting may be associated with the mid-Tertiary orogeny. The northwest strike of the proposed “paleo-Lime Creek fault” is also characteristic of the structural grain of the mid-Tertiary orogeny (Spencer and Reynolds, 1989; Menges and Pearthree, 1989).

Extensive basaltic volcanism in the area must have began by about 15.1 Ma, as this is the age of the base of the Hickey Formation basalts in the project area. The youngest date produced in the project area is 13.5 Ma, indicating accumulation of up to 600 m in ~1.6 Ma. At this point in time, the project area must have been covered by an

areally extensive sheet of Hickey Formation basalts (Fig. 21). Although the southeast corner of the project area near Sunset Mountain does not have any Hickey Formation basalts, Wrucke and Conway (1987) have mapped Hickey Formation basalts to the east along the Verde River, indicating that flows probably once covered the area and have merely been erosionally removed in the Sunset Mountain area.

Extension and fault block rotation in the project area are constrained to have occurred between 13.5 and 5-8 Ma, and must have been dominantly oriented east-west, controlling the rotation of west-dipping fault blocks. This timing and orientation of extension in the project area is synchronous with the Basin and Range disturbance in Arizona. Fault patterns in the project area, however, are characterized by both north- and northwest-striking faults that appear to have formed contemporaneously. It appears that during extension in the project area there was interaction of the Basin and Range stress field (east-west extension) with that of the southwestern margin of the Colorado Plateau (northeast-southwest extension). Interaction of these two oblique stress fields controlled the north and northwest strikes of the faults in the project area.

Half-grabens formed during extension are filled with a conglomerate composed of detritus derived mainly from Hickey Formation basalts. The half-grabens were small, local basins which filled late syn- to post-extension phase in the project area. This is indicated by both the slightly fanning dips within the bedded parts of the unit and the fact that it onlaps against fault exposures without being in faulted contact.

Minor basaltic volcanism around 6.4 Ma, which is correlative in time with eruption of the Ramp basalts to the north, is only present in the lowest structural portions of the Lower Verde Valley graben. Here, the basalt covers tilted Hickey Formation basalt and overlying Younger Conglomerate. The areal extent of the younger basalt flows was probably controlled by the structural, and resulting topographic, effects of the graben, rather than erosion of the unit elsewhere.

Extension in the northwest part of the project area and adjoining area to the east and northeast was active after 5-8 Ma. This extension appears to have been minor, with little offset of Late Miocene Younger Basalt. Extension occurred along northwest-striking faults that were active during the main pulse of extension and fault block rotation in the project area. This activity may represent an episode of reactivation of these structures due to the continued extension along the margin of the Colorado Plateau and the preferential alignment of these faults with respect to this stress state (northeast-southwest extension). Figure 31 summarizes the Tertiary geologic history of the project area as described above in a diagrammatic fashion.

## Conclusions

The East and West Cedar Mountains of the central Arizona Transition Zone are west-dipping fault blocks which encompass part of the larger Lower Verde Valley graben structure. West-dipping fault blocks related to extension and formation of this graben are found through the entire project area. These blocks are composed of a basement of

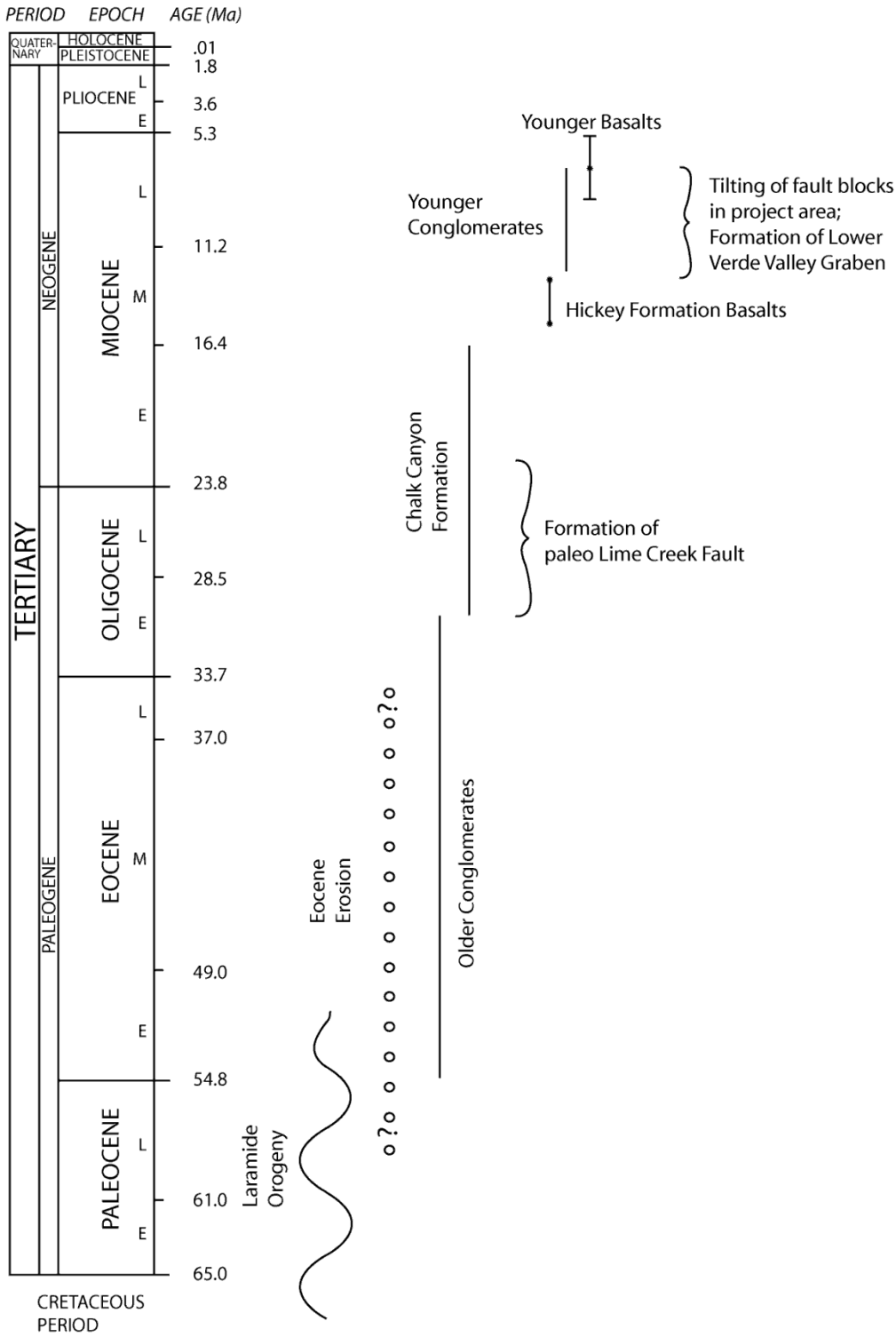


**Figure 31. Diagram summarizing Tertiary geologic history of the project area.**

undifferentiated Early Proterozoic metamorphic rocks and the Early Proterozoic Verde River Granite successively overlain by the Paleogene Older Conglomerate, Early Oligocene to Early Miocene Chalk Canyon Formation, and Middle Miocene Hickey Formation basalts. These units were tilted during extension along high-angle normal faults which merge with a listric fault at depth, the Cooks Mesa fault. This fault is the master fault in the project area as it marks the main boundary between unextended terrain to the west from the area of extension and tilting to the east. Extension in the project area is approximately 8.5 – 10%. In map view it is clear that north- and northwest-striking faulting patterns in the area are dominant. This relationship forms a gridded pattern and rhomb-shaped fault blocks. These gridded patterns are apparently controlled by the interaction of two oblique stress fields in the project area. These are the east-west directed extension of the Basin and Range province to the south and the northeast-southwest directed extension along the southwestern margin of the Colorado Plateau to the north. The timing of extension is constrained to be between 13.5 and 5-8 Ma in the project area, indicating that it is synchronous with both the Basin and Range disturbance in Arizona and the formation of the Verde Valley and Tonto Basins. Major faults bounding the Lower Verde Valley graben, including the Cooks Mesa fault, appear to eventually merge with the Verde fault to the north of the field area, indicating that the extension in the field area may be related to the formation of the Verde Valley. Further investigation is needed, however, to understand this association.

Tilt-block domains are characteristic of the mid-Tertiary orogeny. The East and West Cedar Mountains area tilt-block domain, however, falls outside of both the temporal

and spatial boundaries set forth for the mid-Tertiary orogeny earlier in the paper. Accordingly, the tilting in the project area is not related to any “last-gasp” of the mid-Tertiary orogeny, instead extension and tilting in the area is constrained to be part of the Basin and Range disturbance, both through $^{40}Ar$-$^{39}Ar$ geochronology and association with the Verde fault and Verde Valley, which is considered a Basin and Range disturbance feature. Extension in the project area, then, provides a new view into the dynamics of the Basin and Range disturbance in Arizona, as it is accommodated by motion along a listric normal fault and tilting of fault-blocks, rather than through graben subsidence along high-angle normal faults, as is typical of the Basin and Range disturbance in Arizona.

This project is important for several reasons. It documents tilted fault blocks in the Transition Zone, a previously unrecognized feature of this physiographic province. It recognizes the larger scale Lower Verde Valley graben for the first time, a feature dominated by extension and tilting of fault blocks along a listric normal fault. This relationship is unexpected with respect to our general understanding of the dynamics of the Basin and Range disturbance in Arizona, but is not completely undocumented. At the very least it documents a little recognized mode of extension related to the Basin and Range disturbance. Finally, it indicates that between 13.5 and 8-5 Ma, extension in this area of the Transition Zone played a powerful role in the formation of the modern landscape. The Lower Verde Valley graben appears to tie into the Verde fault, and therefore may be associated with the formation of the Verde Valley. Formation of the Tonto Basin, which has a similar timing and is along strike to the southeast of the Verde Valley, may also be related to the formation of the Lower Verde Valley graben and the

Verde Valley. These structural features provided a powerful control over the modern landscape of this part of Arizona, and probably, if one compares the structural lows of the Lower Verde Valley and the Verde Valley with the modern course of the Verde River, even directed the path of this major river through the Transition Zone.

## REFERENCES


Aldrich, Jr., M.J., and Laughlin, A.W., 1984, A model for the tectonic development of the southeastern Colorado Plateau boundary, Journal of Geophysical Research, v. 89, no. B12, p. 10,207-10,218.

Aldrich, Jr., M.J., and Laughlin, A.W., 1986, Implications of stress data on tectonic history of Arizona and contiguous areas, *in* Beatty, B., and Wilkinson, P.A.K., eds., Frontiers in geology and ore deposits of Arizona and the southwest, Arizona Geological Society Digest, Volume 16, p. 447.

Anderson, C.A, and Creasy, S.C., 1958, Geology and ore deposits of the Jerome area, Yavapai County, Arizona, United States Geological Survey Professional Paper 308, 185 p.

Anderson, P., 1980, Proterozoic convergent plate tectonics, 25th International Geologic Congress, v. 1, p. 73.

Anderson, P., 1989a, Proterozoic plate tectonic evolution of Arizona, *in* Jenney, J.P., and Reynolds, S.J., eds., Geologic Evolution of Arizona: Arizona Geological Society Digest 17, p. 17-55.

Anderson, P., 1989b, Stratigraphic framework , volcanic-plutonic evolution, and vertical deformation of the Proterozoic volcanic belts of central Arizona, *in* Jenney, J.P., and Reynolds, S.J., eds., Geologic Evolution of Arizona: Arizona Geological Society Digest 17, p. 57-148.

Canney, F.C., Lehmbeck, W.L., and Williams, F.E., 1967, Mineral resources of the Pine Mountain Primitive Area, Arizona, United States Geological Survey Bulletin 1230-J, p. J1-J45.

Coney, P.J., 1976, Plate tectonics and Laramide orogeny, *in* New Mexico Geological Society Special Publication 6, p. 5-10.

Coney, P.J., 1978a, The plate tectonic setting of southeastern Arizona, *in* New Mexico Geological Society Guidebook, 29th Field Conference, Land of Cochise, p. 285-290

Coney, P.J., 1978b, Mesozoic – Cenozoic cordilleran plate tectionics, *in* Smith, R.B., and Eaton, G.P., eds., Cenozoic tectonics and regional geophysics of the western cordillera: Geological Society of America Mem. 152, p. 33-50.

Coney, P.J., and Reynolds, S.J., 1977, Cordilleran Benioff Zones, Nature, Vol. 270, p. 403-406.

Conway, C.M., and Silver, L.T., 1989, Early Proterozoic (1710-1615 Ma) in central Arizona to southeastern Arizona, *in* Jenney, J.P., and Reynolds, S.J., eds., Geologic Evolution of Arizona: Arizona Geological Society Digest 17, p. 165-186.

Damon, P.E., Shafiqullah, M., and Clark, K.F., 1981, Age trends of igneous activity in relation to metallogenesis in the southern Cordillera, *in* Dickinson, W.R., and Payne, W.D., eds., Relations of tectonics to ore deposits in the southern Cordillera: Arizona Geological Society Digest, v. 14, p. 137-154.

Damon, P.E., Lynch, D.J., Shafiqullah, M., 1984, Cenozoic Landscape Development in the Basin and Range Province of Arizona, *in* Smiley, T.L., Nations, J.D., Pewe, T.L., and Schafer, J.P., eds., Landscapes of Arizona: University Press of America, p. 175-206.

Davis, G.A., Anderson, J.L., Frost, E.G., and Shackelford, T.J., 1980, Mylonization and detachment faulting in the Whipple – Buckskin – Rawhide Mountains terrane, southeastern California and western Arizona, *in* Crittenden, M.D., Coney, P.J., and Davis, G.H., eds., Cordilleran metamorphic core complexes: Geological Society of America Memoir 153, p. 79-129.

Dickinson W.R., 1989, Tectonic Setting of Arizona through Geologic Time, *in* Jenney, J.P., and Reynolds, S.J., eds., Geologic Evolution of Arizona: Arizona Geological Society Digest 17, p. 1-16.

Eaton, G.P., 1980, Geophysical and geological characteristics of the crust of the Basin and Range Province, *in* Continental tectonics, Geophysical research board, National Academy of the Sciences, Washington, D.C., p. 96-113.

Eberly, L.D. and Stanley, T.B., 1978, Cenozoic stratigraphy and geologic history of southwestern Arizona, Geological Society of America Bulletin, v. 89, p. 921-940

Effimoff, I., and Pinezich, A.R., 1986, Tertiary structural development of selected basins: Basin and Range province, northeastern Nevada, *in* Mayer, L., Extensional tectonics of the southwestern United States, Geological Society of America Special Paper 208, p. 31-42.

Elston, D.P., 1984, Rocks, Landforms, and Landscape Development *in* Central Arizona, in Smiley, T.L., Nations, J.D., Pewe, T.L., and Schafer, J.P., eds., Landscapes of Arizona: University Press of America, p. 151-173.

Elston, D.P., and McKee, E.H., 1982, Age and correlation of the late Proterozoic Grand Canyon disturbance, northern Arizona, Geological Society of America Bulletin, v. 93, p. 681-699.

Elston, D.P., and Young, R.A., 1991, Cretaceous-Eocene (Laramide) landscape development and Oligocene-Pliocene drainage reorganization of transition zone and Colorado Plateau, Arizona, Journal of Geophysical Research, v. 96, no. B7, p. 12,389–12,406.

Faulds, J.E., 1988, Cenozoic structural and geomorphic evolution of part of the Transition Zone, Salt River Canyon region, east-central Arizona, *in* Anderson, L., and Piety, L., 1988, Guide to the Tonto Basin of Arizona, Friends of the Pleistocene Rocky Mountain Cell Field Trip: p. 109-128.

Faulds, J.E., Schreiber, C., Reynolds, S.J., Gonzalez, L.A., Okaya, D., 1997, Origin and paleogeography of an immense, nonmarine Miocene salt deposit in the Basin and Range (western USA), The Journal of Geology, v. 105, p. 19-36.

Ferguson, C.A., Gilbert, W.G., and Leighty, R.S., 1998, Geoloic map of the New River Mesa 7.5' quadrangle, Maricopa County, Arizona, Arizona Geological Survey, Open-File Report 98-12, 29 p., 3 sheets, scale 1:24,000.

Ferguson, C.A., Gilbert, W.G., Skotnicki, S.J., Wrucke, C.T., and Conway, C.M., 1999, Geologic map of the Horsehoe Dam 7.5' quadrangle, Maricopa County, Arizona, Arizona Geological Survey, Open-File Report 99-15, 11 p., scale 1:24,000, 1 sheet.

Gibbs, A.D., 1983, Balanced cross-section construction from seismic sections in areas of extensional tectonics, Journal of Structural Geology, v. 5, p. 153-160.

Gilbert, W.G., Ferguson, C.A., Leighty, R.S., 1998, Geologic map of the Humboldt Mountain 7.5' quadrangle, Maricopa County, Arizona, Arizona Geological Survey, Open-File Report 98-11, 17 p., 3 sheets, scale 1:24,000.

Gomez, E., 1979, Geology of the south-central part of the New River Mesa quadrangle, Cave Creek Area, Maricopa County, Arizona, United States Geological Survey, Open-File Report 79-1312, 156 p., 1 sheet, scale 1:12,000.

Hendricks, J.D. and Plescia, J.B., 1991, A review of the regional geophysics of the Arizona transition zone, Journal of Geophysical Research, v. 96, no. B7, p. 12,351–12,373

Jagiello, K.J., 1987, Structural evolution of the Phoenix basin, Arizona, M.S. thesis, Arizona State University, 156 p.

Kamilli, R.J., and Richard, S.M., eds., 1998, Geologic Highway Map of Arizona, Arizona Geological Society, 1 sheet containing text and figures, scale 1:1,100,000.

Karlstrom, K.E., Bowring, S.A., and Conway, C.M., 1987, Tectonic significance of an Early Proterozoic two-province boundary in central Arizona, Geological Society of America Bulletin, v. 99, p. 529-538.

Keith, S.B., and Wilt, J.C, 1985, Late Cretaceous and Cenozoic orogenesis of Arizona and adjacent regions: a strato-tectonic approach, *in* Flores, R. M. and Kaplan, S. S., Cenozoic paleogeography of west-central United States, RMS, SEPM Symposium 3, p. 402-437.

Laubach, S.E., Vendeville, B.C., and Reynolds, S.J., 1992, Patterns in the development of extensional fault-block shapes from comparison of outcrop-scale faults and experimental physical models, *in* Larsen, R.M., Brekke, H., Larsen, B.T., and Talleraas, E., eds., Structural and Tectonic Modelling and its Application to Petroleum Geology, NPF Special Publication 1, p. 231-241.

Leighty, R.S., 1997, Neogene tectonism and magmatism across the Basin and Range – Colorado Plateau boundary, central Arizona, Ph.D dissertation, Arizona State University, 1019 p.

Leighty, R.S., 1998, Tertiary volcanism, sedimentation, and extensional tectonism across the Basin and Range – Colorado Plateau boundary in central Arizona, *in* Duebendorfer, E. M., ed, Geologic Excursions in Northern and Central Arizona, Field Trip Guidebook, Geological Society of America, Rocky Mountain Section Meeting, p. 59-95.

Lindberg, P.A., 1989, Precambrian ore deposits of Arizona, *in* Jenney, J.P., and Reynolds, S.J., eds., Geologic Evolution of Arizona: Arizona Geological Society Digest 17, p. 187-210.

Lindsay, E.H., and Lundin, R.F., 1972, An Oligocene oreodont (Mammalia: Artiodactyla) from central Arizona, Journal of Paleontology, v. 46, p. 115-119.

Livingston, D.E., and Damon, P.E., 1968, The ages of stratified Precambrian rock sequences in central Arizona and northern Sonora, Canadian Journal of Earth Science, v. 5, p. 763-772.

Lucchita, I., and Hendricks, J.D., 1983, Characteristics, depositional environment, and tectonic interpretations of the Proterozoic Cardenas Lavas, eastern Grand Canyon, Arizona, Geology, v. 11, p. 177-181.

McClay, K.R., and Ellis, P.G., 1987, Analogue models of extensional fault geometries, *in* Coward, M.P., Dewey, J.F., and Hancock, P.L, eds., Continental Extensional Tectonics, Geological Society London, Special Publication 28, p. 109-127.

McKee, E.H., and Anderson, C.A., 1971, Age and chemistry of Tertiary volcanic rocks in north-central Arizona and relation of the rocks to the Colorado Plateau, Geological Society of America Bulletin, v. 85, no. B1, p. 327-337.

Menges, C.M. and Pearthree, P.A., 1989, Late Cenozoic tectonism in Arizona and its impact on regional landscape evolution, *in* Jenney, J.P, and Reynolds, S.J, eds., Geologic evolution of Arizona: Arizona Geological Society Digest 17, p. 649-680.

Muehlberger, E.W., and Brumbaugh, D.S., 1986, Structural and stratigraphic analysis of the Payson basin, Gila County, Arizona, Geological Society of America Abstracts with Programs, Rocky Mountain Section Meeting, v. 18, no. 5, p. 398.

Nations, J.D., 1990, Late Cenozoic stratigraphy and tectonics of the Tonto Basin, central Arizona, in Gehrels, G.E., and Spencer, J.E., eds., *in* Geologic Excursions through the Sonoran Desert region, Arizona and Sonora: Arizona Geological Survey Special Paper 7, p. 24-27.

Nations, J.D., 1989, Cretaceous history of northeastern and east-central Arizona, *in* Jenney, J.P, and Reynolds, S.J, eds., Geologic evolution of Arizona: Arizona Geological Society Digest 17, p. 435-446.

Nations, J.D., 1988, Stratigraphy and tectonic significance of Cenozoic basin-fill sediments, Tonto Basin, Arizona, *in* Anderson, L., and Piety, L., 1988, Guide to the Tonto Basin of Arizona, Friends of the Pleistocene Rocky Mountain Cell Field Trip: p. 165-179.

Nations, J.D., Wilt, J.C., and Hevly, R.H., 1985, Cenozoic paleogeography of Arizona, *in* Flores, R. M. and Kaplan, S. S., Cenozoic paleogeography of west-central United States, RMS, SEPM Symposium 3, p.335-356.

Peirce, H.W., 1984, Some Late Cenozoic basins and basin deposits of southern and western Arizona, *in* Smiley, T.L., Nations, J.D., Pewe, T.L., and Schafer, J.P., eds., Landscapes of Arizona: University Press of America, p. 207-227.

Peirce, H.W., Damon, P.E., and Shafiqullah, M., 1979, An Oligocene (?) Colorado Plateau edge in Arizona, Tectonophysics, v. 61, p. 1-24.

Peirce, H.W., and Nations, J.D, 1986, Tectonic and paleogeographic significance of Tertiary rocks in the southern Colorado Plateau and Transition Zone, *in* Nations, J.D, Conway, C.M, and Swann, G.A, eds., Geology of Central and Northern Arizona: Geological Society of America, Rocky Mountain Section Guidebook, p. 111-124.

Potochnik, A.R., 1989, Depositional style and tectonic implications of the Mogollon Rim formation (Eocene), east-central Arizona, New Mexico Geological Society 40th Annual Field Conference Guidebook, p. 107-118.

Potochnik, A.R., 2001, Cenozoic structural and paleographic evolution of the Transition Zone, central Arizona, Ph.D. dissertation, Arizona State University, 173 p.

Ramberg, I.B., Cook, F.A., and Smithson, S.B, 1978, Structure of the Rio Grande rift in southern New Mexico and west Texas based on gravity interpretation, Geological Society of America Bulletin, v. 89, p. 107-123.

Ramberg, I.B., and Smithson, S.B., 1975, Gridded fault patterns in a late Cenozoic and a Paleozoic continental rift, Geology, v. 3, no. 4, p. 201-205.

Reynolds, S.J., and DeWitt, E., 1991, Proterozoic geology of the Phoenix region, central Arizona, *in* Karlstrom, K.E, ed., Proterozoic geology and ore deposits of Arizona, Arizona Geological Society Digest 19, p. 237-250.

Scarborough, R.B, and Peirce, H.W., 1978, Late Cenozoic basins of Arizona, *in* New Mexico Geological Society Guidebook, 29th Field Conference, Land of Cochise, p. 253-259

Scarborough, R., and Wilt, J.C., 1979, A study of Uranium favorability of Cenozoic sedimentary rocks, Basin and Range province, Arizona: Part 1, General Geology and Chronology of pre-late Miocene Cenozoic Sedimentary Rocks, United States Geological Survey, Open File Report 79-1429, 101 p.

Shafiqullah, M., Damon, P.E., Lynch, D.J., Reynolds, S.J., Rehrig, W.A., and Raymond, R.H., 1980, K-Ar Geochronology and Geologic History of Southwestern Arizona and Adjacent Areas, *in* Jenney, J.P., and Stone, C., eds., Studies in Western Arizona: Arizona Geological Society Digest, Volume XII, p. 201-260.

Shride, A.F., 1967, Younger Precambrian geology in southern Arizona, United States Geological Survey Professional Paper 566, 89 p.

Silver, L.T., Bickford, M.E., and Van Schmus, W.R., 1977, The 1.4-1.5 b.y. transcontinental anorogenic plutonic perforation of North America, Geological Society of America Abstracts with Programs, v. 9, p. 1176-1177.

Silver, L.T., Conway, C.M., and Ludwig, K.R., 1986, Implications of a precise chronology for early Proterozoic crustal evolution and caldera formation in the Tonto Basin-Mazatzal Mountains region, Arizona, Geological Society of America Abstracts with Programs, v. 18, no. 5, p. 413.

Spencer, J.E., and Reynolds, S.J., 1989, Middle Tertiary tectonics of Arizona and adjacent areas, *in* Jenney, J.P., and Reynolds, S.J., eds., Geologic Evolution of Arizona: Arizona Geological Society Digest 17, p. 539-574.

Spencer. J.E., Richard, S.M., Reynolds, S.J., Miller, R.J., Shafiqullah, M., Gilbert, W.G., and Grubensky, M.J., 1995, Spatial and temporal relationships between mid-Tertiary magmatism and extension in southwestern Arizona, Journal of Geophysical Research, v. 100, No. B7, p. 10321-10351.

Stewart, J.H., 1980, Regional tilt patterns of late Cenozoic basin-range fault blocks, western United States, Geological Society of America Bulletin, v. 91, p. 460-464

Thompson, G.A., and Burke, D.B, 1974, Regional Geophysics of the Basin and Range Province, Annual Review of Earth and Planetary Sciences, Vol. 2: 213-238

Thompson, G.A., and Zoback, M.L., 1979, Regional geophysics of the Colorado Plateau, Tectonophysics, v. 61, p. 149-181.

Titley, S.R., 1984, Arizona Landforms Viewed from the Perspective of Geologic History, *in* Smiley, T.L., Nations, J.D., Pewe, T.L., and Schafer, J.P., eds., Landscapes of Arizona: University Press of America, p. 37-53.

Twiss, R.J. and Moores, E.M., 1992, Structural Geology (Textbook), University of California at Davis, W.H. Freeman and Company, New York, 532 p.

Wernicke, B., and Burchfiel, B.C., 1982, Modes of extensional tectonics, Journal of Structural Geology, v. 4, p. 105-115.

Wessels, R.L., and Karlstrom, K.E., 1991, Evaluation of the tectonic significance of the Proterozoic Slate Creek shear zone in the Tonto Basin area, *in* Karlstrom, K.E, ed., Proterozoic geology and ore deposits of Arizona, Arizona Geological Society Digest 19, p. 193-209.

Wilt, J.C., and Scarborough, R.B, 1981, Cenozoic sediments, volcanics, and related uranium in the Basin and Range Province of Arizona, *in* Goodell, P.C., and Waters, A.C., eds., Uranium in volcanic and volcaniclastic rocks: American Association of Petroleum Geologists, Studies in Geology No. 13, p. 123-143.

Wolfe, E.W., 1981, Verde fault of central Arizona, United States Geological Survey Professional Paper 1275, p. 78

Wrucke, C.T., and Conway, C.M., 1987, Geologic map of the Mazatzal Wilderness and Contiguous roadless area, Gila, Maricopa, and Yavapai counties, Arizona, United States Geological Survey, Open File Report 87-664, 22 p., scale 1:48,000.

Young, R.A., Peirce, H.W., Faulds, J.E., 1987, Geomorphology and structure of the Colorado Plateau/ Basin and Range transition zone, Arizona, *in* Davis, G.H, and VandenDolder, E.M., eds., Geologic Diversity of Arizona and its margins: Excursions to choice areas: Arizona Bureau of Geology and Mineral Technology, Geological Survey Branch, Special Paper 5, p. 182-196.

Zoback, M.L., Anderson, R.E., and Thompson, G.A., 1981, Cainozoic evolution of the state of stress and style of tectonism of the Basin and Range Province of the western United States, Philosophical Transactions of the Royal Society of London, v. 300, no 1454, p. 407-434.

Zoback, M.L., and Zoback, M.D., 1989, Tectonic stress field of the continental United States, *in* Pakiser, L.C., and Mooney, W.D., eds., Geophysical framework of the continental United States, Geological Society of America Memoir 172, p. 523-539.

APPENDIX A

ANALYTICAL TECHNIQUES

## Introduction

In prepararation for $^{40}Ar/^{39}Ar$ analyses of basalt samples, groundmass concentrates were prepared by crushing and cleaning with hydrochloric acid and distilled water and then removing the phenocrysts. The mineral separates were then loaded into aluminum discs and irradiated for 14 hours at the Nuclear Science Center in College Station, Texas. The samples were analyzed with the furnace incremental heating age spectrum method. Details are discussed below.

## Irradiation Details

The following statement is from the New Mexico Geochronological Research Laboratory (NMGRL) regarding their analytical techniques. The NMGRL uses either the Ford reactor at the University of Michigan or the Nuclear Science Center reactor at Texas A&M University. In this case the Texas A&M facilities were used. The D-3 position is always used at the Texas A&M reactor. Texas irradiations are carried out in a dry location which is shielded with B and Cd. Depending upon the reactor used, the mineral separates are loaded into either holes drilled into Al discs or into 6 mm I.D. quartz tubes. Various Al discs are used. For Texas, 2.4 cm diameter discs contain either sixteen or six sample holes with smaller holes used to hold the standards. For the six hole disc, sample locations are 30, 90, 150, 210, 270 and 330° and standards are at 0, 60, 120, 180, 240 and

300°. Samples are located at 18, 36, 54, 72, 108, 126, 144, 162, 198, 216, 234, 252, 288, 306, 324, 342 degrees and standards at 0, 90, 180 and 270 degrees in the sixteen hole

disc. Following sample loading into the discs, the discs are stacked, screwed together and sealed in vacuo in Pyrex tubes.

**Extraction Line and Mass Spectrometer Details**

The NMGRL argon extraction line has both a double vacuum Mo resistance furnace and a $CO_2$ laser to heat samples. The Mo furnace crucible is heated with a W heating element and the temperature is monitored with a W-Re thermocouple placed in a hole drilled into the bottom of the crucible. A one inch long Mo liner is placed in the bottom of the crucible to collect the melted samples. The furnace temperature is calibrated by either melting Cu foil or with an additional thermocouple inserted in the top of the furnace down to the liner. The $CO_2$ laser is a Synrad 10W laser equipped with a He-Ne pointing laser. The laser chamber is constructed from a 3 3/8” stainless steel conflat and the window material is ZnS. The extraction line is a two stage design. The first stage is equipped with a SAES GP-50 getter, whereas the second stage houses two SAES GP-50 getters and a tungsten filament. The first stage getter is operated at 450°C as is one of the second stage getters. The other second stage getter is operated at room temperature and the tungsten filament is operated at ~2000°C. Gases evolved from samples heated in the furnace are reacted with the first stage getter during heating.

Following heating, the gas is expanded into the second stage for two minutes and then isolated from the first stage. During second stage cleaning, the first stage and furnace are pumped out. After gettering in the second stage, the gas is expanded into the mass spectrometer. Gases evolved from samples heated in the laser are expanded through a cold finger operated at -140°C and directly into the second stage. Following cleanup, the gas in the second stage and laser chamber is expanded into the mass spectrometer for analysis.

The NMGRL employs a MAP-215-50 mass spectrometer which is operated in static mode. The mass spectrometer is operated with a resolution ranging between 450 to 600 at mass 40 and isotopes are detected on a Johnston electron multiplier operated at ~2.1 kV with an overall gain of about 10,000 over the Faraday collector. Final isotopic intensities are determined by linear regression to time zero of the peak height versus time following gas introduction for each mass. Each mass intensity is corrected for mass spectrometer baseline and background and the extraction system blank.

Blanks for the furnace are generally determined at the beginning of a run while the furnace is cold and then between heating steps while the furnace is cooling. Typically, a blank is run every three to six heating steps. Periodic furnace hot blank analysis reveals that the cold blank is equivalent to the hot blank for temperatures less than about 1300°C. Laser system blanks are generally determined between every four analyses. Mass discrimination is measured using atmospheric argon which has been dried using a Ti-sublimation pump. Typically, 10 to 15 replicate air analyses are measured to determine a mean mass discrimination value. Air pipette analyses are generally conducted 2-3 times

per month, but more often when samples sensitive to the mass discrimination value are analyzed. Correction factors for interfering nuclear reactions on K and Ca are determined using K-glass and CaF2, respectively. Typically, 3-5 individual pieces of the salt or glass are fused with the $CO_2$ laser and the correction factors are calculated from the weighted mean of the individual determinations.

# APPENDIX B

## ANALYTICAL RESULTS

The following is a statement from the New Mexico Geochronological Research Laboratory regarding the analytical results. 3704A groundmass concentrate yielded a fairly well-behaved age spectrum (Fig. 27). The initial 27.3% of the $^{39}$Ar released yields increasing apparent ages (5.4 Ma to 12.79 Ma) and radiogenic yields (0.5% to 56.4%). The remaining $^{39}$Ar released yielded a weighted mean age of 13.53±0.14 Ma with a MSWD value of 1.69. This MSWD value suggests that much or all of the observed scatter can be attributed to analytical error. The K/Ca values and radiogenic yields reveal an overall decrease across the later 72.7% of the $^{39}$Ar released. Inverse isochron analysis of steps D-I reveal a $^{40}$Ar/$^{36}$Ar intercept of 290.3±6.6, within error of the atmospheric intercept of 295.5 and an isochron age (13.68±0.22 Ma) within error to the weighted mean age calculated from the age spectrum (Fig. 27b).

31304A groundmass concentrate yields a slightly disturbed age spectrum (Fig. 26). The initial 16.6% of the $^{39}$Ar released reveals old apparent ages. The next three heating steps contain 55.5% of the $^{39}$Ar released and are used to calculate a weighted mean age of 15.14±0.13 Ma with a MSWD value of 1.35. The following two steps reveal slightly younger apparent ages. The final heating step contains only ~1.5% of the $^{39}$Ar released but reveals a slightly older apparent age than the mid-portion of the age spectrum. The radiogenic yields and K/Ca values are somewhat oscillatory. Inverse

isochron analysis of steps B-I reveals a $^{40}Ar/^{39}Ar$ intercept of 296.2±5.4 and an isochron age of 15.07±0.42 Ma with a MSWD value of 4.4 (Fig. 26b).

| Sample | Lab # | Irradiation | mineral | age analysis | # of crystals/steps | Age | ±2σ | comments |
|---|---|---|---|---|---|---|---|---|
| 31304A | 55116 | NM-181 | groundmass concentrate | age spectrum | 3 | 15.14 | 0.13 | |
| 3704A | 55117 | NM-181 | groundmass concentrate | age spectrum | 6 | 13.53 | 0.14 | |
| 31304B | 55115 | NM-181 | groundmass concentrate | age spectrum | 8 | 6.4 | 1.3 | low confidence |

**Sample preparation and irradiation:**

Mineral separates were prepared using standard crushing, dilute acid treatment and hand-picking techniques.
Separates were loaded into a machined Al disc and irradiated for 14 hours in the D-3 position, Nuclear Science Center, College Station, TX.
Neutron flux monitor Fish Canyon Tuff sanidine (FC-1). Assigned age = 27.84 Ma (Deino and Potts, 1990)
equivalent to Mmhb-1 at 520.4 Ma (Samson and Alexander, 1987).

**Instrumentation:**

Mass Analyzer Products 215-50 mass spectrometer on line with automated all-metal extraction system.
The groundmass concentrates were step-heated for 10 minutes using a Mo double-vacuum resistance furnace.
Reactive gases removed during furnace analysis by reaction with 3 SAES GP-50 getters, 2 operated at ~450°C and
1 at 20°C. Gas also exposed to a W filiment operated at ~2000°C.

**Analytical parameters:**

Electron multiplier sensitivity averaged 2.63 x 10-16 moles/pA.
Total system blank and background averaged 1000, 10.3, 0.78, 8.5, 1.4 x $10^{-18}$ moles at masses 40, 39, 38, 37 and 36, respectivelyfor the biotite analyses
J-factors determined to a precision of ± 0.1% by $CO_2$ laser-fusion of 6 single crystals from each of 6 radial positions around the irradiation tray.
Correction factors for interfering nuclear reactions were determined using K-glass and $CaF_2$ and are as follows:
$(^{40}Ar/^{39}Ar)_K = 0.00020 \pm 0.0003$; $(^{36}Ar/^{37}Ar)_{Ca} = 0.00028 \pm 0.000005$; and $(^{39}Ar/^{37}Ar)_{Ca} = 0.0007 \pm 0.00002$.

31304B groundmass concentrate yields an imprecise and very disturbed age spectrum (Fig. 28). The apparent ages are oscillatory and are correlated with oscillations in the radiogenic yields. The radiogenic yields are very low (1.4-6.9 %). Yields of 50% or greater would be more typical for a basalt of this age. The initial heating step is of very poor quality and yields an apparent age of -1510±190 Ma. Due to the negative first step, the integrated age calculated for 31304B is -23.1±4.6 Ma. We have calculated a weighted mean age of 6.4±1.3 Ma from steps B-I. Due to the uniformly low radiogenic yields, the points on the inverse isochron cluster near the y axis. An inverse isochron age of 9.6±3.0 Ma with a MSWD value of 4.5 and a 40Ar/36Ar intercept of 290.3±5.1 is calculated for steps B-I (Fig. 28b).

| | ID | Power (°C) | $^{40}Ar/^{39}Ar$ | $^{37}Ar/^{39}Ar$ | $^{36}Ar/^{39}Ar$ (x $10^{-3}$) | $^{39}Ar_K$ (x $10^{-15}$ mol) | K/Ca | $^{40}Ar^*$ (%) | $^{39}Ar$ (%) | Age (Ma) | ±1σ (Ma) |
|---|---|---|---|---|---|---|---|---|---|---|---|
| | **31304B,** Groundmass Concentrate, J=0.0015981, D=1.0064, NM-181G, Lab#=55115-06 | | | | | | | | | | |
| # | A | 605 | 1302.0 | 2.790 | 5600.0 | 4.46 | 0.18 | -27.2 | 2.8 | -1510 | 190 |
| | B | 680 | 91.71 | 2.350 | 304.8 | 13.7 | 0.22 | 2.0 | 11.6 | 5.34 | 0.74 |
| | C | 730 | 49.09 | 2.548 | 157.6 | 6.54 | 0.20 | 5.6 | 15.7 | 7.89 | 0.60 |
| | D | 780 | 88.87 | 3.171 | 297.5 | 9.1 | 0.16 | 1.4 | 21.5 | 3.54 | 0.70 |
| | E | 855 | 108.4 | 3.865 | 362.6 | 6.73 | 0.13 | 1.4 | 25.8 | 4.5 | 1.1 |
| | F | 955 | 85.29 | 3.028 | 281.5 | 92.6 | 0.17 | 2.8 | 84.9 | 6.78 | 0.92 |
| | G | 1055 | 49.40 | 2.745 | 156.5 | 4.06 | 0.19 | 6.9 | 87.5 | 9.76 | 0.83 |
| | H | 1230 | 54.51 | 16.90 | 181.9 | 17.2 | 0.030 | 4.0 | 98.4 | 6.32 | 0.55 |
| | I | 1680 | 37.33 | 13.11 | 122.9 | 2.46 | 0.039 | 5.7 | 100.0 | 6.12 | 0.78 |
| | **Integrated age ± 2σ** | | | n=9 | | 156.9 | | | | -23.1 | 4.6 |
| | **Plateau ± 2σ** | steps B-I | | n=8 | MSWD=6.37 | 152.4 | 0.15 | | 97.2 | 6.4 | 1.3 |
| | **31404A,** Groundmass Concentrate, J=0.0015956, D=1.0064, NM-181G, Lab#=55116-02 | | | | | | | | | | |
| # | A | 605 | 2290.0 | 5.613 | 7562.0 | 3.65 | 0.091 | 2.4 | 2.8 | 154 | 14 |
| # | B | 680 | 32.02 | 0.7771 | 90.48 | 9.8 | 0.66 | 16.7 | 10.5 | 15.34 | 0.40 |
| # | C | 730 | 13.51 | 0.6496 | 27.28 | 7.89 | 0.79 | 40.8 | 16.6 | 15.79 | 0.24 |
| | D | 780 | 13.78 | 0.6086 | 29.17 | 17.1 | 0.84 | 37.8 | 29.9 | 14.95 | 0.13 |
| | E | 855 | 16.19 | 0.9579 | 37.14 | 26.3 | 0.53 | 32.7 | 50.4 | 15.18 | 0.13 |
| | F | 955 | 9.227 | 0.7031 | 13.50 | 27.9 | 0.73 | 57.4 | 72.1 | 15.19 | 0.07 |
| # | G | 1055 | 9.465 | 1.400 | 15.36 | 7.79 | 0.36 | 53.3 | 78.2 | 14.47 | 0.20 |
| # | H | 1230 | 15.33 | 11.55 | 37.79 | 26.0 | 0.044 | 33.4 | 98.4 | 14.78 | 0.17 |
| # | I | 1680 | 28.90 | 11.57 | 81.60 | 2.06 | 0.044 | 19.8 | 100.0 | 16.56 | 0.88 |
| | **Integrated age ± 2σ** | | | n=9 | | 128.6 | | | | 19.19 | 0.95 |
| | **Plateau ± 2σ** | steps D-F | | n=3 | MSWD=1.35 | 71.4 | 0.68 | | 55.5 | 15.14 | 0.13 |
| | **3704A,** Groundmass Concentrate, J=0.0015958, D=1.0064, NM-181G, Lab#=55117-02 | | | | | | | | | | |
| # | A | 605 | 366.9 | 2.129 | 1235.7 | 4.90 | 0.24 | 0.5 | 6.0 | 5.4 | 2.8 |
| # | B | 680 | 10.15 | 1.713 | 21.41 | 9.4 | 0.30 | 39.1 | 17.7 | 11.39 | 0.17 |
| # | C | 730 | 7.896 | 2.532 | 12.37 | 7.78 | 0.20 | 56.4 | 27.3 | 12.79 | 0.16 |
| | D | 780 | 7.116 | 2.642 | 8.991 | 13.6 | 0.19 | 65.7 | 44.1 | 13.44 | 0.09 |
| | E | 855 | 7.042 | 2.779 | 8.600 | 16.4 | 0.18 | 67.2 | 64.4 | 13.60 | 0.10 |
| | F | 955 | 7.762 | 3.577 | 11.20 | 14.1 | 0.14 | 61.2 | 81.8 | 13.66 | 0.10 |
| | G | 1055 | 10.49 | 4.528 | 20.88 | 6.21 | 0.11 | 44.8 | 89.5 | 13.51 | 0.21 |
| | H | 1230 | 15.87 | 28.48 | 46.96 | 5.42 | 0.018 | 27.4 | 96.2 | 12.75 | 0.36 |
| | I | 1680 | 18.60 | 16.46 | 52.23 | 3.11 | 0.031 | 24.3 | 100.0 | 13.14 | 0.57 |
| | **Integrated age ± 2σ** | | | n=9 | | 81.0 | | | | 12.68 | 0.40 |
| | **Plateau ± 2σ** | steps D-I | | n=6 | MSWD=1.69 | 58.9 | 0.15 | | 72.7 | 13.53 | 0.14 |

Isotopic ratios corrected for blank, radioactive decay, and mass discrimination, not corrected for interfering reactions.
Ages calculated relative to FC-1 Fish Canyon Tuff sanidine interlaboratory standard at 27.84 Ma.
Errors quoted for individual analyses include analytical error only, without interfering reaction or J uncertainties.
Integrated age calculated by recombining isotopic measurements of all steps.
Integrated age error calculated by recombining errors of isotopic measurements of all steps.
Plateau age is inverse-variance-weighted mean of selected steps.
Plateau age error is inverse-variance-weighted mean error (Taylor, 1982) times root MSWD where MSWD>1.
Plateau and integrated ages incorporate uncertainties in interfering reaction corrections and J factors.
Decay constants and isotopic abundances after Steiger and Jaeger (1977).
# symbol preceding sample ID denotes analyses excluded from plateau age calculations.
Discrimination = 1.0064 ± 0.0005
Correction factors:
$(^{39}Ar/^{37}Ar)_{Ca}$ = 0.0007 ± 2e-05
$(^{36}Ar/^{37}Ar)_{Ca}$ = 0.00028 ± 5e-06
$(^{38}Ar/^{39}Ar)_K$ = 0.01077
$(^{40}Ar/^{39}Ar)_K$ = 0.0002 ± 0.0003